Department of Civil and Environmental Engineering
Stanford University

A Preliminary Investigation of the Dynamic Response of the Imperial County Services Buildings during the October 15, 1979 Imperial Valley Earthquake

by

Joy M. Pauschke, Carlos S. Oliveira,
Haresh C. Shah and Theodore C. Zsutty

Report No. 49

January 1981

The John A. Blume Earthquake Engineering Center was established to promote research and education in earthquake engineering. Through its activities our understanding of earthquakes and their effects on mankind's facilities and structures is improving. The Center conducts research, provides instruction, publishes reports and articles, conducts seminar and conferences, and provides financial support for students. The Center is named for Dr. John A. Blume, a well-known consulting engineer and Stanford alumnus.

Address:

The John A. Blume Earthquake Engineering Center
Department of Civil and Environmental Engineering
Stanford University
Stanford CA 94305-4020

(650) 723-4150
(650) 725-9755 (fax)
earthquake @ce. stanford.edu
http://blume.stanford.edu

A PRELIMINARY INVESTIGATION OF THE DYNAMIC RESPONSE OF THE IMPERIAL COUNTY SERVICES BUILDING DURING THE OCTOBER 15, 1979 IMPERIAL VALLEY EARTHQUAKE

By

Joy M. Pauschke

Carlos S. Oliveira

Haresh C. Shah

Theodore C. Zsutty

The John A. Blume Earthquake Engineering Center
Department of Civil Engineering
Stanford University
Stanford, California 94305

A Research Report Supported by the

National Science Foundation
Grant ENV77-17834

January 1981

Acknowledgements

The authors of this report wish to thank Fritz Matthiesen, Chris Rojahn and Gerry Brady of USGS, Menlo Park, CA, and Larry Porter, formerly of the California Division of Mines and Geology, for providing the records from the October 15, 1979 Imperial Valley earthquake. Slides of the damaged Imperial County Services Building were generously provided by Jim Stratta.

Help and suggestions provided by Marty McCann are also gratefully acknowledged.

The financial support provided by the National Science Foundation Grant ENV77-17834 and the John A. Blume Earthquake Engineering Center is gratefully acknowledged.

TABLE OF CONTENTS

LIST OF FIGURES

LIST OF FIGURES (CONT.)

LIST OF FIGURES (CONT.)

LIST OF FIGURES (CONT.)

LIST OF TABLES

PREFACE

On October 15, 1979 during the Imperial Valley earthquake, the Imperial County Services Building, located in El Centro, California, became the first extensively instrumented building to sustain significant structural damage induced by seismic loads. This report presents a preliminary assessment of the dynamic behavior of this building based on the vibration data recorded prior to (ambient), during, and after (ambient) the October 15, 1979 earthquake. The thirteen building and the three nearby free field records obtained during this earthquake are analyzed in detail in the time and frequency domains to trace the nonlinear response.

The results show that the building initially vibrated in higher modes. A study of the relative displacement time histories shows that yielding initiated in the first story columns between 6 and 7 seconds after the initial triggering followed by collapse of the east end columns at about 11.2 seconds. Column failure resulted from high axial loads and moments imposed on the columns. The east end columns failed but the west end columns did not because the relative displacements at the east end were on the order of 2 to 3 times larger than at the west end. Throughout the earthquake, the first and second translational and torsional modes in the north-south direction were closely coupled. At the end of the strong motion (approximately 12.0 seconds) and beyond, the fundamental frequencies in both the north-south and east-west directions decreased to values of about 0.4 times the ambient vibration frequencies.

Chapter 1 presents background information on the seismicity of the Imperial Valley, structural characteristics of the Imperial County Services

Building, strong motion instrumentation in the building, structural damage observed during the October 15, 1979 earthquake, and vibration records obtained in the building prior to, during, and after the earthquake. In Chapter 2, the building response characteristics during the October 15, 1979 earthquake are studied as a function of time using the absolute acceleration and relative displacement time histories. The time variation of the frequency content is quantitatively assessed in Chapter 3 using moving time window analysis. Differences between the free field and base motion are discussed. Based on recent strong ground motion research, the root mean square (rms) acceleration response and Arias intensity (energy dissipation) are investigated in Chapter 4. It should be mentioned that the results obtained in Chapter 2, 3 and 4 are not mutually exclusive; analyses in the time and frequency domains can duplicate results as well as provide additional information not as readily obtainable in the other domain. Chapter 5 interprets the dynamic behavior determined in the preceding chapters and suggests further research prompted by this study.

CHAPTER 1: BACKGROUND INFORMATION AND AVAILABLE DATA

1.1 Seismicity of the Imperial Valley

In historic time, the seismicly active Imperial Valley region has experienced only moderate to small earthquakes. Located in southern California near the Mexican border, this region is dominated by the San Andreas and San Jacinto fault systems and by other northwesterly trending faults as shown in Figure 1.1. Most of these faults are right lateral strike - slip faults. More moderate to small ($M_L < 6.0$) earthquakes and earthquake swarms have occurred in this region than in any other area along the San Andreas fault system. The recorded history of earthquakes occurring with magnitude M_L greater than 6.0 is summarized in Table 1.1. In spite of the frequent rate of earthquake occurrences, Table 1.1 shows that there have been no great earthquakes ($M > 8$) in the Imperial Valley in historic time, suggesting that the rather frequent occurrence of moderate size earthquakes is sufficient to release the accumulated strain energy. The only other recorded earthquake activity prior to the November 9, 1852 Fort Yuma event occurred on June 23, 1843 with a MMI of VII (Ulrich, 1941).

The moderate magnitude Imperial Valley earthquake ($M_L = 6.6$ CalTech Seismological Laboratory) occurred at 16:16 Pacific Daylight Time on October 15, 1979, with the epicenter located at 32.64° N and 115.33° W. The earthquake had a shallow focal depth and was generated by right lateral slip on the northwest trending Imperial Fault. This earthquake had similar local Richter magnitude, peak horizontal ground acceleration, and measure of the closest distance to the rupture surface as the May 18, 1940, earthquake. Damage estimated to be 30 million dollars was evident in residential areas of southern Imperial County and northeastern Baja California. As will be discussed later, the foundation and structure of the Imperial County Services

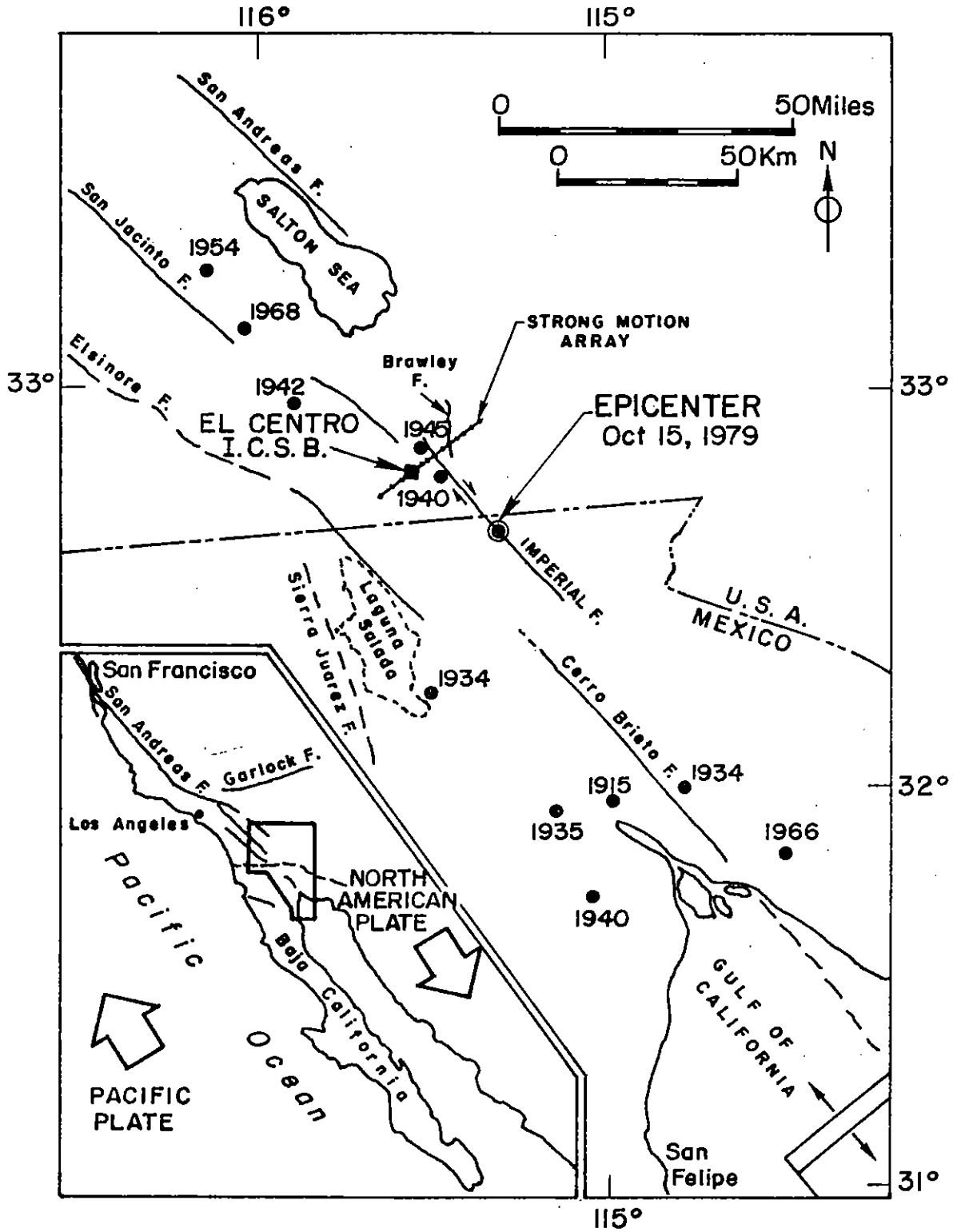

FIGURE 1.1 Major Faults and Seismicity (M_L > 6.0) of the Imperial Valley Region. Location of the Imperial County Services Building (I.C.S.B.), El Centro

TABLE 1.1 SEISMICITY OF THE IMPERIAL FAULT REGION, $M_L \geq 6.0$*

DATE	GMT	LAT.	LONG.	MAGNITUDE	I max (MM)	Felt area ($x10^3 km^2$)	Reference
1852 29 Nov.	20:00	32.5	115.0	M = 6.5	9		1
1906 19 Apr.	00:30	32.5	115.5	M = 6.0	8	100	2
1915 23 Jun.	03:59	32.8	115.5	M = 6.3	8	200	2
1915 23 Jun.	04:56	32.8	115.5	M = 6.3	8	200	2
1927 1 Jan.	08:16:45	32.5	115.5	M = 5.8	8	130	2
1940 19 May	04:36:40.9	32.733	115.50	M_L = 6.4	10	155	3,4,5,6
				M_s = 7.1			
1979 15 Oct.	23:16:54.3	32.644	115.312	M_L = 6.6			6,7
				M_s = 6.8			

References to Table 1.1

1. Toppozada, T., Real, C., Bezore, S., and Parke, D., 1979. Compilation of pre-1900 California earthquake history, Annual Technical Report, U.S.G.S. Grant No. 14-08-0001-G-513.
2. Toppozada, T., Parke, D., and Higgins, C., 1978. Seismicity of California 1900-1931, CDMG Special Rpt. 135, Sacramento, California.
3. Hileman, J.A., Allen, C.R., and Nordquist, J.M., 1973. Seismicity of the Southern California Region 1 January 1932 to 31 December 1972 (Seismological Laboratory, California Institute of Technology).
4. Richter, C.F., 1958. Elementary Seismology, W.H. Freeman, San Francisco, p. 768.
5. Neumann, F., 1942. United States Earthquakes, 1940, Serial #647, U.S. Dept. of Commerce Coast and Geodetic Survey, Washington.
6. Pechmann, J., 1979, pers. comm. (see Table 2).
7. German, P., 1980, pers. comm.

* From (Leivas, et al, 1980, p. 28)

Building in El Centro were extensively damaged. Other damaged structures included mobile homes, a concrete block wall, bridge abutments, and metal grain elevators.

1.2 Structural Characteristics of the Imperial County Services Building

The six story reinforced concrete Imperial County Services Building is one of the few tall buildings in the highly seismic Imperial Valley. Located approximately 7.5 km southwest from the Imperial fault and 29 km northwest of the October 15, 1979 epicenter, this building was designed to the 1967 Uniform Building Code (UBC) and built in 1971. Figure 1.2a shows the south and east exterior faces of the building. The plan and elevation dimensions are shown schematically in Figure 1.2b. With a plan dimension of 136'-10" x 85'-4" (41.7 m x 26.0 m), the building is five bays wide in the east-west (longitudinal) direction and three bays wide in the north-south (transverse) direction, with all bays 25'-0" long. Lateral loads are resisted by reinforced concrete moment resisting frames in the E-W direction. In the N-S direction, lateral load resistance is provided by exterior facade full width shear walls on lines A and H (Figure 1.2b) above the second floor and by four 25'-0" long center bay shear walls on lines B, D, E and F in the first story. The shear walls are 12" thick with two curtains of reinforcement in the first story, 7-1/2" thick with a single curtain of reinforcement in the second story, and 7" thick above the second level with a single curtain of reinforcement. According to the design calculations, the design "K" factor was 1.33 for the N-S shear walls, 0.67 for the E-W exterior frames and 1.0 for the E-W interior frames.

The first story columns are square. Above the second floor, the interior columns are square but the exterior columns on the north and south

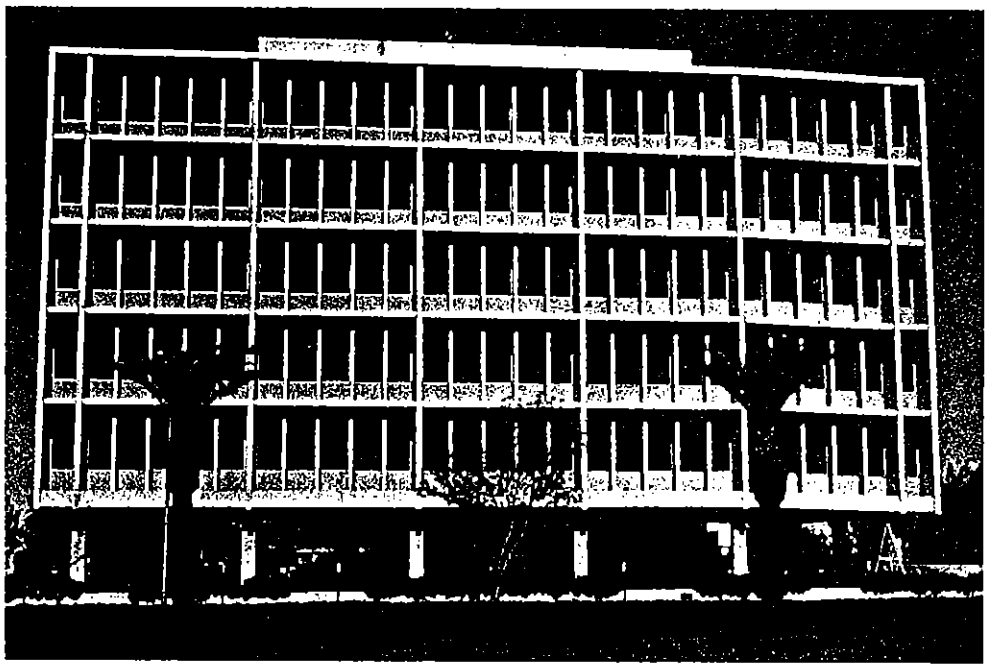

South Face.

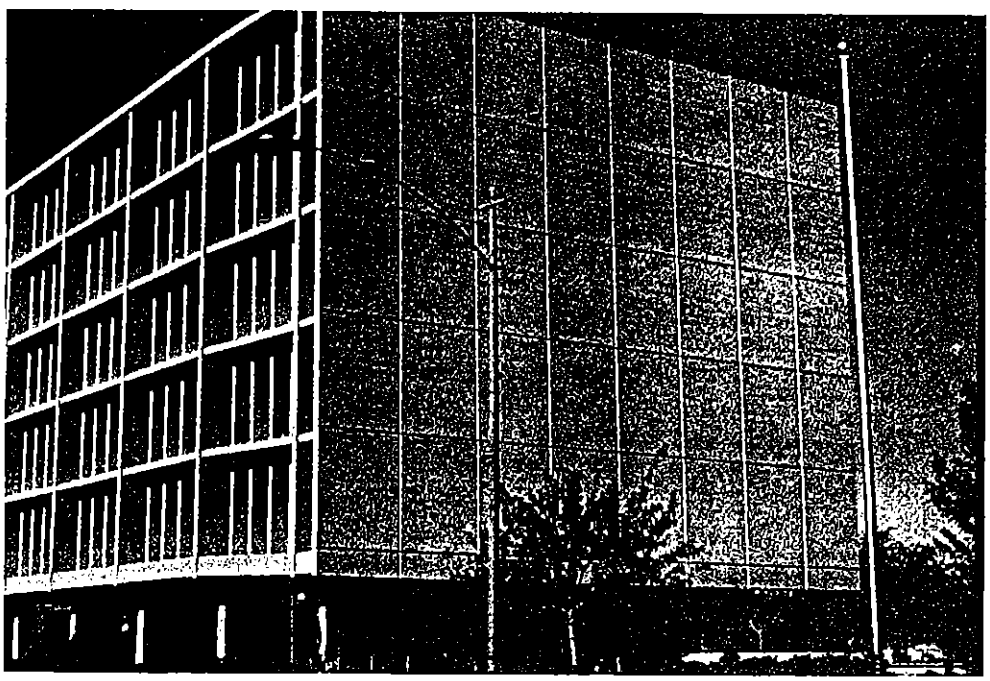

East Face.

Figure 1.2(a) Elevation Views of South and East Exterior Faces of the Imperial County Services Building.

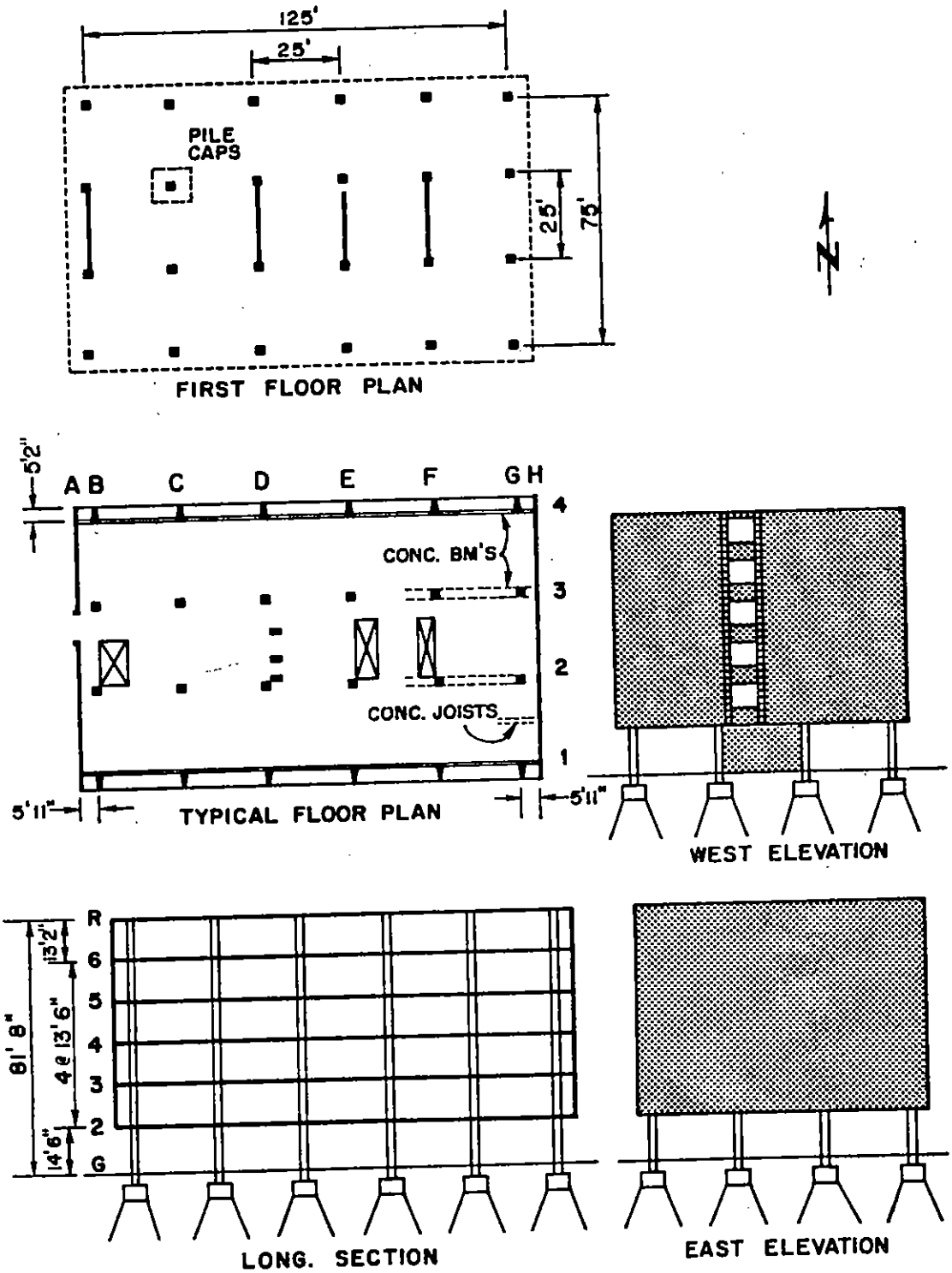

FIGURE 1.2b Structural Configuration of the Imperial County Services Building (From Wosser, et al, 1980)

faces are elongated to the outside tapering from 18" wide to 10" wide over a depth of 5'-10". The column reinforcement is Grade 40 steel consisting of ten #11 bars in the exterior columns and eight #11 bars in the interior columns. The reinforcement layout for the east end corner columns which were severely damaged during the October 15, 1979 earthquake is shown in Figure 1.3. At the first floor level, the pile caps are 2'-2" below the floor line with #4 tie bars at 3" spacing. Above the first floor level to 2'-2" below the girder framing, i.e., over the midsection of the column, the ties are #3 bars at 12" spacing. For 3'-0" above and 2'-2" below the girder framing, #4 bars are used at 2 1/2" and 3" spacings, respectively.

Except at the second floor, the longitudinal framing consists of 10" thick x 4'-6" deep spandrel sections below the floor level on the exterior column lines and 24" x 30" girders on the two interior column lines. At the second floor level, the exterior girders are also 24" x 30". Above the second floor the slabs are 3" thick supported by 5 1/2" x 14" reinforced concrete joists at 36" o.c. in the transverse direction. The 5" thick floor slab at the second level allows the shear transfer in the diaphragm between the first and second stories. The design strength of the concrete was 4 ksi in the beams and slabs and 5 ksi in the columns and shear walls. The building is supported on tapered piles 45' to 60' long which extend into an alluvium (sand and clay) layer.

1.3 Strong Motion Instrumentation and Data

Because of its structural characteristics, size and location in a known highly seismic area, the Imperial County Services Building was initially instrumented in May 1976 with the 9-channel Kinemetrics CRA-1 accelerograph system shown in Figure 1.4a. The instrumentation consisted of a tri-axial

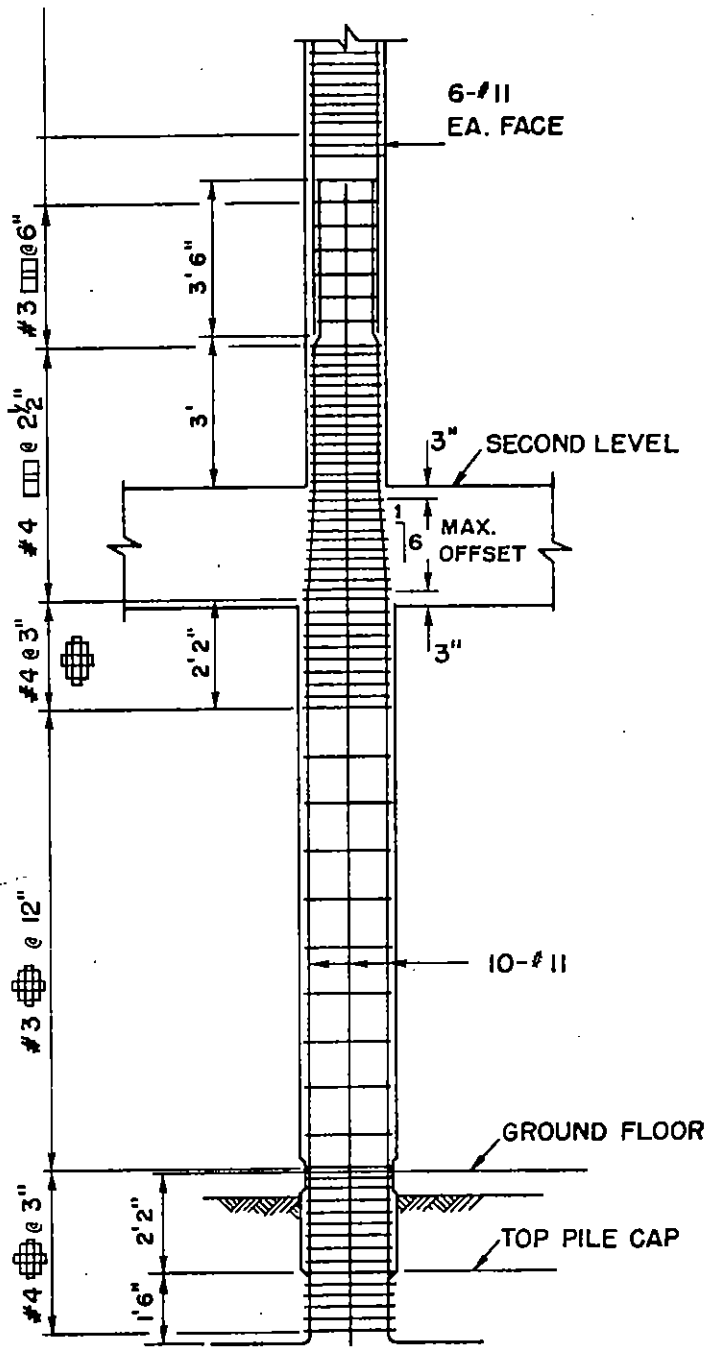

EXTERIOR FRAME COLUMN REINFORCEMENT
ALONG LINE G AT 1 & 4

FIGURE 1.3 Exterior Frame Column Reinforcement Along Line G at 1 and 4 (See FIGURE 1.2b)
(From drawing by Brandow & Johnston Associates in Wosser, et al, 1980)

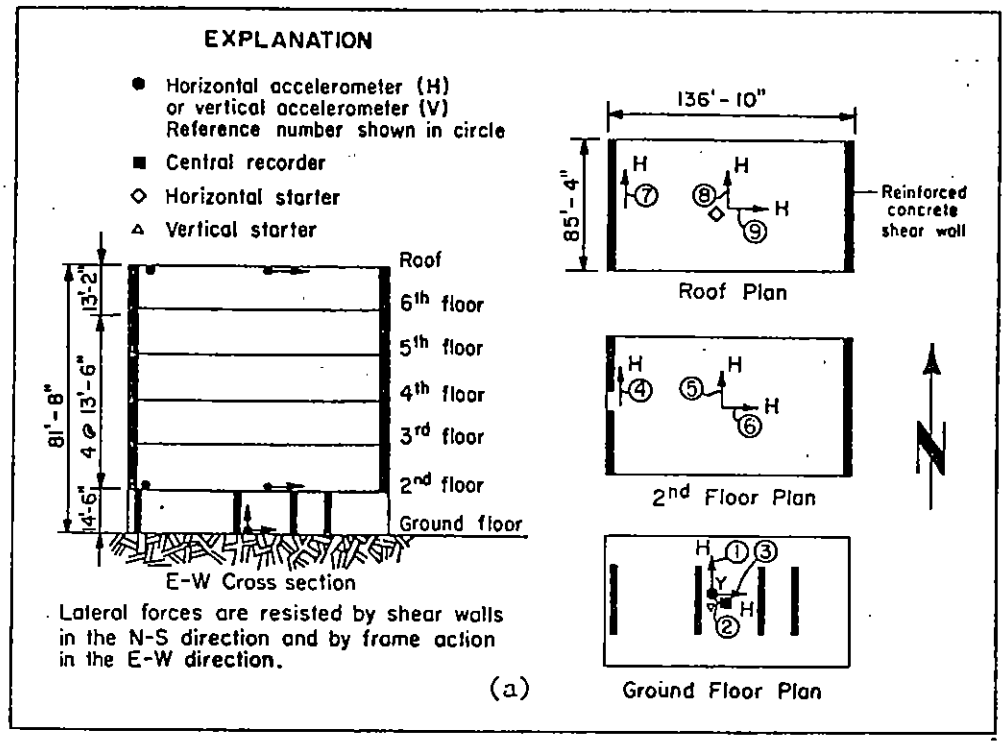

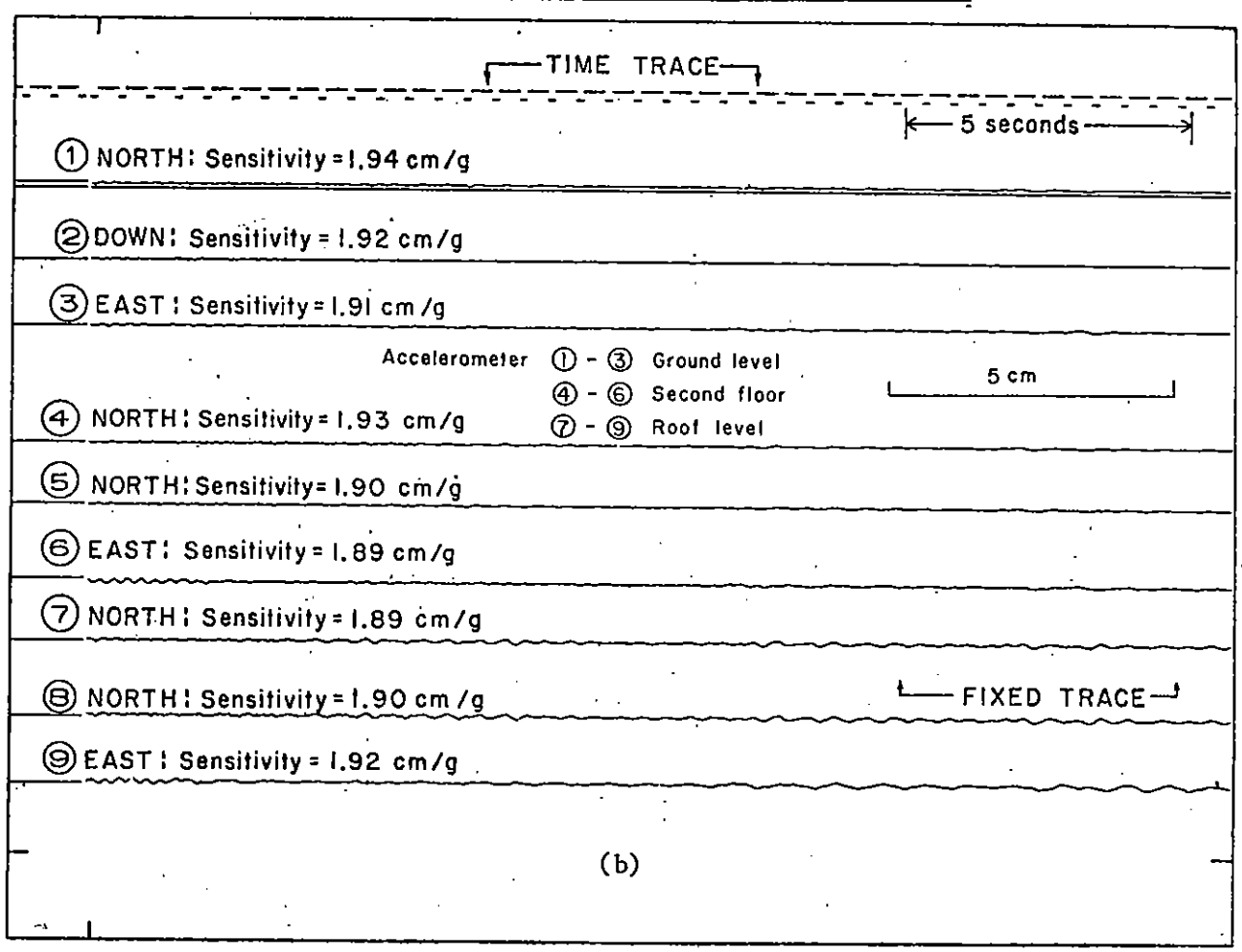

FIGURE 1.4 Acceleration Time Histories from the Imperial Valley Earthquake of November 4, 1976
(a) Location of Strong Motion Instrumentation
(b) Acceleration Time Histories

package of accelerometers at the ground level and 3 single-axis horizontal accelerometers each at the second and roof levels. The 9 channel system was triggered by the magnitude M_L = 4.9 Imperial Valley earthquake of November 4, 1976. The epicenter of this earthquake was about 20 miles (32 km) north of the building. Because the amplitudes of the recorded building accelerations were very low (peak values less than 0.1 g) as shown in Figure 1.4b, the records were not processed. After a review of the 1976 earthquake, the instrumentation was upgraded in May 1978 to its present 13 channel configuration and a triaxial Kinemetrics SMA-1 accelerograph, intended to record the nearby free field motion, was added at the ground level approximately 340' east of the building. Locations of the sixteen accelerometers are shown in Figure 1.5. The revised system was maintained by the California Division of Mines and Geology (CDMG) Office of Ground Motion Studies.

The thirteen building and three free field accelerometers produced high quality records of almost 60 seconds duration of the October 15, 1979 Imperial Valley earthquake. All building records had triggered at the same time. The building and the free field records were processed by the CDMG Office of Ground Motion Studies and are shown in Figure 1.6. The peak acceleration values and times of occurrences are summarized in Table 1.2 and plotted in Figure 1.7.

1.4 Structural Damage from the October 15, 1979 Earthquake

During the October 15, 1979 earthquake, the foundation and first story of the Imperial County Services Building were irreparably damaged. As documented in detail by Wosser et al (1980) and shown in Figure 1.8a, the most significant structural damage was the failure just above ground

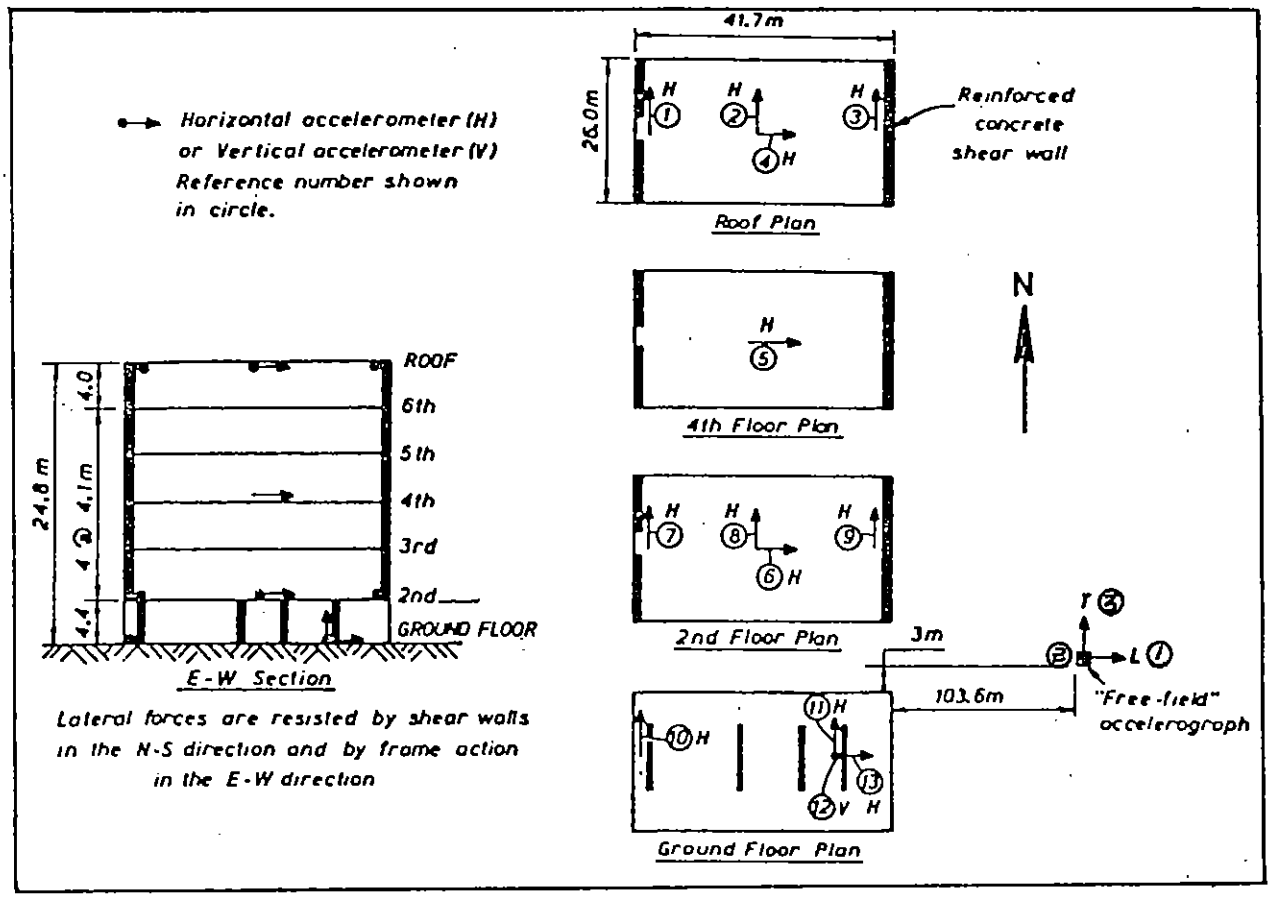

FIGURE 1.5 Location of Strong Motion Instrumentation in the Imperial County Services Building which Triggered during the Imperial Valley Earthquake of October 15, 1979

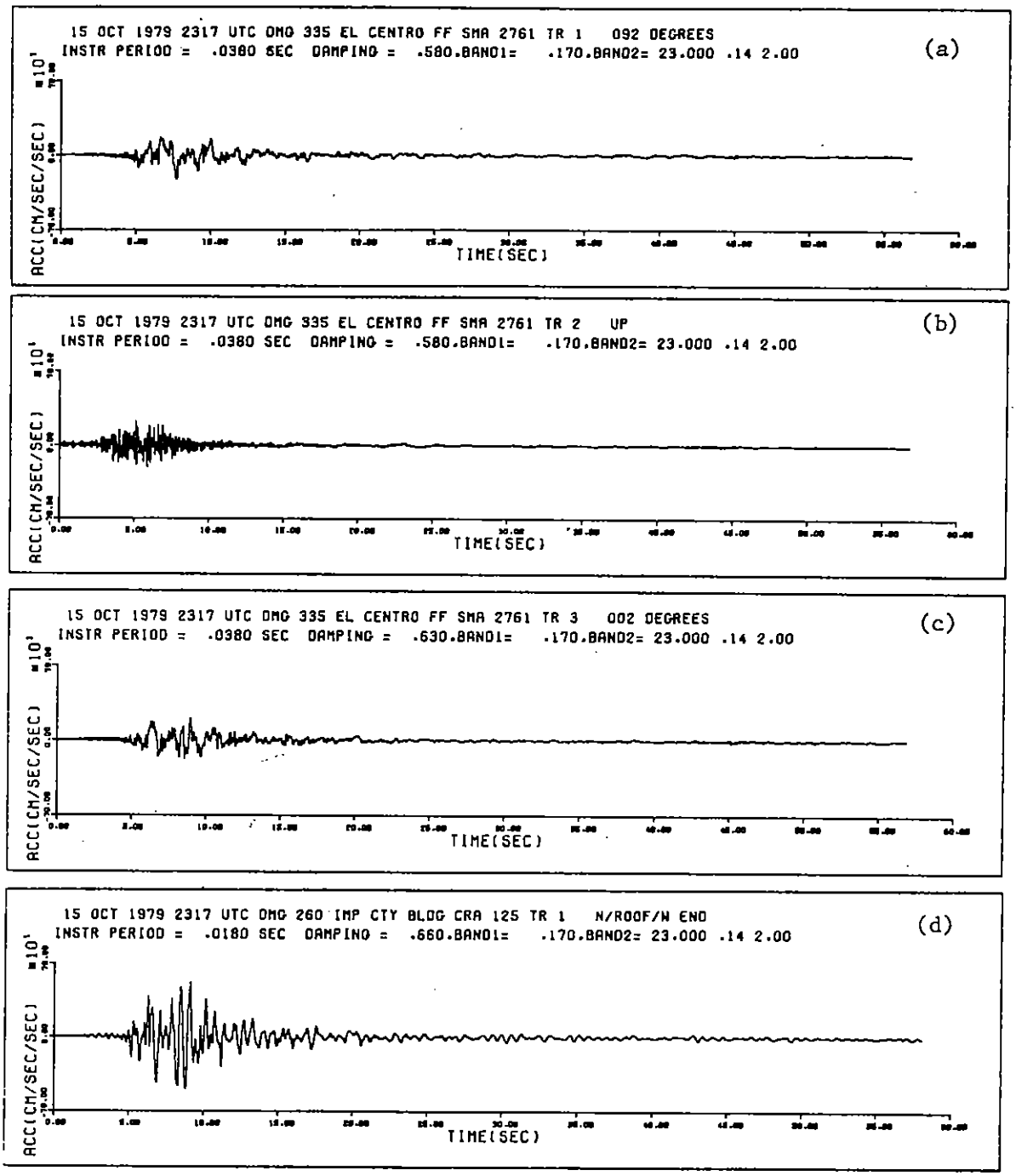

FIGURE 1.6 Acceleration Time Histories from the Imperial Valley Earthquake of October 15, 1979

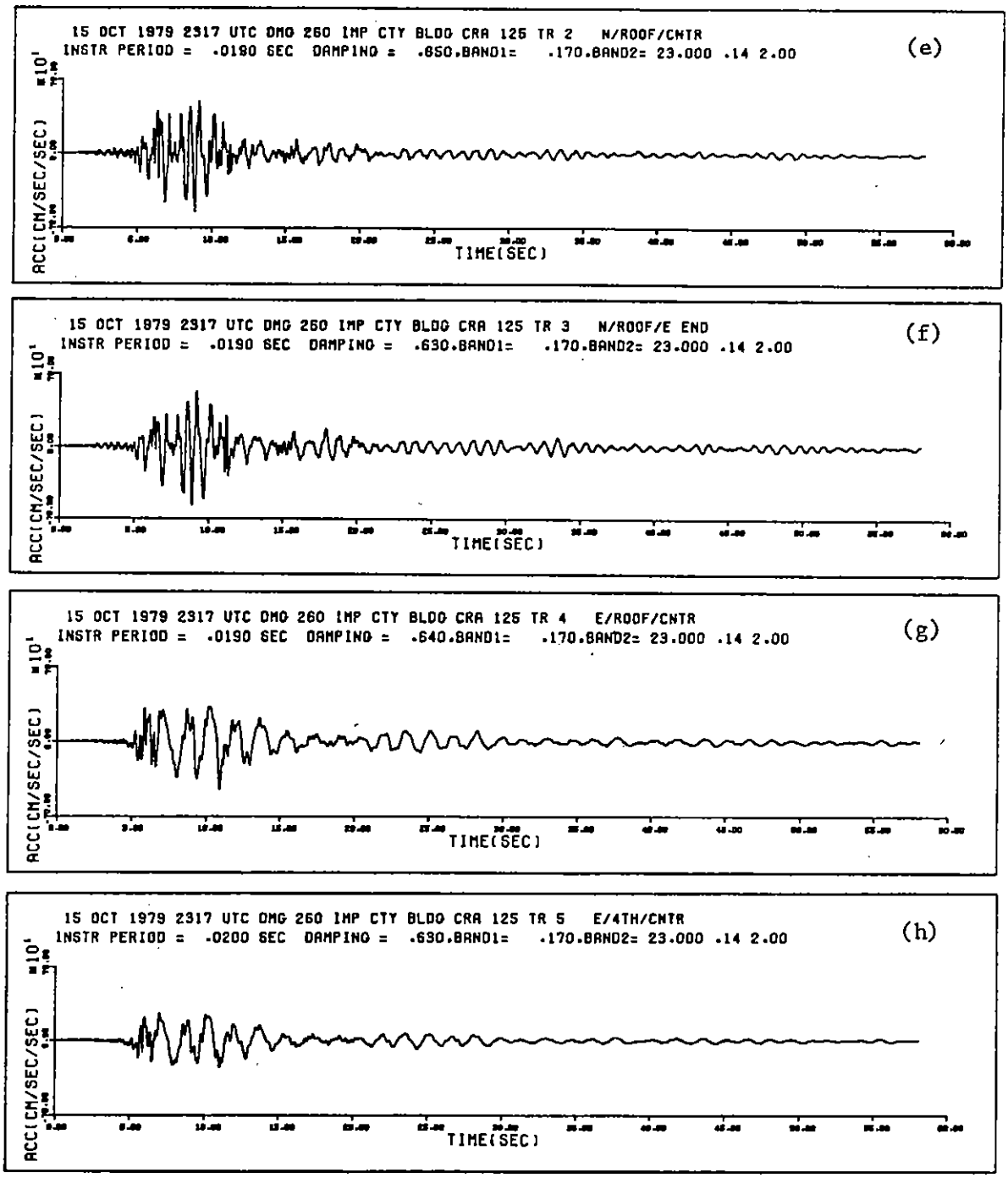

FIGURE 1.6 (cont'd) Acceleration Time Histories from the Imperial Valley Earthquake of October 15, 1979

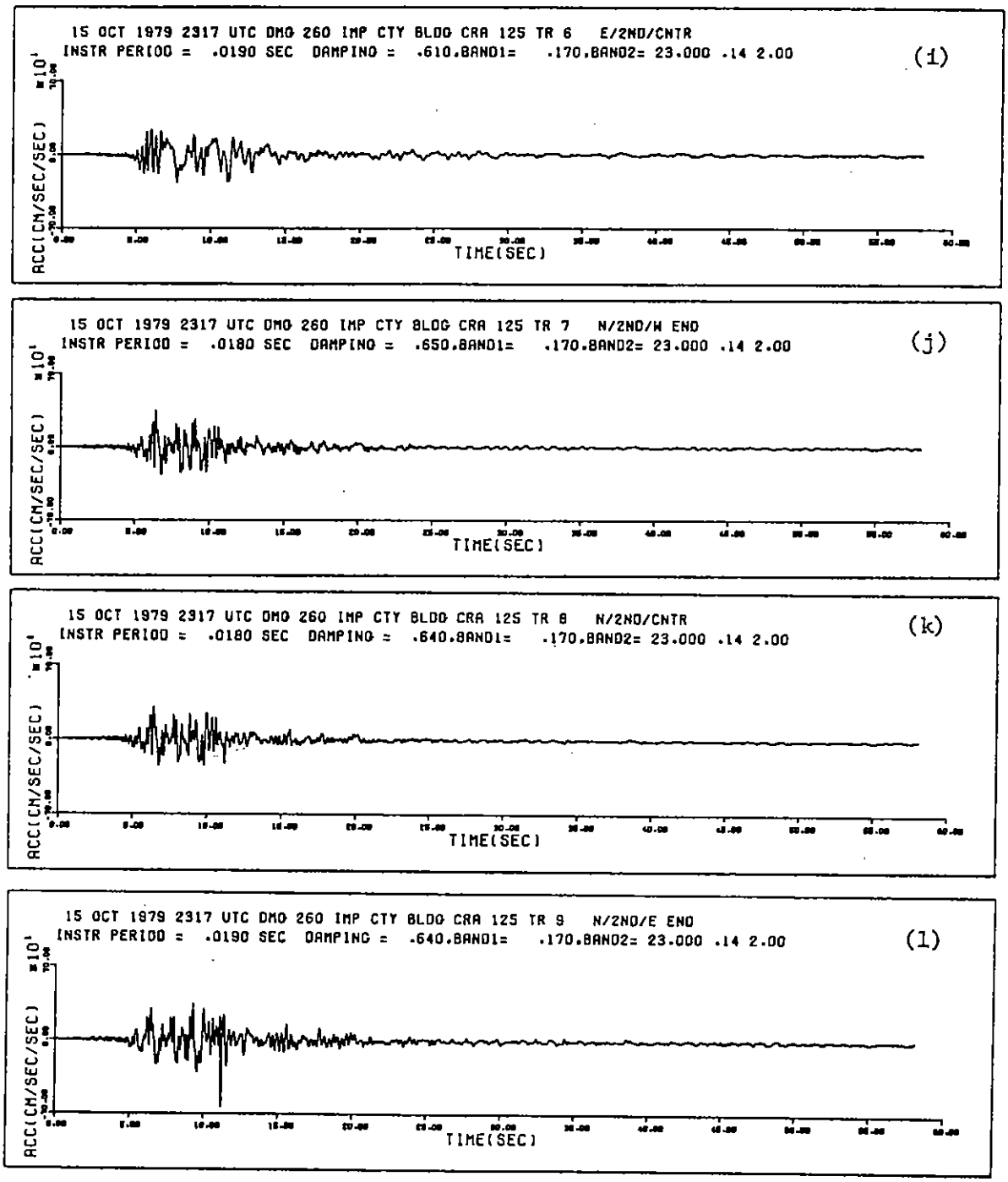

FIGURE 1.6 (cont'd) Acceleration Time Histories from the Imperial Valley Earthquake of October 15, 1979

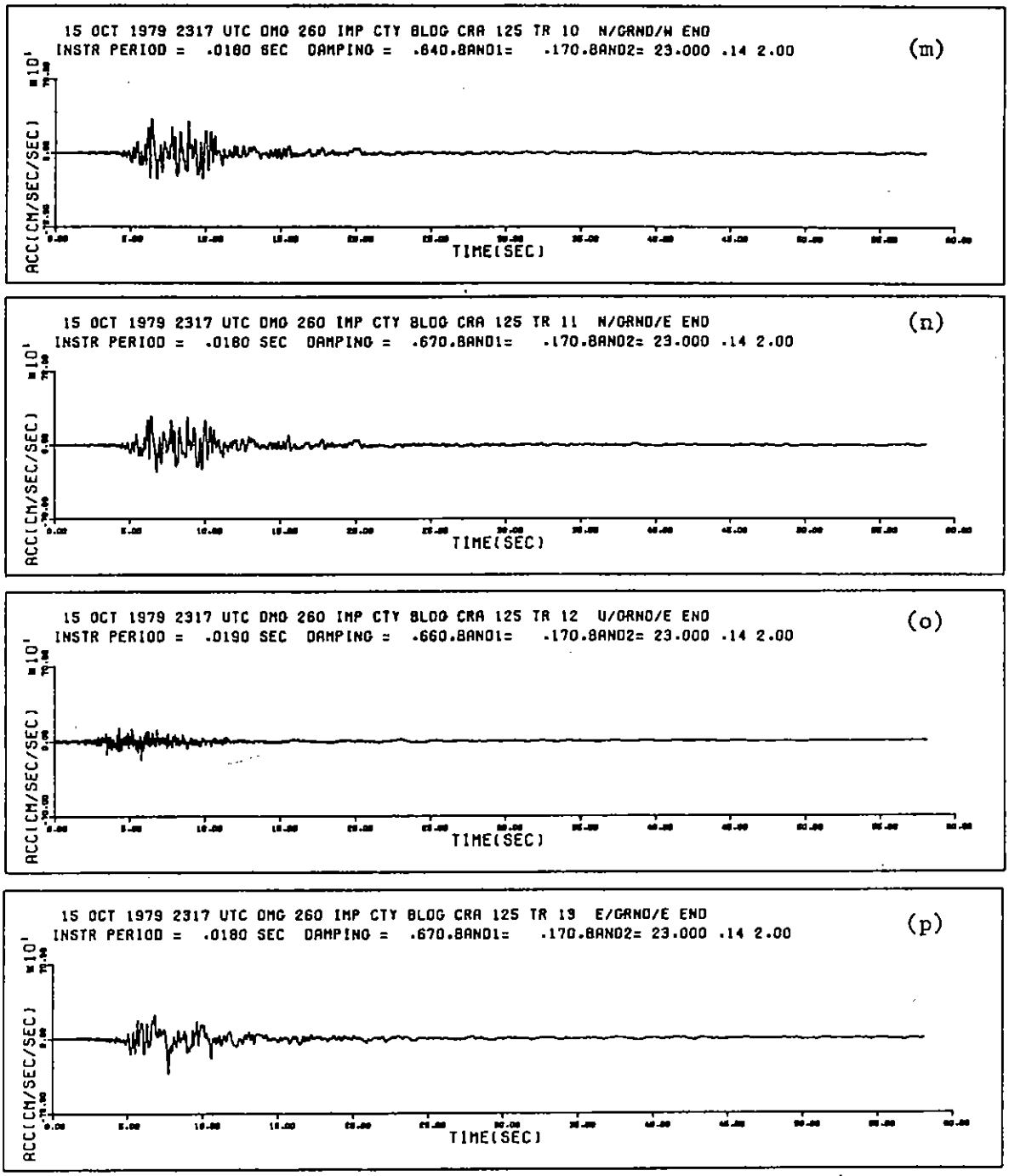

FIGURE 1.6 (cont'd) Acceleration Time Histories from the Imperial Valley Earthquake of October 15, 1979

TABLE 1.2 MAXIMUM ACCELERATIONS IN THE IMPERIAL COUNTY SERVICES BUILDING FROM THE OCTOBER 15, 1979 EARTHQUAKE

Trace No.*	Location**	Direction	Maximum Acceleration cm/sec^2	Time of Maximum Acceleration (sec)
TR1	FF 092	588E	-231.44	7.75
TR2	FF UP	UP	230.90	5.10
TR3	FF 002	N02E	209.02	8.95
TR1	N/R/W	N00E	531.34	9.12
TR2	N/R/C	N00E	-551.56	8.89
TR3	N/R/E	N00E	-569.38	8.89
TR4	E/R/C	N90E	-443.90	10.92
TR5	E/4/C	N90E	258.21	6.97
TR6	E/2/C	N90E	-268.54	7.77
TR7	N/2/W	N00E	355.80	6.40
TR8	N/2/C	N00E	307.44	6.42
TR9	N/2/E	N00E	-641.95	11.20
TR10	N/G/W	N00E	330.57	6.41
TR11	N/G/E	N00E	284.03	6.44
TR12	U/G/E	UP	-174.26	5.79
TR13	E/G/E	N90E	-324.96	7.72

* See Figure 1.5

** N/R/W is the abbreviation for North-South Direction/Roof Level/ West End of the Building. These abbreviations will be used in the remainder of this report.

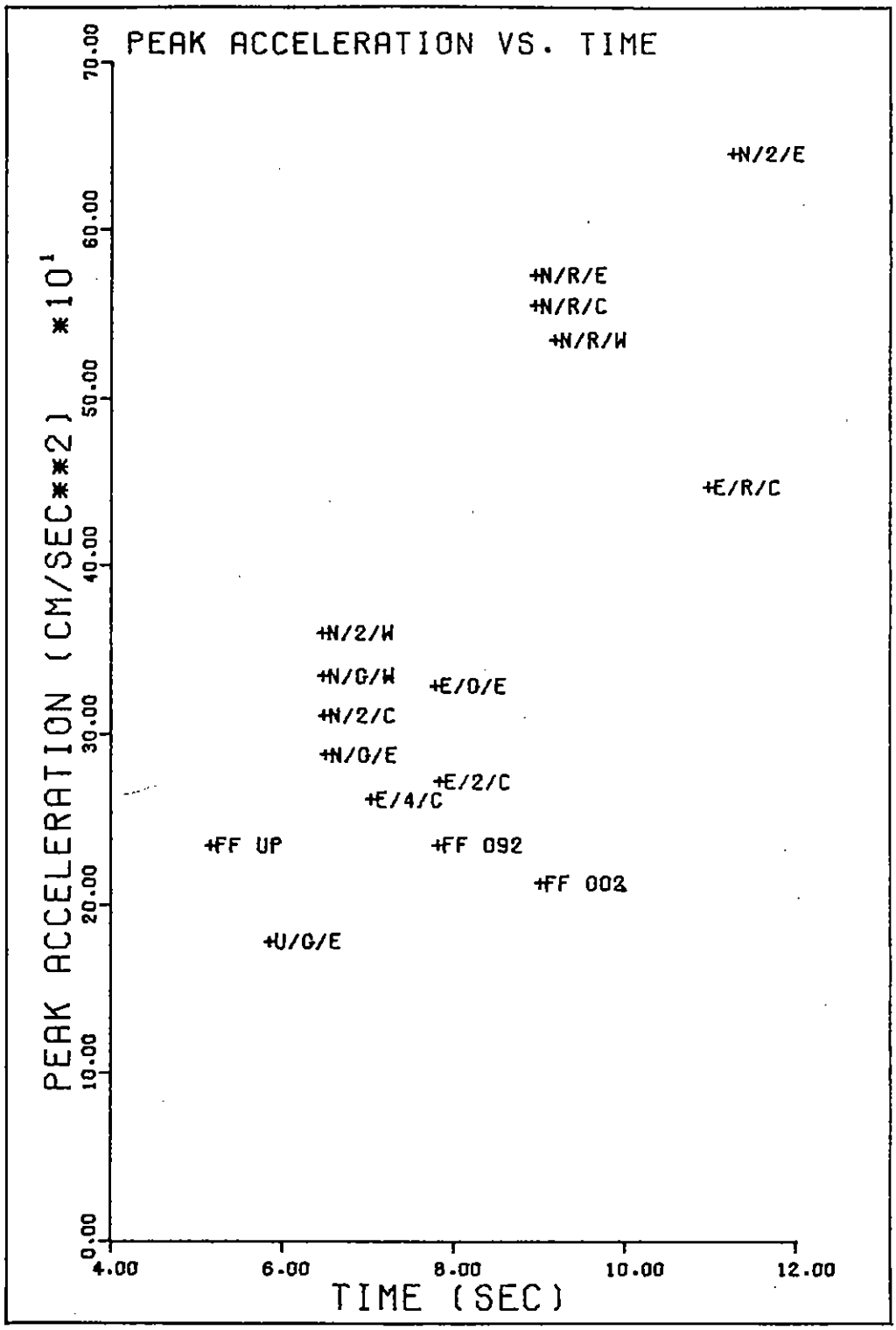

FIGURE 1.7 Peak Acceleration vs. Time in Imperial County Services Building during the October 15, 1979 Earthquake

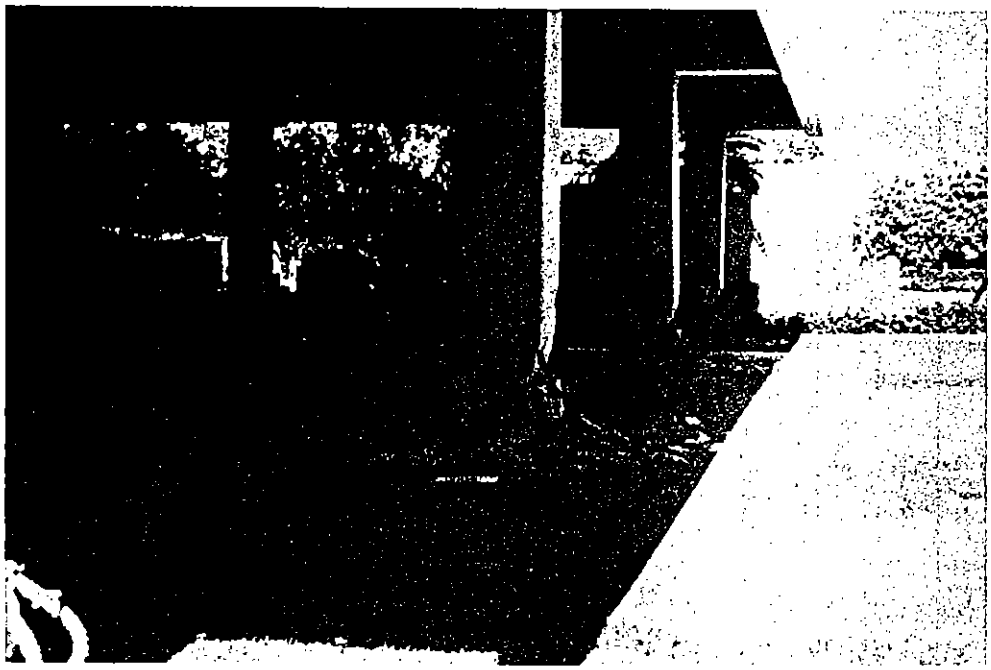

Failure of Ground Level Column Line G at East End of the Building.

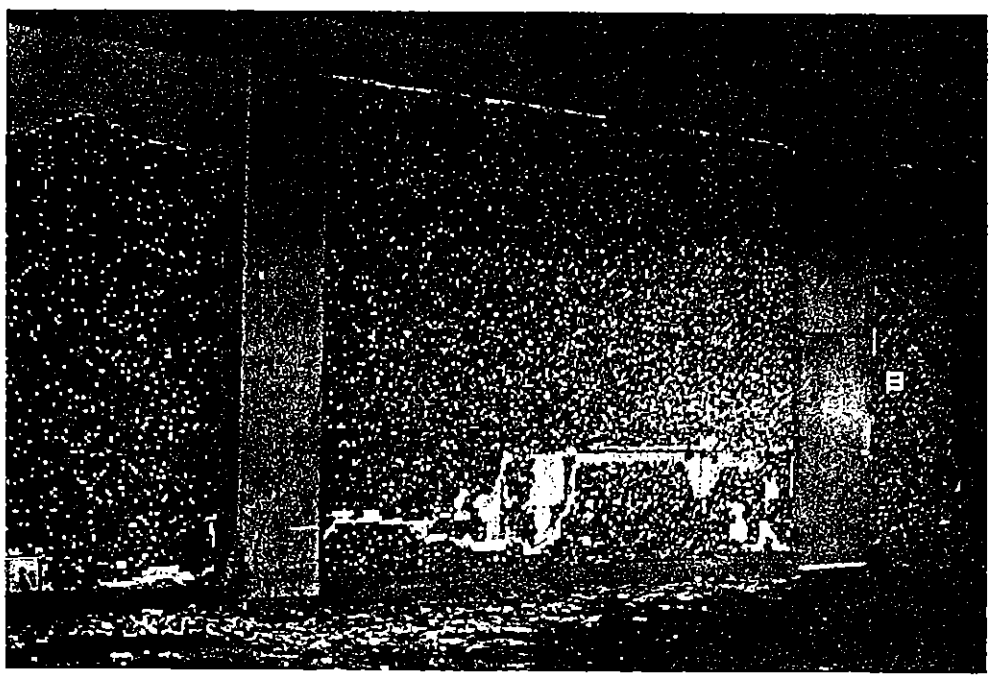

Ground Level Column 3E from the North.

Figure 1.8 Structural Damage to the Imperial County Services Building During the Imperial Valley Earthquake of October 15, 1979.

level of the four reinforced concrete columns located along the east end of the building (column line G in Figure 1.2b). The concrete at the base of each column was badly shattered, the vertical reinforcing bars had severely buckled, and the horizontal tie bars had loosened. The columns shortened about 12 inches during the main event and after shocks but the building did not appear to lean in any direction. The settlement of these four columns caused hinging at the first story of the east end bays of the longitudinal moment resisting frames as evidenced by minor cracking of the girders and incipient spalling at the tops of the columns. Spalling of concrete was evident in the first story columns in line 1 (Figure 1.2b) but nothing approaching complete failure. As shown in Figure 1.8b, column 3E shows a steep shear crack in the E-W direction which cracked the adjacent infilled wall and created a 3 cm gap between the top of the column and wall (permanent displacement at the second floor).

In the upper stories only minor damage due to the first story east end column failures was evident. Shear cracks in the floor diaphragms and some longitudinal frame yielding was observed. The exterior shear walls showed minor diagonal tension cracks.

1.5 Ambient Vibration Test Results

Ambient vibration tests were performed on the Imperial County Services Building prior to and after the October 15, 1979 earthquake. The pre-earthquake ambient vibration test was performed by Pardoen (1979) in February 1979. Measurements were recorded at floor levels 2, 4 and 6 and the roof in both the N-S and E-W directions. The measured frequencies and damping ratios are summarized in Table 1.3a. Values for the first two N-S and E-W translational modes and for the first torsional mode are given by Pardoen; the

TABLE 1.3 FREQUENCIES AND DAMPING RATIOS OF IMPERIAL COUNTY SERVICES BUILDING OBTAINED FROM AMBIENT VIBRATION TESTS

a) February 1979

Direction	1st Mode		2nd Mode		3rd Mode		Damping %
	Frequency (Hz)	P.F.*	Frequency (Hz)	P.F.	Frequency (Hz)	P.F.	
E-W	1.54	1.50	5.1	-0.42	8.9	0.43	6
N-S	2.24	1.72	9.0	-0.146	-	-	10
Torsion	2.85	1.13	-	-	-	-	8

b) March 1980

Direction	Frequency (Hz)		
	1st Mode	2nd Mode	3rd Mode
E-W	1.20	2.88	7.28
N-S	1.92	~6.4	-
Torsion	2.32	-	-

* Participation Factor

frequency of third translational mode was derived from the given power spectra. The power spectra show a small perturbation near 4 Hz that could not be identified. The damping values were obtained by Pardoen using three methods: from the width of the peak of the spectral density function at half the peak value, from the parameters of the exponential curve fit to the auto-correlation envelope, and the random decrement technique. Mode shapes derived from the power spectra at the various floor levels are sketched in Figure 1.9. Pardoen presents similar mode shapes for the first N-S and E-W translational modes but a slightly different shape for torsion. The participation factors are computed for each mode shape from the mass distribution assumed in Figure 1.9.

In March 1980 Pardoen performed a post-earthquake ambient vibration test. The new frequency values, listed in Table 1.3b, reflect the building in its shored up configuration. The second ambient test frequencies show a decrease of 22%, 14%, and 19%, in the E-W, N-S, and torsional mode frequencies, respectively, from the first test and show that the foundation movement at the building base was very important. It is interesting to note in Figure 1.10 that the post-earthquake ambient ground motion spectra at the nearby free field site is nearly flat (wide band) with the peak envelope at 3-4 Hz and is completely different from the motion recorded at the base of the building. The influence of the pile-foundation is strongly evident.

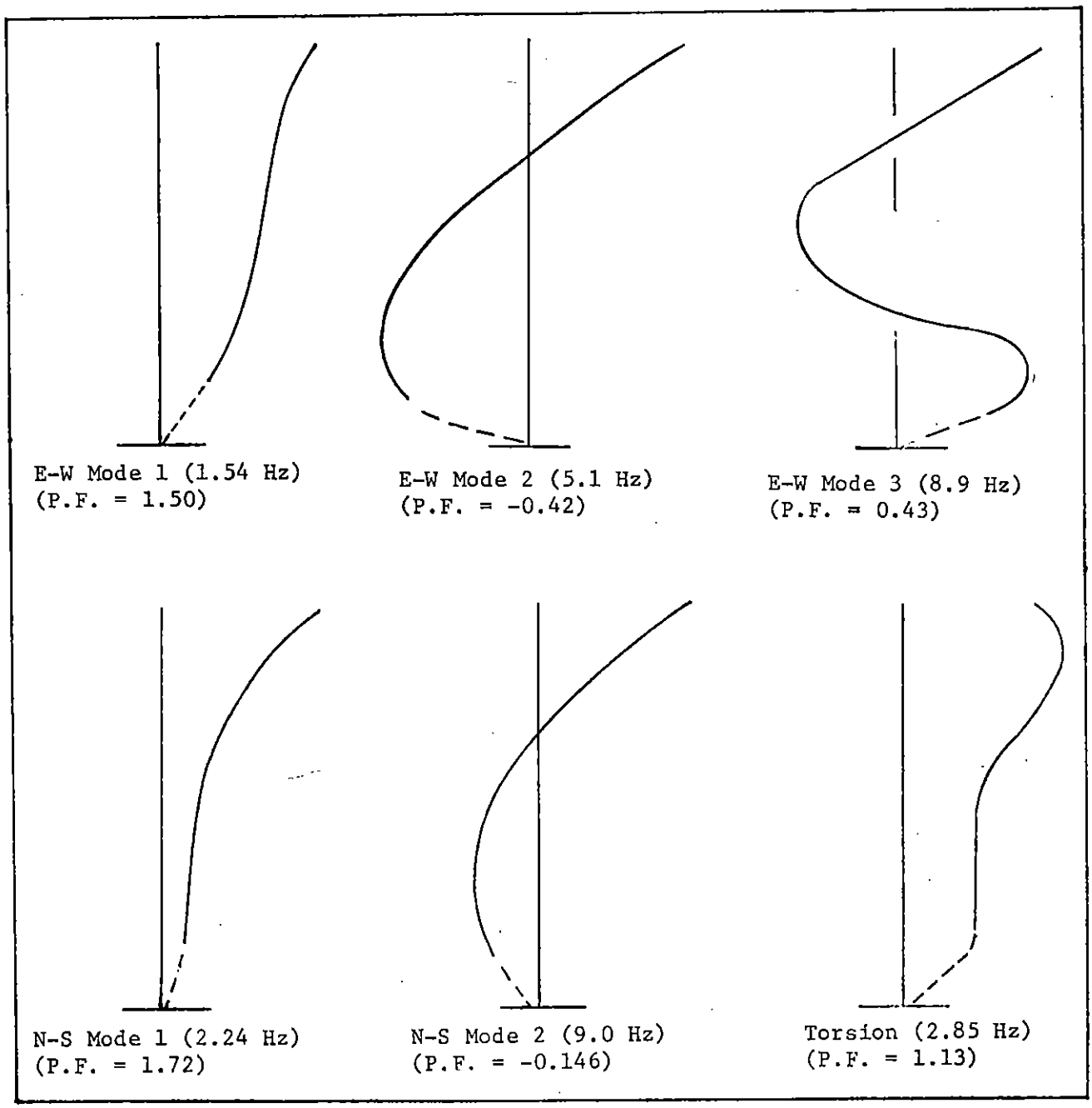

Assumed Mass Distribution	
Level	Mass x 10^3 cu.ft.
Roof	8.9
6	12.4
5	12.4
4	12.4
3	12.5
2	13.7

FIGURE 1.9 Mode Shapes Obtained from 1979 Ambient Vibration Test

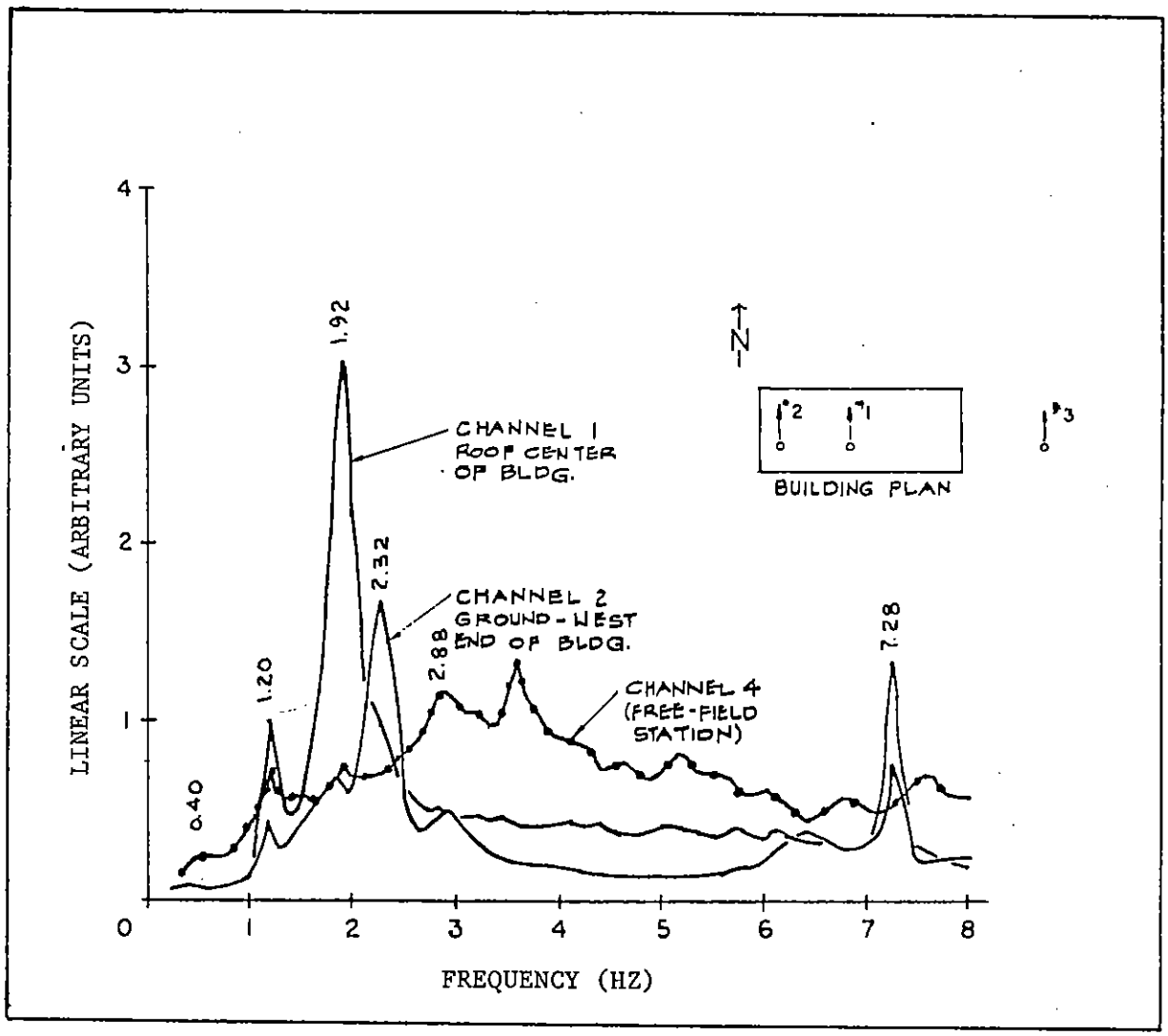

FIGURE 1.10 March 1980 Post Earthquake Ambient Vibration Ground Level Spectra (From Pardoen, Hart, and Bunce, 1980)

CHAPTER 2: TIME DOMAIN ANALYSIS

2.1 Introduction

The number of strong motion building records obtained from past earthquakes are few. Nonetheless, the few available records are invaluable for furthering an understanding of the dynamic response of structures as an aid to design practice. On October 15, 1979, the Imperial County Services Building became the first extensively instrumented building to sustain significant structural damage. The records obtained in this building make it possible to trace the nonlinear response in the time and frequency domains with the goal of recreating the building vibration and following the time variation of the frequency content.

In this chapter, the records are analyzed in the time domain. The absolute acceleration, relative velocity and relative displacement histories are studied in detail. The objective of this chapter is to portray the building response as a function of time, especially to identify the times of initial yielding and final collapse of the east end ground level columns. As discussed below, the highly nonstationary ground motion and building response can be roughly divided into three time intervals: 0 to 6 seconds, low amplitude free field motion producing linear building response; 6 to 12 seconds, large amplitude motion in both the free field and the building with yielding and eventual failure of the ground level columns; and 12 seconds to the end of the record, small amplitude motion, degraded building response. Chapter 3 will quantitatively assess the frequency content during these time intervals.

2.2 Absolute Acceleration Time Histories

A study of the three nearby free field and the thirteen building acceleration time histories (Figure 1.6) gives a preliminary understanding of the characteristics of the strong ground motion and building response. The peak absolute acceleration values and times of occurrence were listed in Table 1.2 and plotted in Figure 1.7. The nomenclature used in Table 1.2 to denote the recorded traces (e.g., N/2/W to denote motion in the N-S direction, 2nd floor, west end of the building) will be followed in the remainder of this report.

A visual inspection of Figures 1.6a, b and c shows that the nearby free field motion was highly nonstationary. The two horizontal free field components, FF 092 (E-W) and FF 002 (N-S), had similar amplitudes and phase throughout the earthquake. During the first six seconds, i.e., the P wave phase, the horizontal components contained low frequency (0 to 3 Hz) motion and low amplitude accelerations (less than 30 cm/sec^2). Between 6 and 12 seconds, an abrupt increase in the amplitudes (about 10 times; maximum was 0.23g) occurred corresponding to the S wave influence. Between 5 and 7 seconds, the N-S component (FF 002) showed a transition stage not present in the E-W component (FF 092). At about 12 seconds, the amplitudes of both components rapidly decayed to about 50 cm/sec^2 and less and by 24 seconds, the amplitudes were less than 15 cm/sec^2. The time history of the vertical component (FF Up) in Figure 1.6b, however, showed less variation with time, consistent high frequency content and an envelope of large amplitude motion between 4 and 8 seconds.

Of special interest is a comparison between the motion at the free field site (Figures 1.6a, b and c) and at the base of the building (Figures 1.6m-p). Visual comparisons show several interesting features. Although the peak horizontal accelerations for all base components were higher than at the free field site (see Table 1.2), the vertical free field motion was generally higher in amplitude than at the base of the building. One way to further compare the horizontal free field vs. base motion is to compare the response of a single degree of freedom oscillator to each of the ground level records. In the E-W direction, the free field (FF092) and base (E/G/E) motions were very similar. In Figures 2.1(a) and (b) the response of a single degree of freedom oscillator (frequency of 1.54 Hz, critical damping of 6%; reference Table 1.3) to each of the above E-W ground motions are shown. Because the response is very similar, it can be concluded that the input motions, i.e., FF092 and E/G/E, also contained similar content at this frequency. On the other hand, the free field (FF002) and base (N/G/E) components in the N-S direction differed significantly. In Figures 2.1(c) and (d) the response of a single degree of freedom oscillator (frequency 2.24 Hz, critical damping of 10%) to these two N-S records are shown and are completely dissimilar. Thus the free field and base N-S components contained different content at this given frequency. The two N-S records at the base of the building, i.e., N/G/W and N/G/E, however were similar in phase (no torsion) and amplitude as shown later in Figure 2.9.

Important features evident in the upper story acceleration time histories (Figures 1.6c through l) are obvious from visual inspection of the records, did not require analysis to arrive at these observations, have been noted by Rojahn and Ragsdale (1980) and are included below for interest:

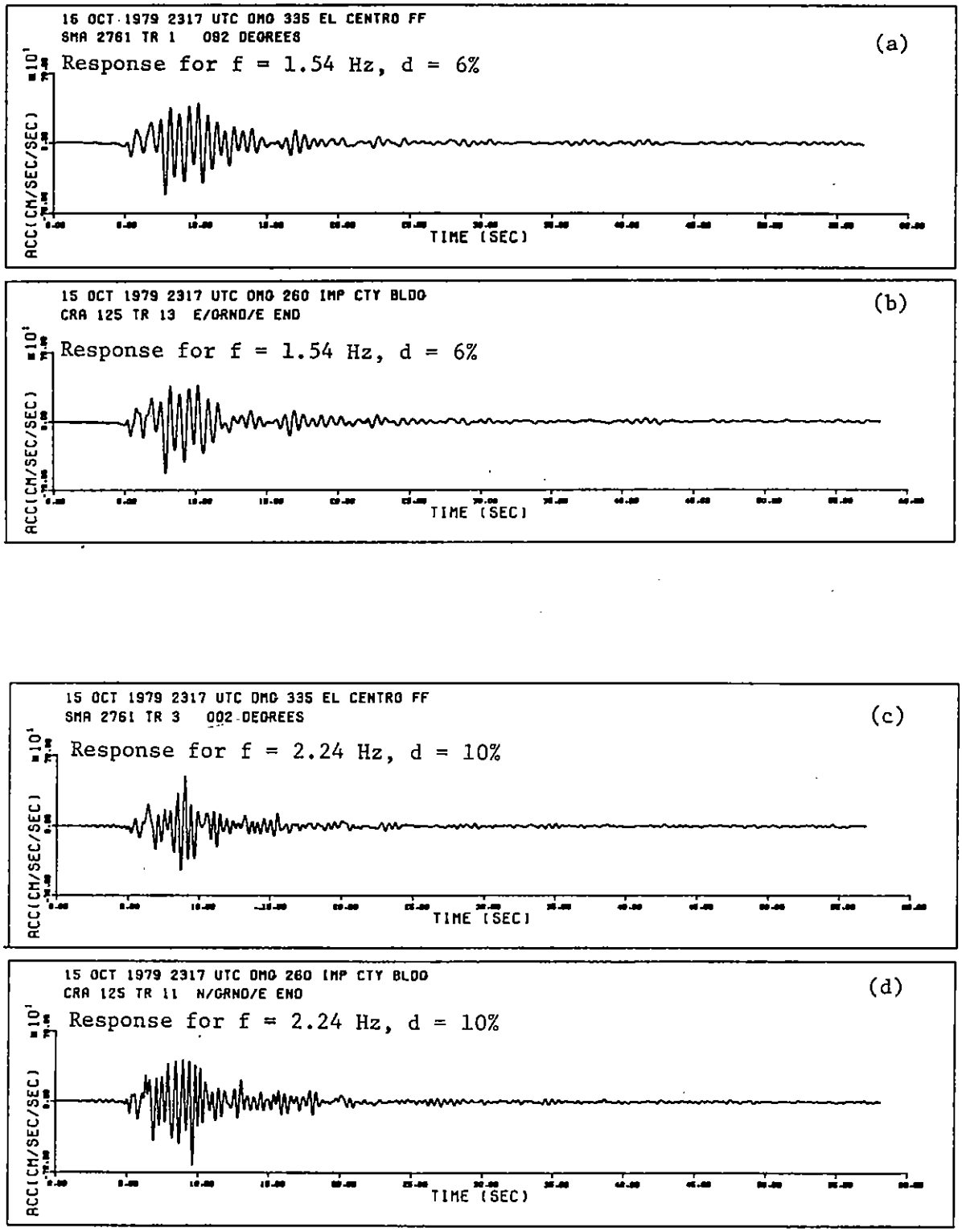

FIGURE 2.1 Response of a Single Degree of Freedom Oscillator to the Ground Motion from the Imperial Valley Earthquake of October 15, 1979

- The abrupt occurrence of long period motion in all E-W direction upper story records at second 6.8.
- Clusters of low amplitude, high frequency components at various times in all upper story traces at and after second 6.8.
- A 0.5 second long cluster of high amplitude, high frequency (50 Hz) motion (visible only in the original, unprocessed record) near second 11 in the N/2/E component directly above the east end column line that failed.

2.3 Relative Velocity and Relative Displacement Time Histories

Using the records at the base, second, fourth and roof levels, the relative velocity and relative displacement time histories are computed. If the relative displacements obtained numerically from the corrected accelerations are accurate, then the relative displacements can be used to trace the building motion with time. A comment about the use of relative displacements in this study, however, is pertinent. It is well-known that the absolute displacements obtained from acceleration records are highly dependent on the data treatment used, and particularly, on the cut-off frequency at the lower end. Relative displacements were also found in this study to be dependent on the filter characteristics: differences in amplitudes up to 40% were observed, but the geometry of deformation remained unchanged. However, for this study, we assume that the techniques used by CDMG to compute the absolute displacements are "state-of-the-art" in data processing. If the current processing methods are reviewed in the future, though, the relative displacements and conclusions discussed below may be subjected to additional adjustments.

The relative velocity and relative displacement time histories for the upper story locations are computed by subtracting the absolute velocity (or displacement) time history at the base of the building for the corresponding absolute velocity (or displacement) time history at the upper level of interest. The relative velocity and displacement time histories are shown in Figures 2.2 and 2.3, respectively. The maximum values and times of occurrence are listed in Table 2.1 and plotted in Figure 2.4. Because the relative displacement time histories are used extensively in the remainder of this section to trace the building motion, these time histories are magnified between 5 and 12 seconds in Figure 2.5. Between 5 and 12 seconds all components experienced about 5 to 7 cycles of large amplitude displacements. As an aid for later use in this section, the peak relative displacements at the second floor at key times within this timespan are summarized in Figure 2.6.

The relative displacements are used below to recreate the building motion in elevation and plan views between 5 and 13 seconds. Such a portrayal of the building vibration facilitates a better understanding of the actual response and enables the approximate times of initiation of yielding and collapse of the ground level east end columns to be determined. After presenting the elevation and plan views of the building motion, an interpretation of the response follows. However, it should be noted that the times of yielding and failure can theoretically be identified in the frequency domain as the times when the frequency characteristics change. Because the building response was highly nonstationary and nonlinear, it was not possible, though, to determine the exact times of yielding and collapse using the method of analysis chosen in Chapter 3.

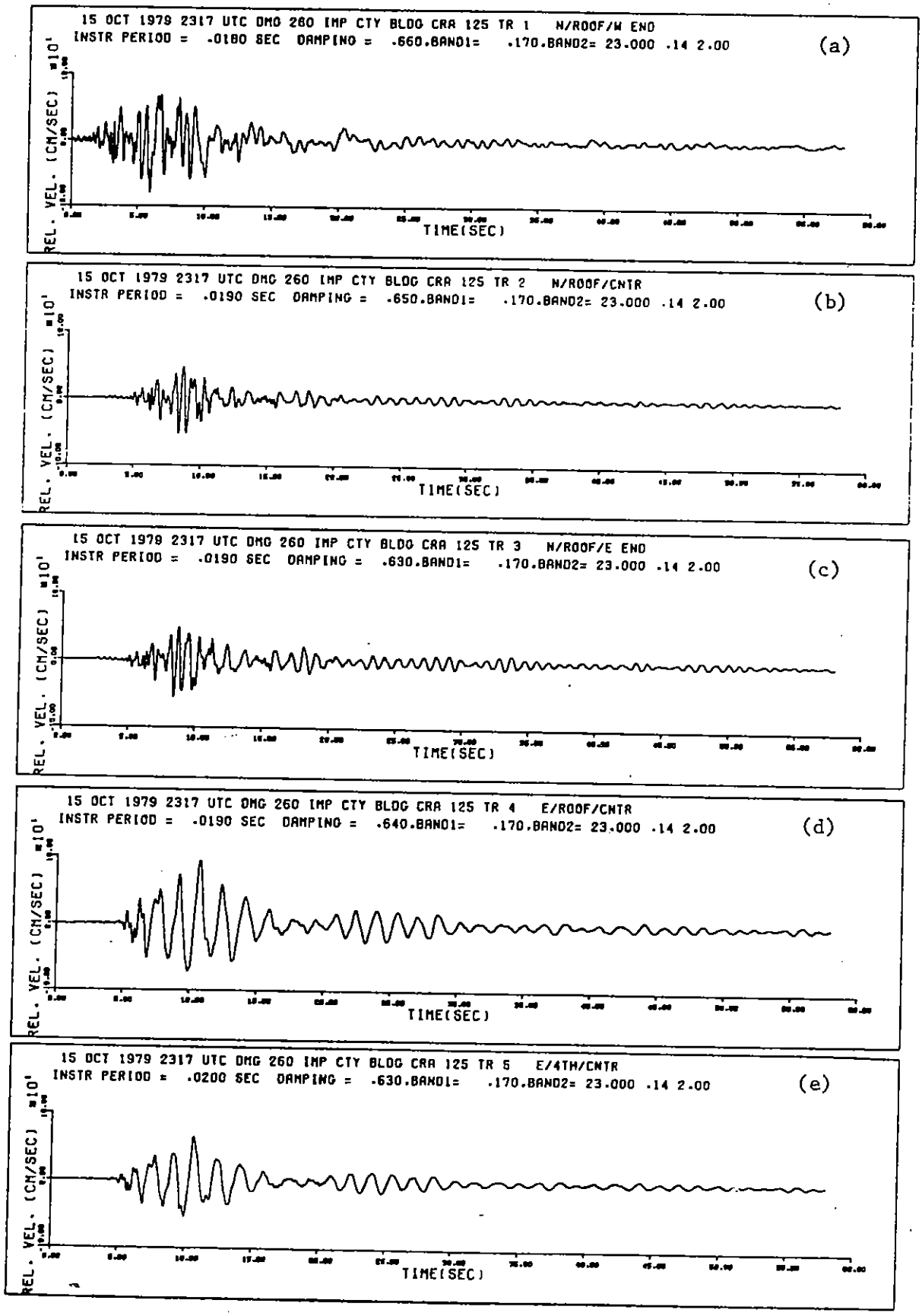

FIGURE 2.2 Relative Velocity Time Histories from the Imperial Valley Earthquake of October 15, 1979

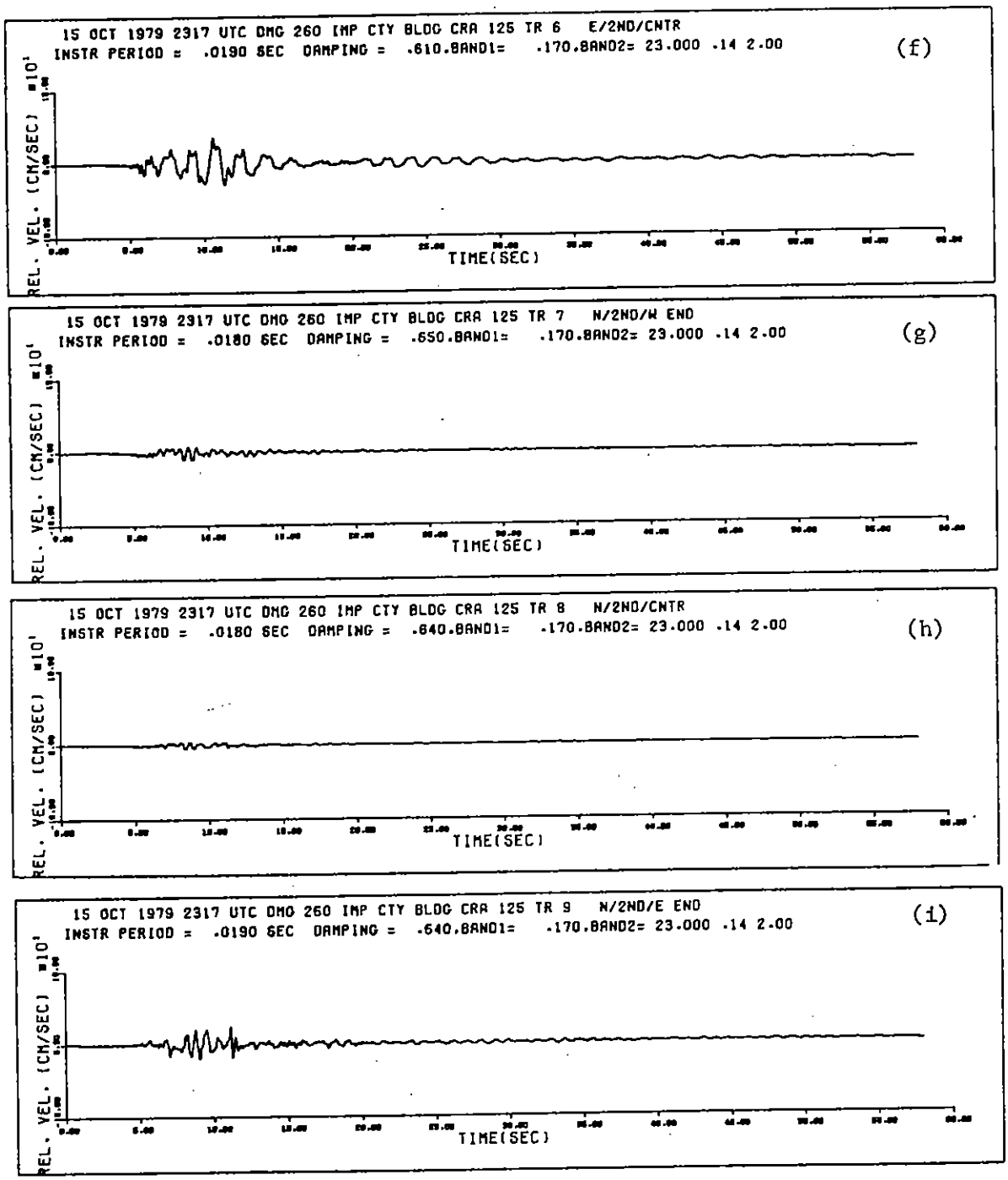

FIGURE 2.2 (cont'd) Relative Velocity Time Histories from the Imperial Valley Earthquake of October 15, 1979

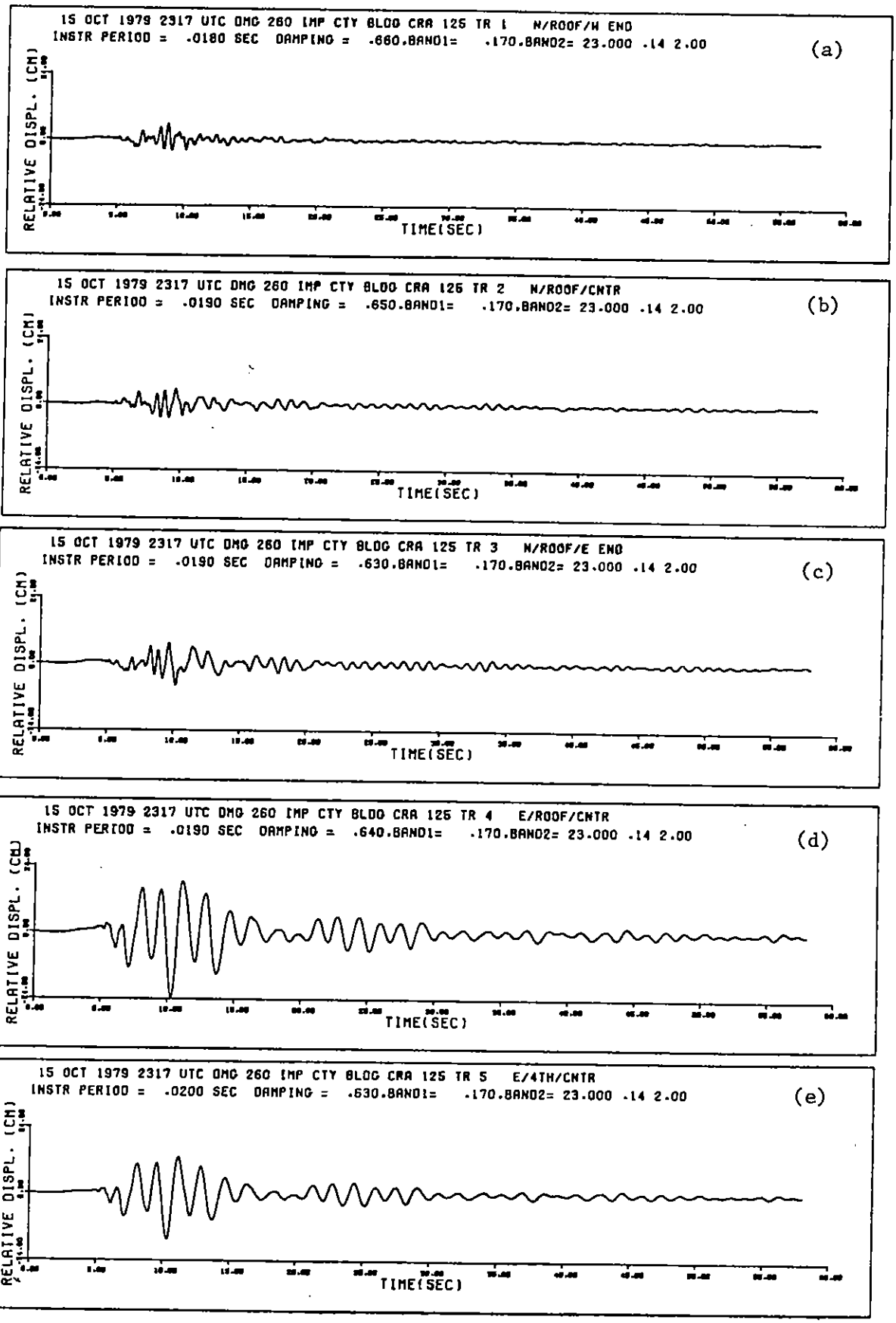

FIGURE 2.3 Relative Displacement Time Histories from the Imperial Valley Earthquake of October 15, 1979

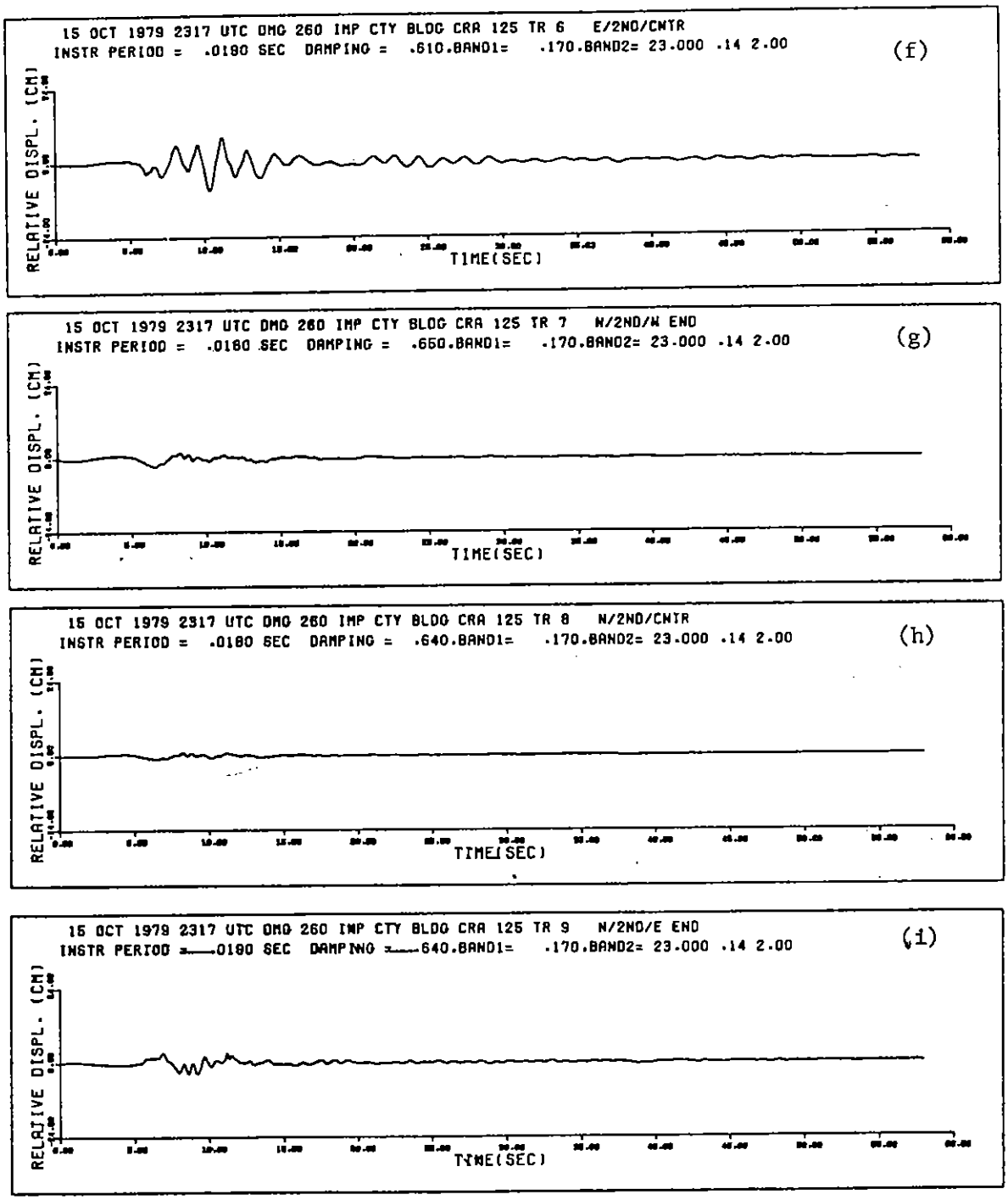

FIGURE 2.3 (cont'd) Relative Displacement Time Histories from the Imperial Valley Earthquake of October 15, 1979

TABLE 2.1 SUMMARY OF MAXIMUM RELATIVE VELOCITIES AND RELATIVE DISPLACEMENTS AND TIMES OF OCCURRENCE

Component	Maximum Relative Velocity (cm/sec)	Time of Occurrence (sec)	Maximum Relative Displacement (cm)	Time of Occurrence (sec)
N/R/W	54.14	8.94	5.62	8.83
N/R/E	56.27	8.44	7.93	10.17
N/2/W	10.78	9.00	2.65	6.58
N/2/E	24.59	11.13	3.44	9.22
E/R/C	95.51	10.74	23.58	10.31
E/4/C	65.61	10.64	16.47	10.32
E/2/C	36.33	10.62	8.90	10.34

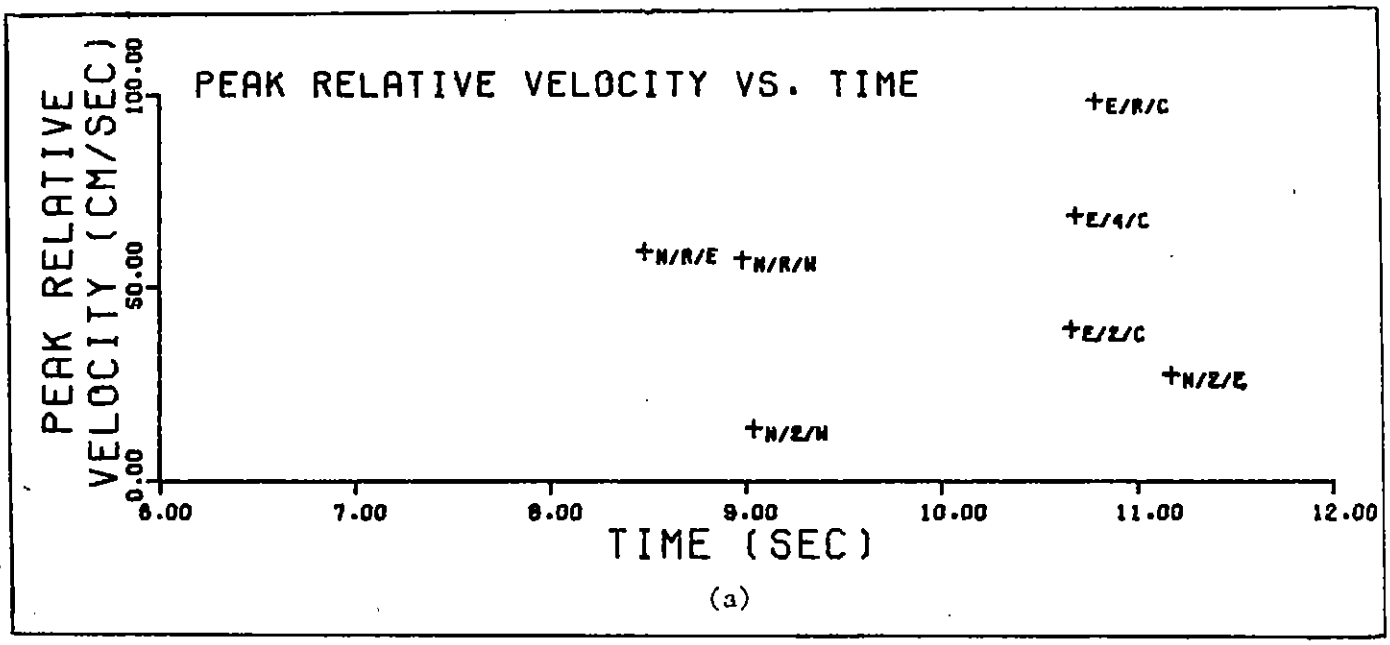

(a)

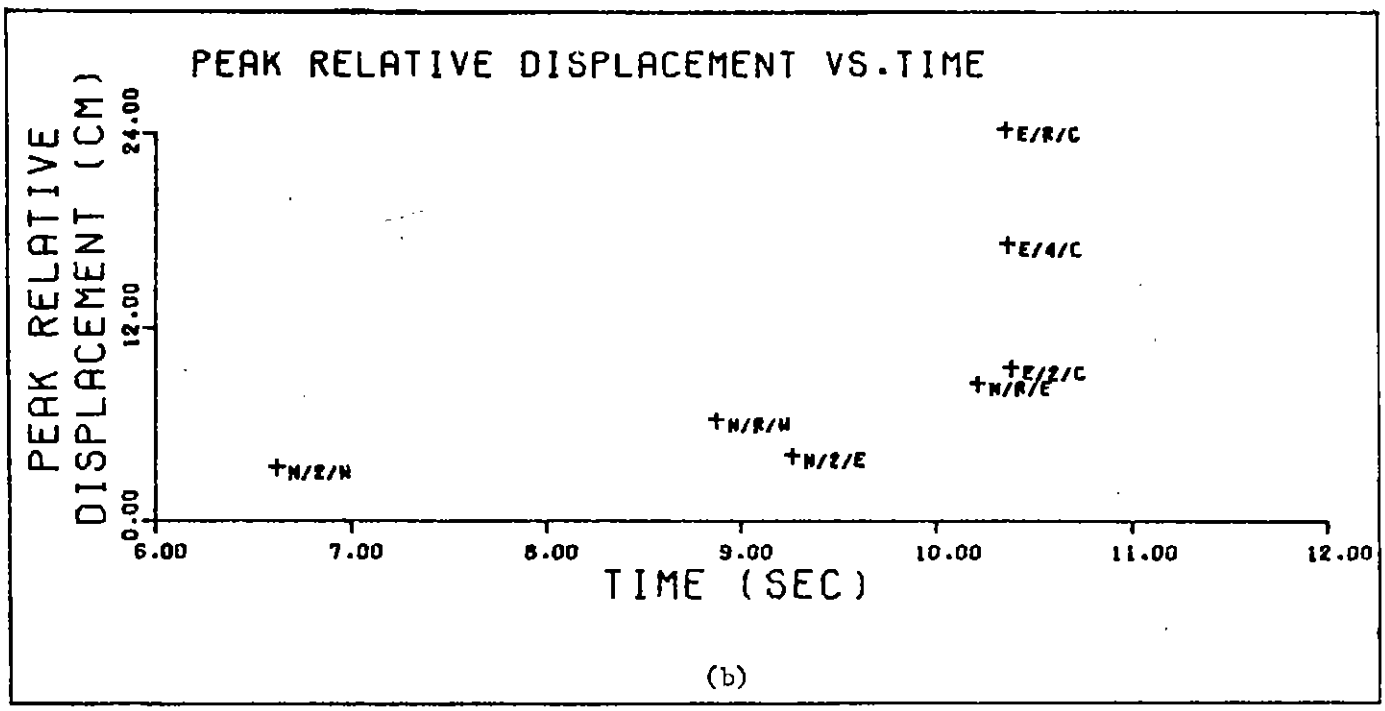

(b)

FIGURE 2.4 (a) Peak Relative Velocity vs. Time
(b) Peak Relative Displacement vs. Time

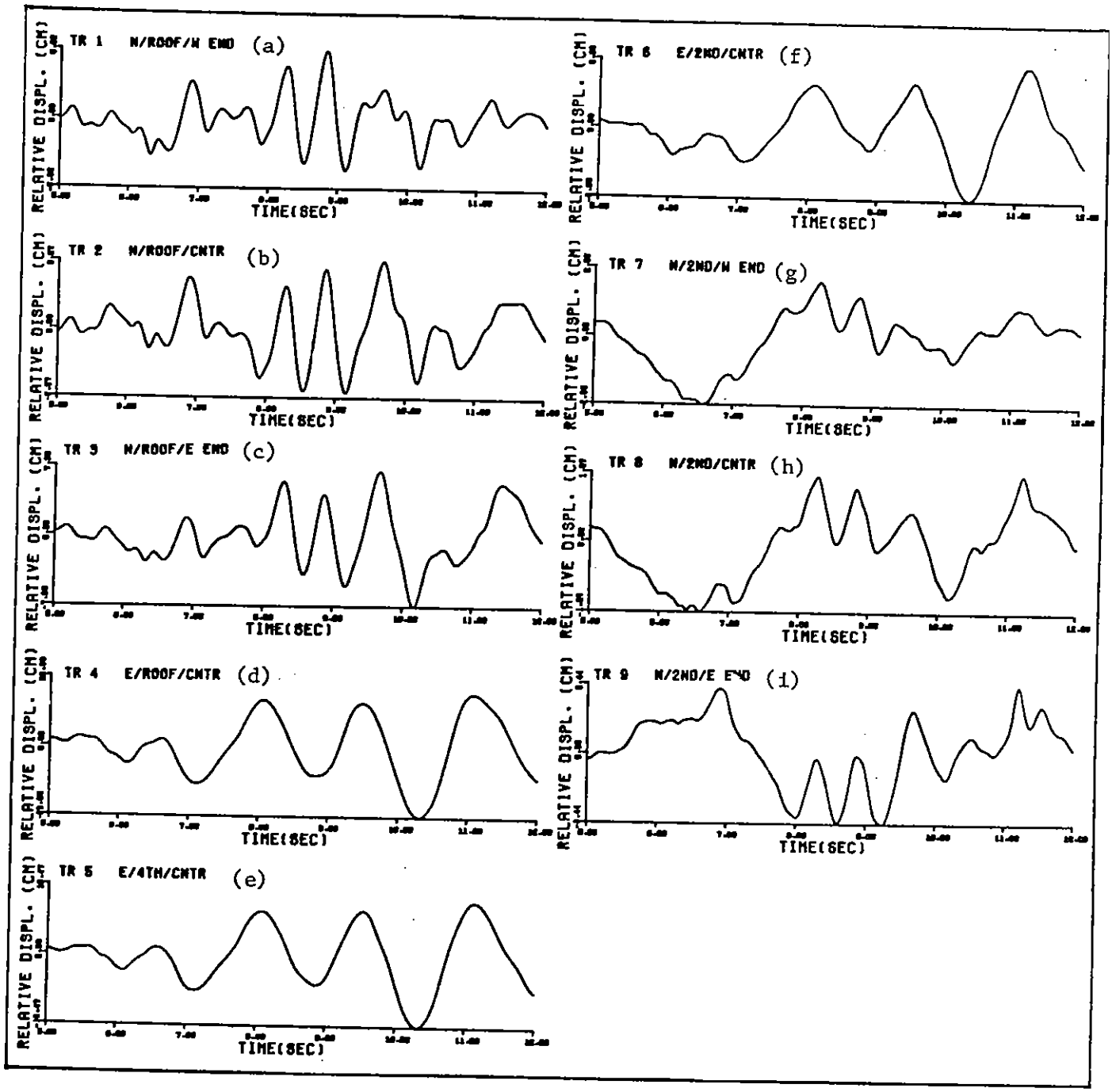

FIGURE 2.5 Relative Displacement Time Histories Between 5 and 12 Seconds during the Imperial Valley Earthquake of October 15, 1979 (Each Time History is Scaled to the Peak Value Listed in Table 2.1)

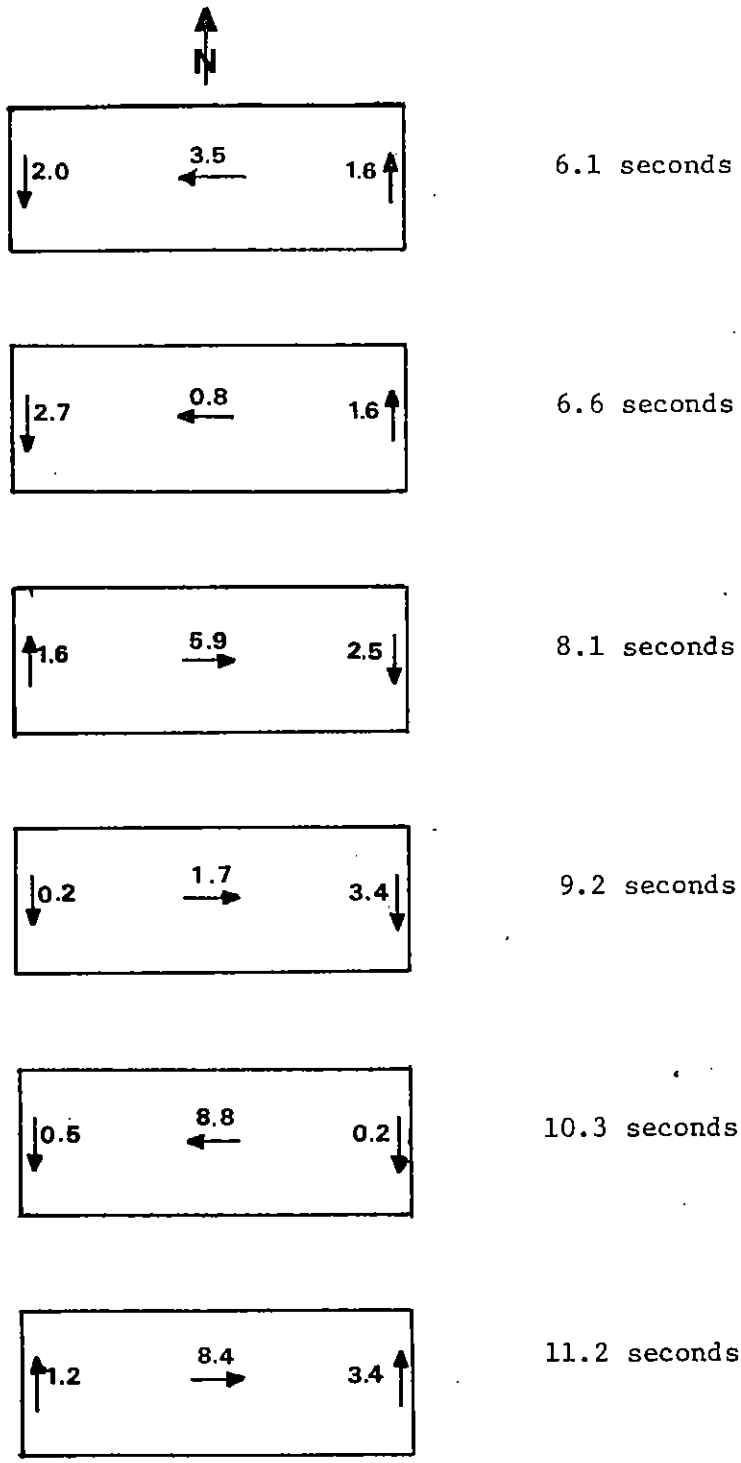

FIGURE 2.6 Maximum Relative Displacements (Cm) at Second Floor Level Between 6 and 12 Seconds

In the N-S direction, the building motion in elevation view is plotted between 5 and 13 seconds at the east and west ends in Figure 2.7 from the relative displacements at the second and roof levels. The relative displacement at the base of the building is assumed to be zero. Between the ground, second and roof levels, the motion is assumed to follow a straight line. This is a reasonable assumption for the east and west shear wall ends between the second and roof levels. Similarly, in the E-W direction, the motion in elevation view is plotted between 5 and 13 seconds in Figure 2.8 based on the computed relative displacements at the base (assumed to be zero), second, fourth and roof levels. Straight line motion is also assumed between these levels since the response at the other intermediate floor levels was not recorded.

The evolution of the building motion in plan view between 5 and 13 seconds is illustrated in Figures 2.9, 2.10 and 2.11 to show the translational and torsional vibrations as well as in-plane floor vibrations at the base, second floor and roof, respectively. Linear motion is assumed between all points of known relative displacements. For illustration purposes, the building dimensions are disproportionately reduced in order to magnify the relative displacements and visually see the motion.

The horizontal vibration shown in Figures 2.5 through 2.11 is now interpreted at key times. It should be noted that because no vertical component of acceleration was recorded at the upper building levels, the influence of the vertical displacement component could not be included in the following discussion.

Between 0 and 6 seconds, the response was linear and the building began to vibrate in modes higher than the fundamental mode. In the N-S

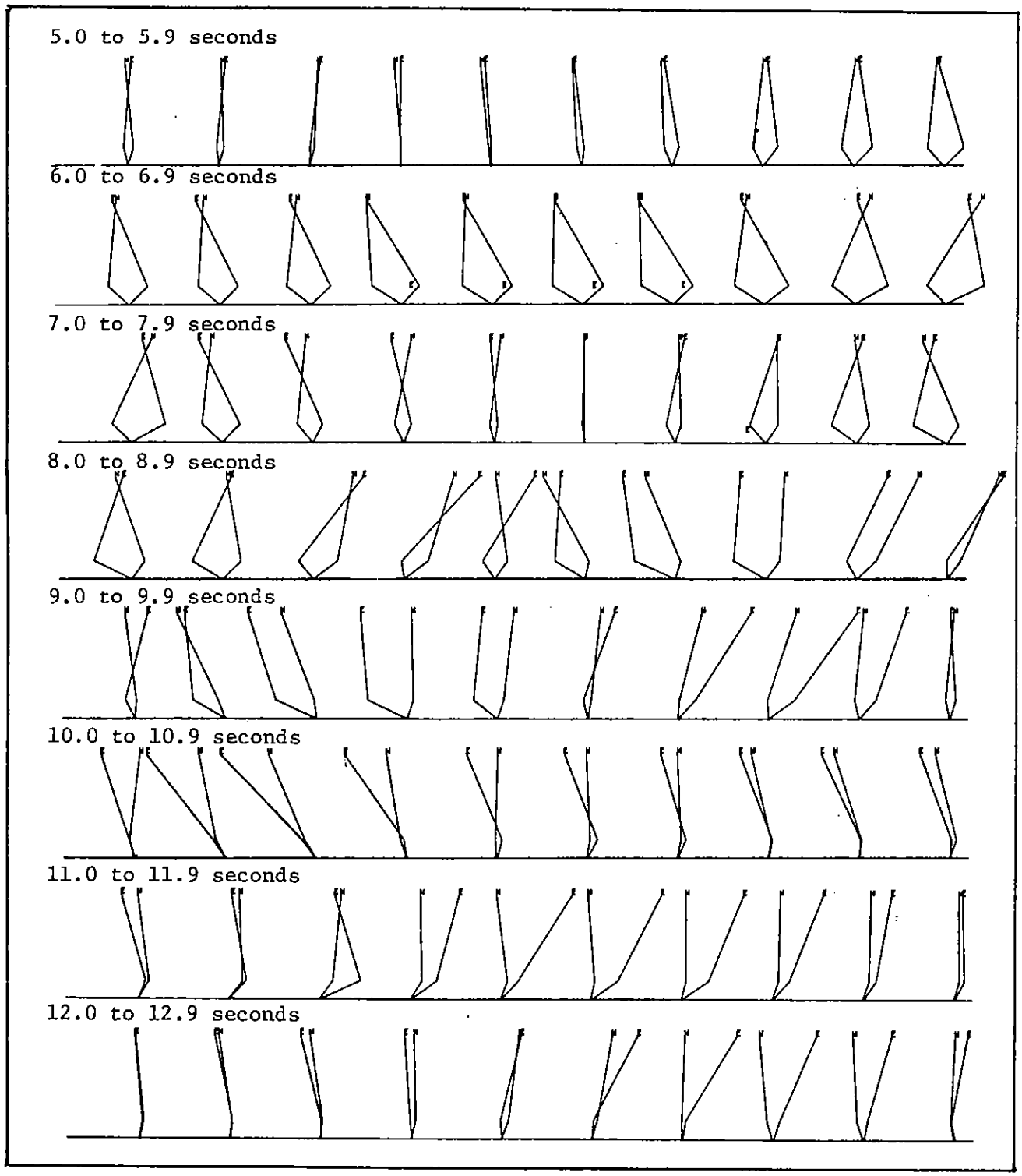

FIGURE 2.7 Elevation View of Building Motion, North-South Direction, East(E) and West(W) Ends, Between 5 and 13 Seconds at 0.1 Second Intervals

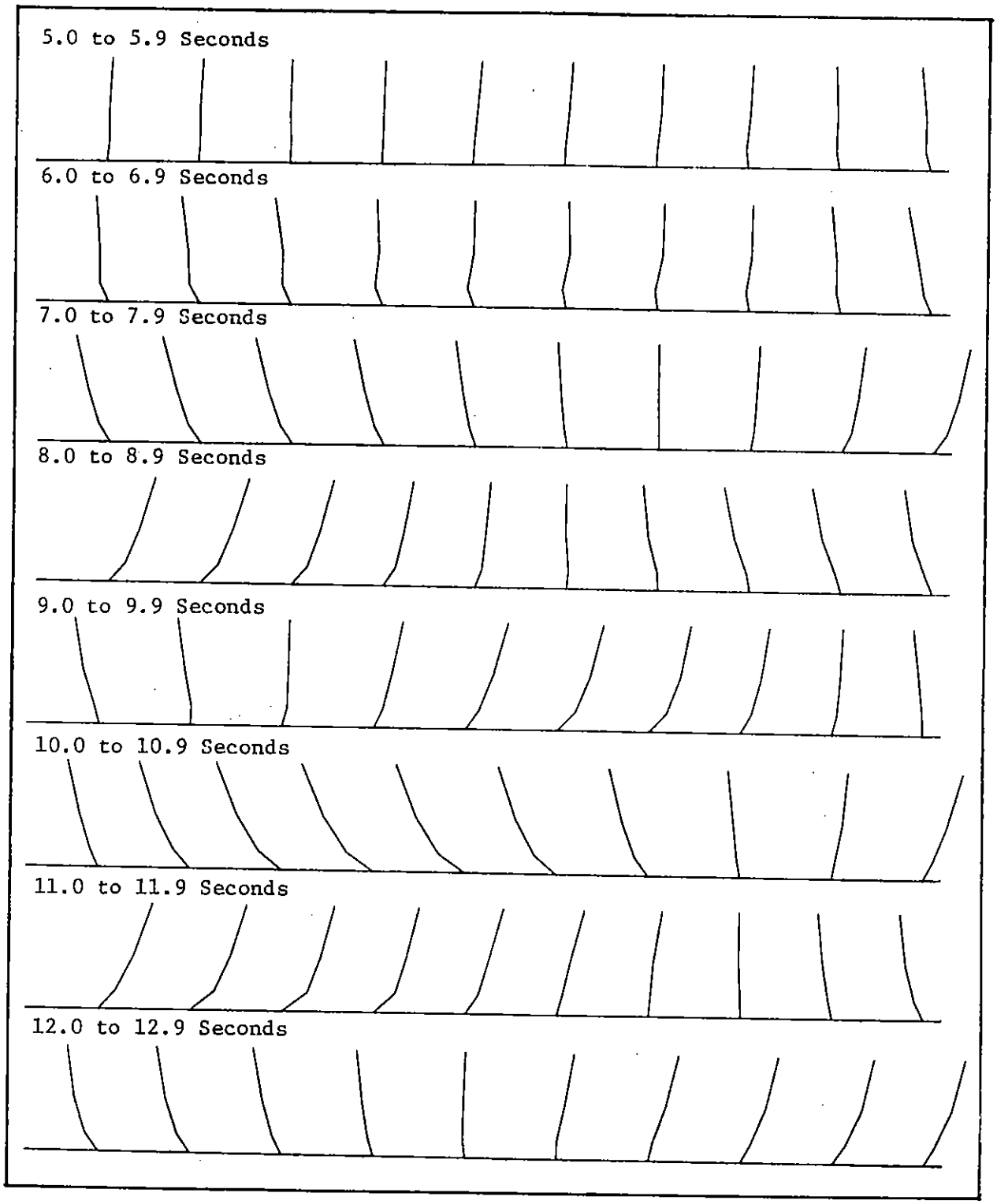

FIGURE 2.8 Elevation View of Building Motion, East-West Direction, Between 5 and 13 Seconds at 0.1 Second Intervals

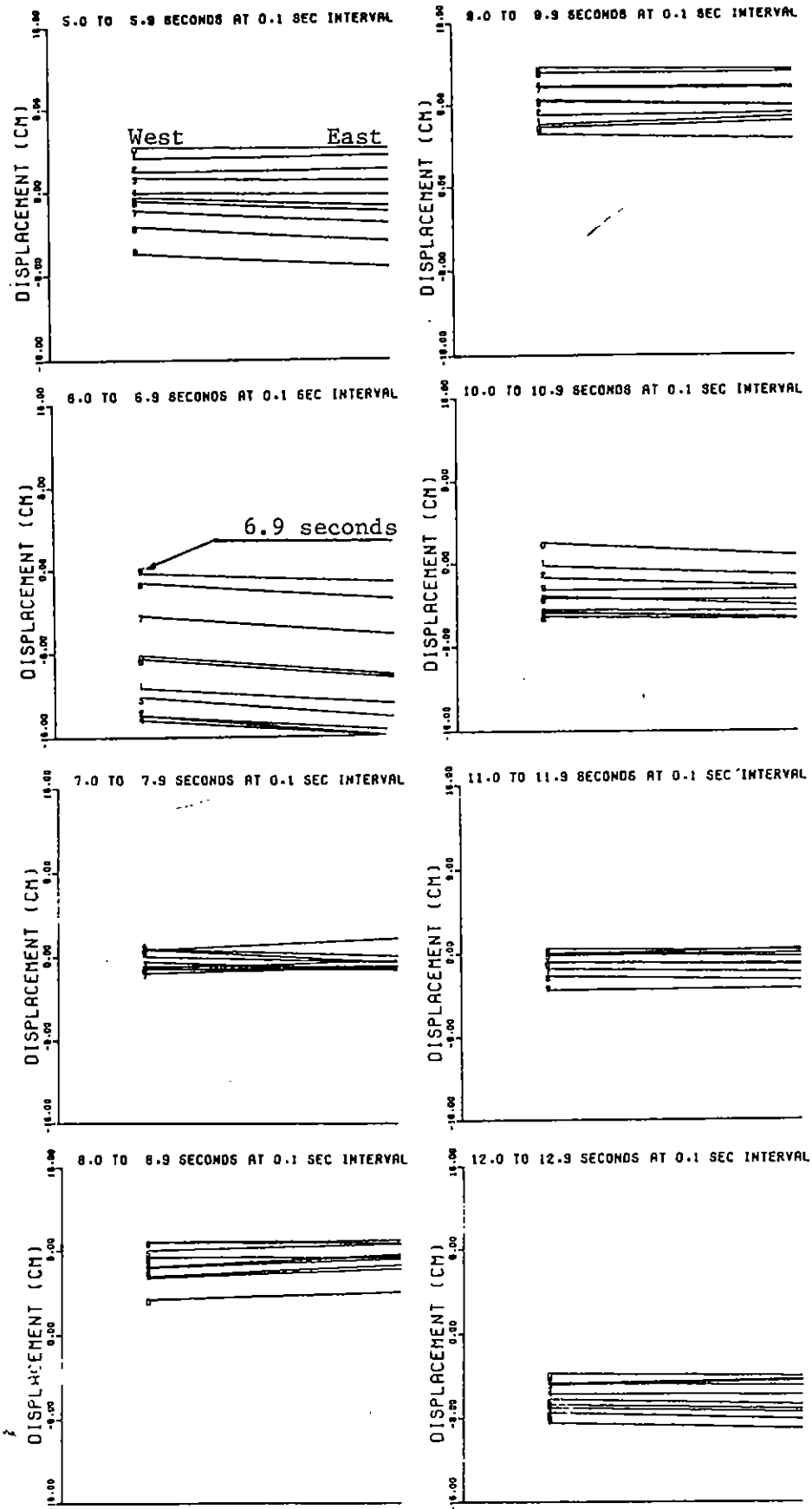

FIGURE 2.9 Plan View of N-S Motion at Base of Building Between 5 and 13 Seconds at 0.1 Second Intervals

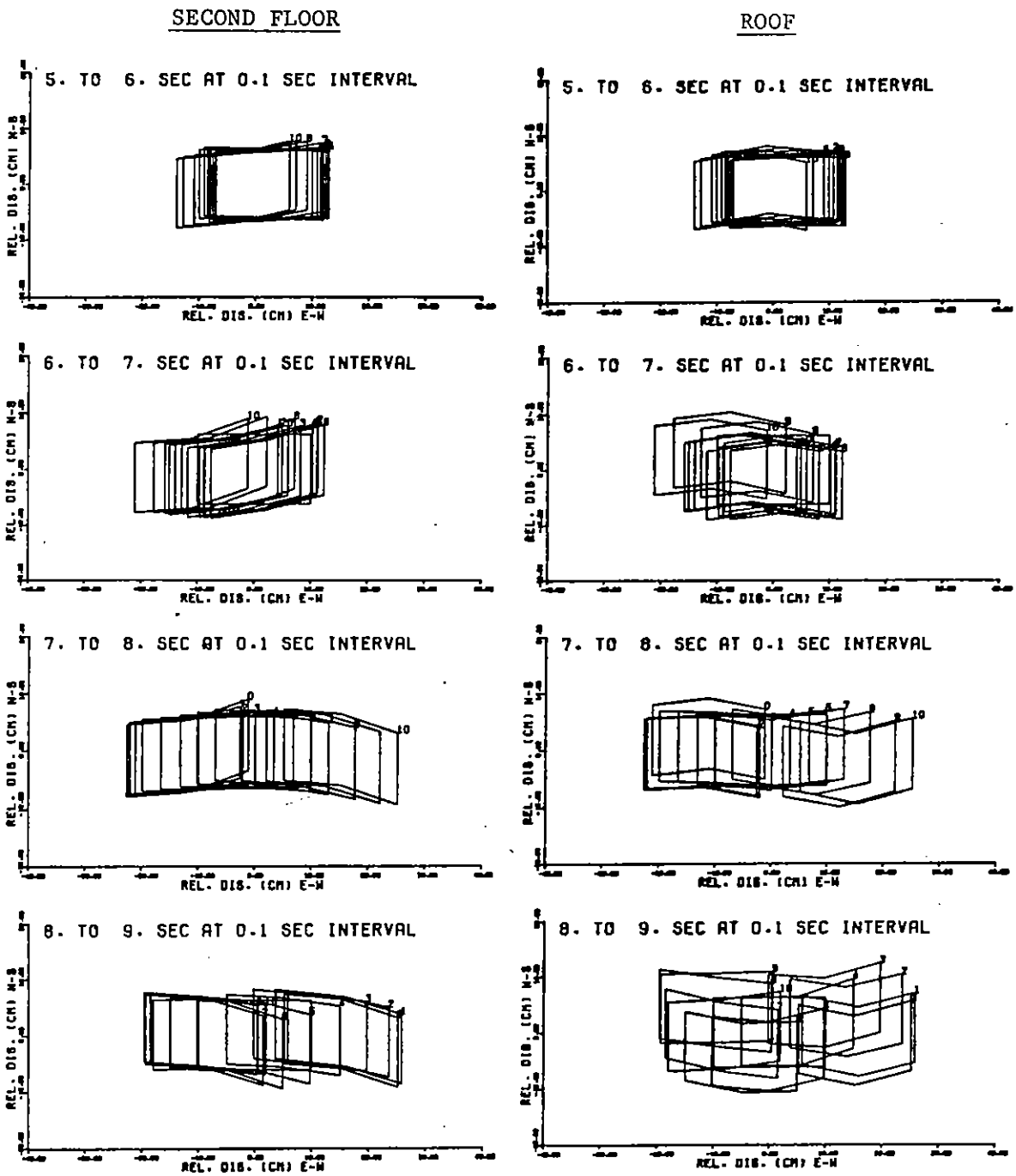

FIGURE 2.10 Plan View of Second Floor and Roof Motion Between 5 and 9 Seconds at 0.1 Second Intervals
X-Axis Range: -40.0 cm to 40.0 cm
Y-Axis Range: -20.0 cm to 20.0 cm

SECOND FLOOR

ROOF

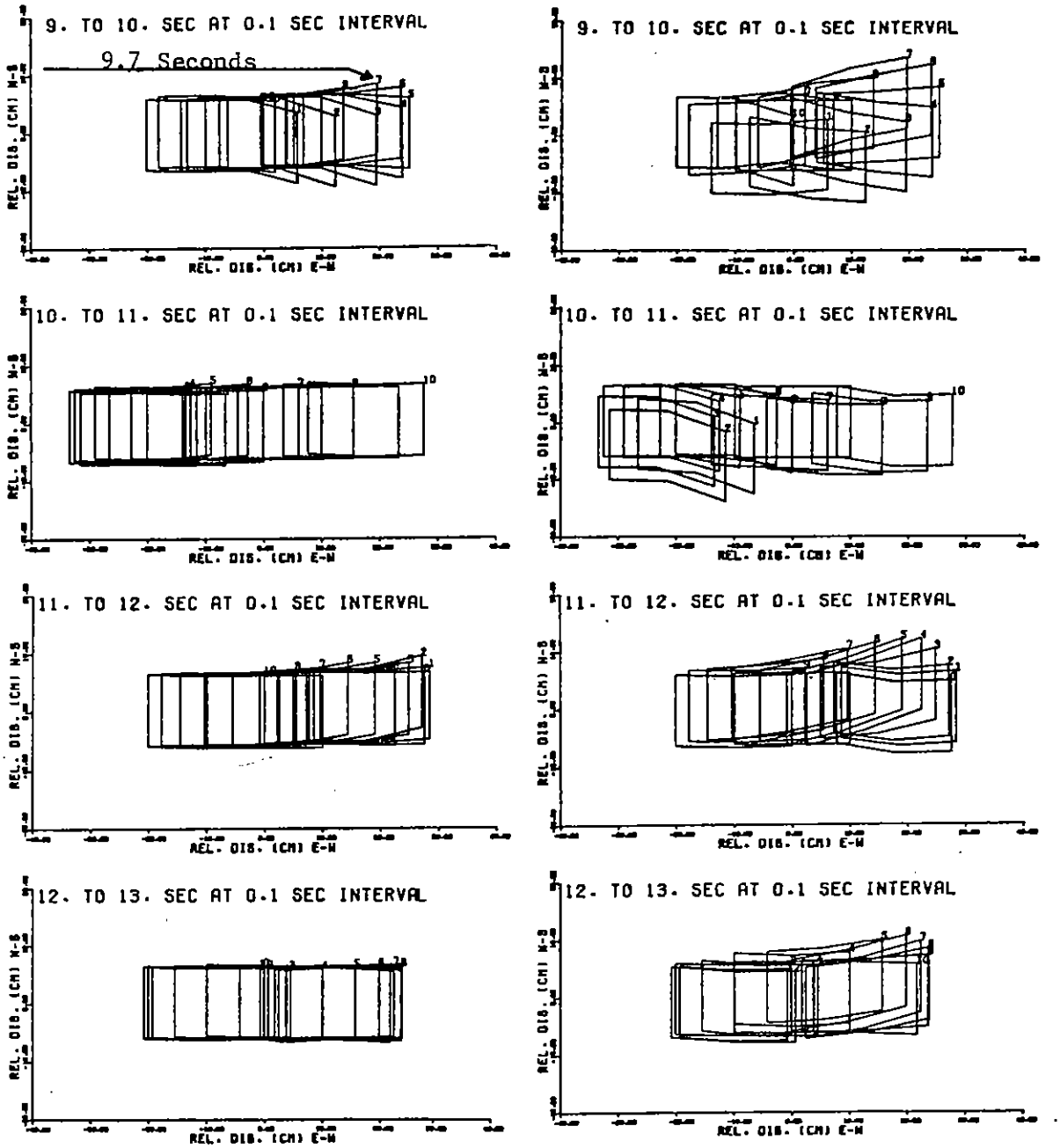

FIGURE 2.11 Plan View of Second Floor and Roof Motion Between 9 and 13 Seconds at 0.1 Second Intervals
X-Axis Range: -40.0 cm to 40.0 cm
Y-Axis Range; -20.0 cm to 20.0 cm

direction, the second torsional mode was indicated. (This mode prevailed during most of the strong motion as well.) As an illustration, the second torsional mode was evident at 5.0 seconds in Figure 2.7 because 1) at both the east and west (shear wall) ends, the motion at the second floor was out of phase with the motion at the roof (see also Figure 2.10) and 2) in elevation view, the east and west ends were out of phase with each other. This torsional mode was influenced by the discontinuity of the exterior shear walls at the first story level and by the slight eccentricity in plan at the first story. At the base of the building, though, Figure 2.9 shows that initially in the N-S direction (and during the strong motion also), the east and west end base motions were mostly in phase (no rotation). Finally, in the E-W direction, the building also started to vibrate in higher modes of vibration as can be seen between 5 and 6 seconds in Figure 2.8.

Yielding may have been initiated in all first story columns between 6 and 7 seconds. At the second floor during this time, the E/2/C frame component, (Figure 2.5f) experienced displacements of about 4 cm coupled with long duration (> 1 second) displacement pulses of about 2 to 3 cm evident in the N/2/W (Figure 2.5g) and N/2/E (Figure 2.5i) components. Also, the building continued to vibrate in the second torsional mode. It is hypothesized therefore, that the second torsional mode configuration combined with the first large N-S second story displacements caused rotation of the upper level exterior shear walls which in turn imposed the first large axial loads on the east and west end columns. These axial loads, coupled with the resulting P-Δ effect from the E-W frame motion, initiated yielding in these columns.

Between 7 and 13 seconds, the second torsional mode still prevailed in the N-S direction, (Figures 2.7, 2.10 and 2.11), but now the first mode was emerging in the E-W direction, (Figure 2.8). Around 11.2 seconds,

in both the N-S (east end) and E-W directions at the second floor, the near maximum relative displacements were simultaneously obtained. (See Table 2.1 and Figures 2.5 and 2.6). This may be the time of collapse of the east end columns. The east and west end elevation configurations in the N-S direction shown at 11.2 seconds in Figure 2.7 may explain why the east end columns failed but the west end columns did not. At this time, observe that at the east end, the second floor was out of phase with the roof. This motion was similar to the motion between 6 and 7 seconds but now the displacements were 2-3 times larger. The resulting shear wall rotation and imposed axial column loads, combined with the P-Δ effect from the E-W frame direction, may have caused collapse. Around 11.2 seconds at the east end, the N-S relative displacement was 2 to 3 times larger than at the west end. The smaller displacements at the west end may have been due to the presence of a single bay shear wall along the west end ground level column line (column line G in Figure 1.2b). Because the second floor was in phase with the roof at the west end, however, there was no rotation of the shear wall and hence the axial loads on the west end columns due to loads from N-S motion were smaller than at the east end.

From the above discussion, it is therefore hypothesized that the building started to vibrate in higher modes. Yielding of the ground level columns may have initiated between 6 and 7 seconds. Collapse of the east end columns occurred at about 11.2 seconds. The large column loads, especially at the east end, may have resulted from the axial loads due to the rotation of the upper shear walls in the N-S direction and from the P-Δ effect due to the E-W frame motion. In Chapter 3, the frequency content will be quantified.

The apparent deformation of the diaphragm at the second floor and roof level seen in Figures 2.10 and 2.11 was due to the difference in the

stiffness between the first and upper stories. The second floor and roof diaphragms may each act as a "simply supported" beam whose supports are the rigid shear walls at the east and west ends of the building. The maximum relative deformations at the center of the second floor and the roof were approximately 1.5 cm and 2.0 cm, respectively. Such deformation may be significant, since diaphragms are usually considered to be rigid bodies in current design practice. The shear walls, however, may also deform but the magnitude cannot be assessed from the given records. No great distress was apparent in the diaphragms since only small cracks were visible.

As a final note of interest, the particle motion between 5 and 13 seconds at the base of the building, second floor, and roof is plotted in Figures 2.12, 2.13 and 2.14, respectively. The horizontal components show that the motion was more pronounced in the E-W direction due to the greater flexibility in that direction.

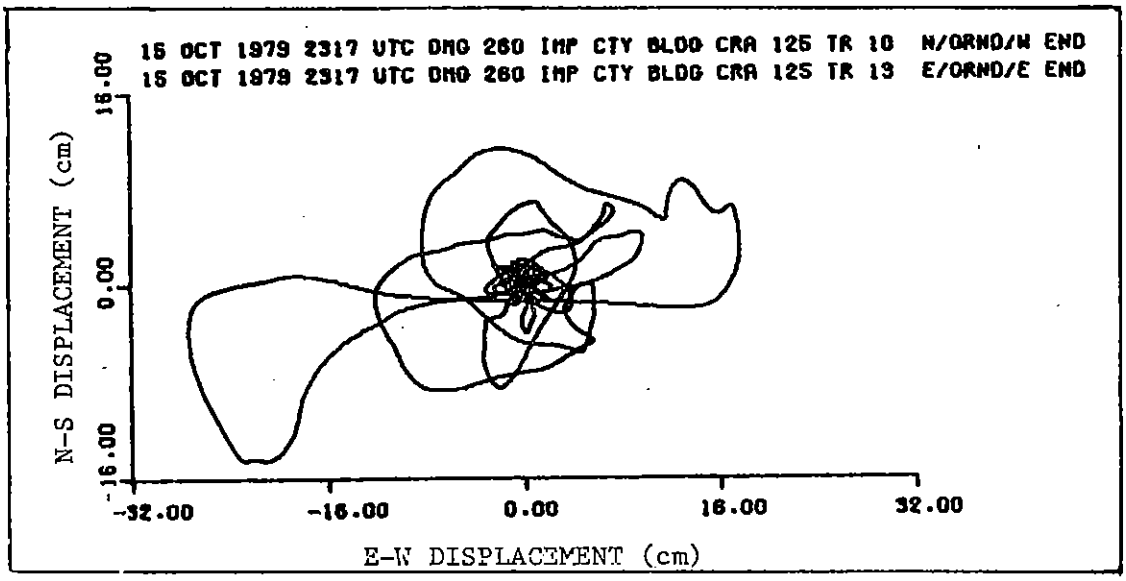

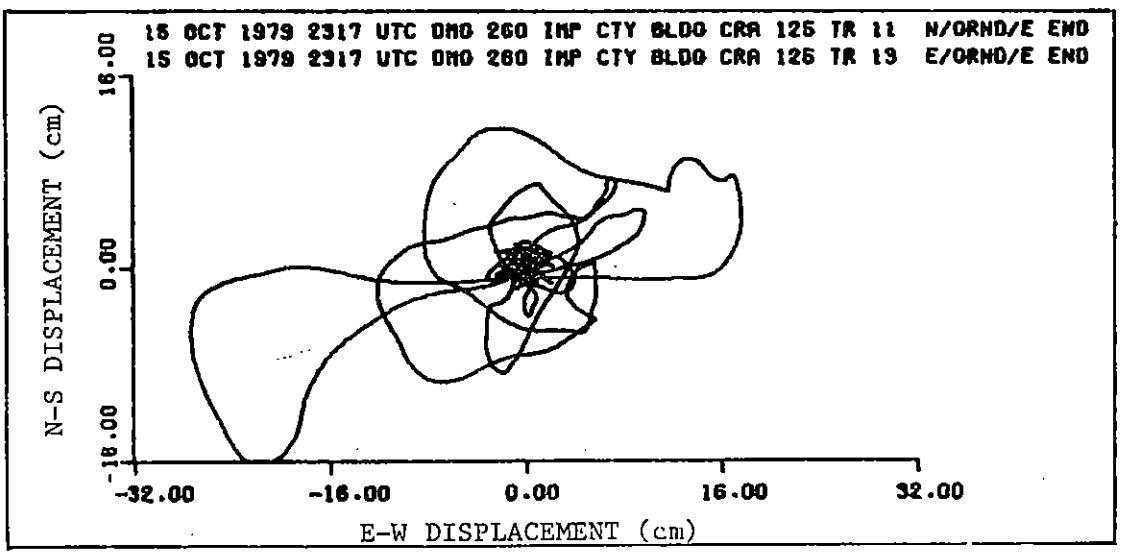

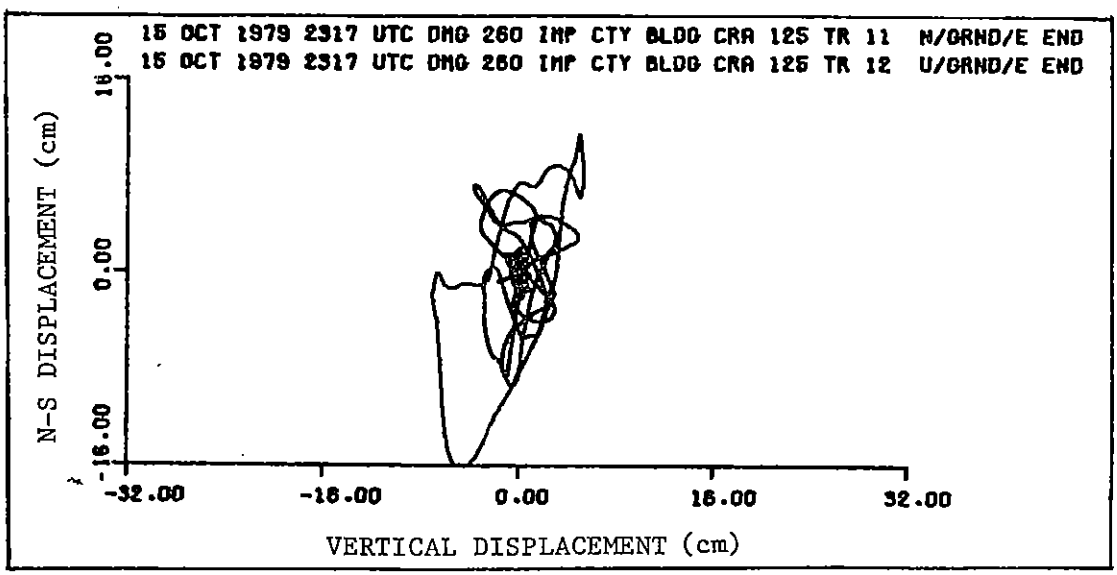

FIGURE 2.12 Directivity of Particle Motion at Base of Building Between 5 and 13 Seconds

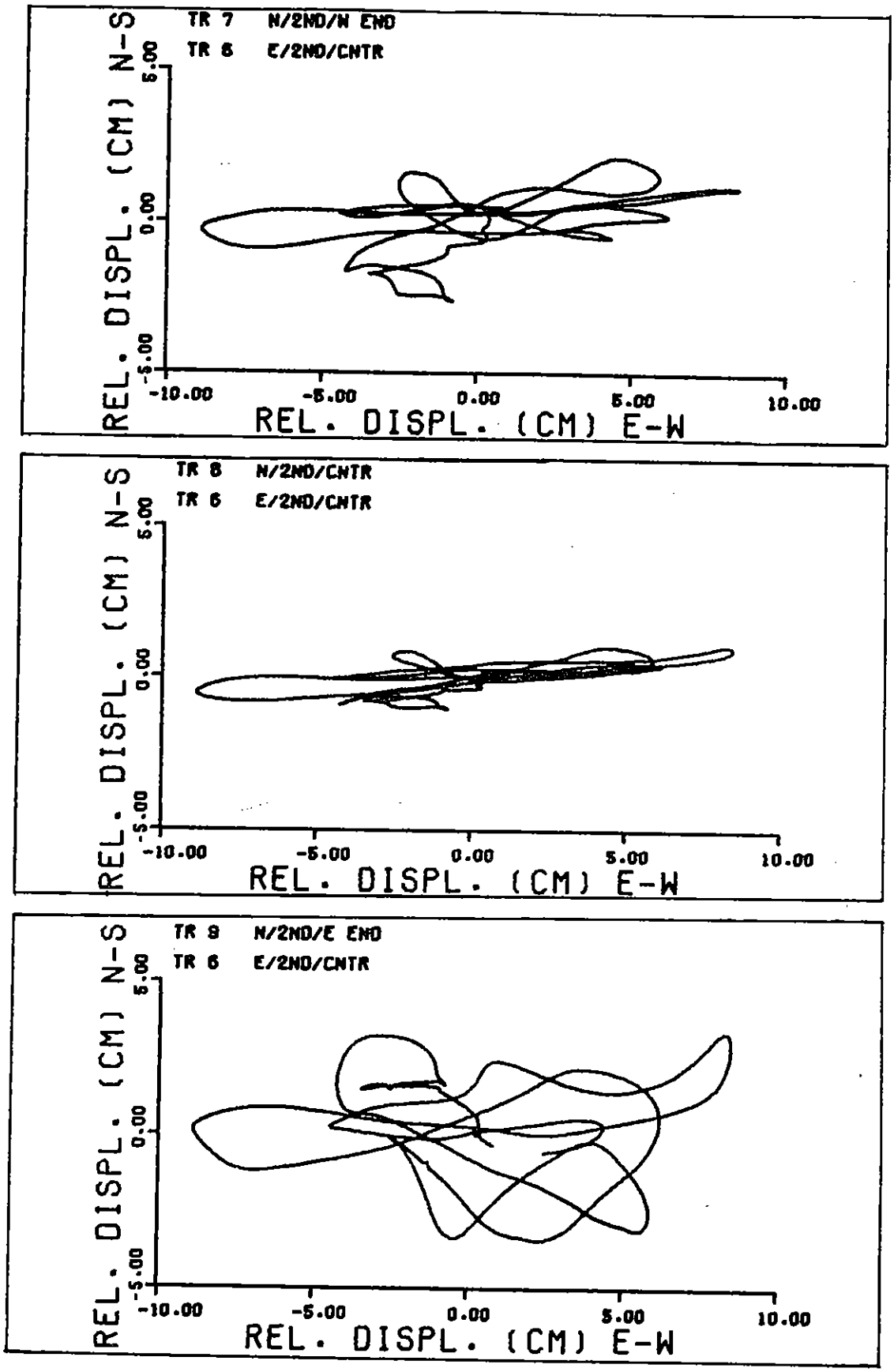

FIGURE 2.13 Directivity of Particle Motion at Second Floor Between 5 and 13 Seconds

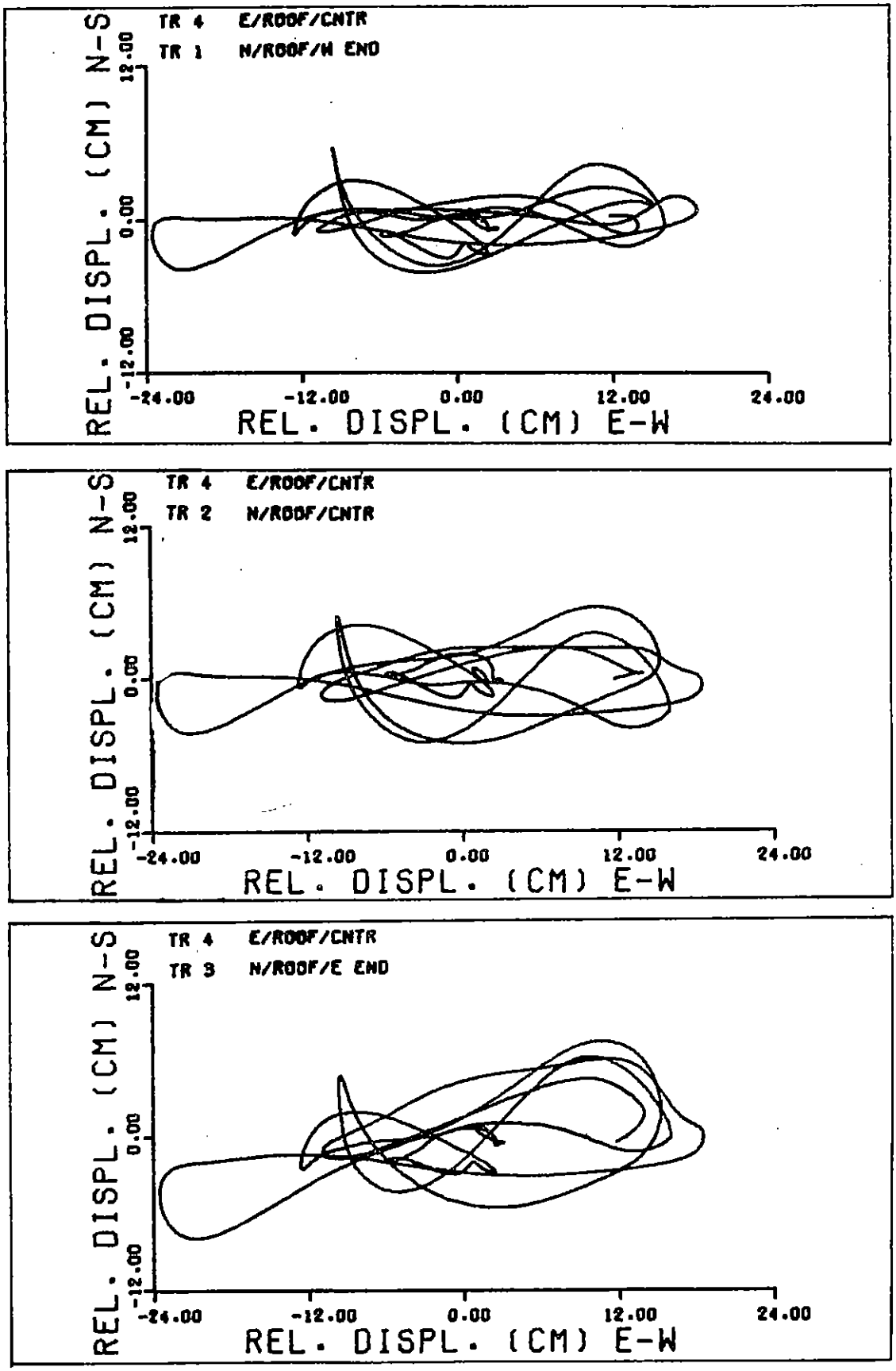

FIGURE 2.14 Directivity of Particle Motion at Roof Between 5 and 13 Seconds

CHAPTER 3: FREQUENCY DOMAIN ANALYSIS

3.1 Introduction

The time domain analysis in Chapter 2 showed that the building not only responded nonlinearly with column yielding initiating between 6 & 7 seconds and east end ground level column collapse occurring near 11.2 seconds but also that the building vibration contained frequencies higher than the fundamental coupled with torsion. Hence, the purpose of this chapter is to quantitatively assess the frequency content. For a linear system subjected to an input motion, the frequency response can be determined from the Fourier amplitude spectra and the transfer functions using the entire record. For nonlinear response, as evidenced in the building, linear methods of analysis and the concept of modes are not rigorously applicable. However, the above linear techniques can be adapted, using moving window time analysis, to trace the time variation of the frequency content of the Imperial County Services Building. Moving window techniques have been used successfully in the past for buildings (Millikan Library, JPL Engineering Building 180) which responded only slightly nonlinearly (Udwadia and Trifunac, 1974; Udwadia and Marmelis, 1976). Because the response of the Imperial County Services Building was highly nonstationary and nonlinear, modal identification using this technique in the range between initiation of yielding and column collapse was very difficult to assess. More elaborate methods of system identification have recently been developed to determine the response of slightly nonlinear structures: McVerry (1979), Udwadia and Marmelis (1976), Beck (1978), and Kaya and McNiven (1978).

3.2 Theory of Moving Time Window Analysis

The principle of superposition allows the total response y(t) of a linear time invariant single degree of freedom system to be the summation of the individual responses to each impulse of the input x(t) occurring from time = $-\infty$ to time = t. In equation form the response y(t) is given as

$$y(t) = \int_{-\infty}^{t} h(t-\tau)\, x(\tau) d\tau \tag{3.1}$$

where $h(t-\tau)$ is the response of the system subjected to a unit impulse $x(\tau)$ of time $t = \tau$ and zero initial conditions are assumed. In the frequency domain for a linear system, the transfer function relates the Fourier transform of the input motion to the Fourier transform of the response. For a given time history z(t), the Fourier transform $Z(\omega)$ is defined as

$$Z(\omega) = \int_{-\infty}^{\infty} z(t) e^{-i\omega t}\, dt \tag{3.2}$$

If the Fourier transform of both sides of equation (3.1) is taken, then the response in the frequency domain becomes

$$Y(\omega) = H(\omega)\, X(\omega) \tag{3.3}$$

where $H(\omega)$ is the transfer function between the Fourier transform $X(\omega)$ of the input and the response Fourier transform $Y(\omega)$. Therefore $H(\omega)$ is computed as

$$H(\omega) = \frac{Y(\omega)}{X(\omega)} \tag{3.4}$$

Because the building responded nonlinearly, the principle of superposition and hence modal concepts are no longer valid in the range between the initiation of yielding and partial or total collapse. The above linear

theory, however can be adapted for nonlinear analysis using moving time window techniques to account for the time variation of the frequency content of the building. Such an approach assumes that the response during a limited time segment of the record can be determined by considering only that segment of the record. During each segment or time window of length T, the structure is assumed to respond as a linear time invariant system, i.e., the nonlinearities are small and the amplitudes and frequencies are slowly varying. With the center of the window located at time T/2, the Fourier transform of those segments of the input and output signals that lie within the time segment T are computed. The resulting Fourier amplitude spectrum or transfer function gives the frequencies in an average sense over that time interval at a time corresponding to the center of the time window.

For this earthquake, the window length T was chosen to be 5.12 seconds (512 points at 0.01 second intervals). The window length was narrow enough so that the system can be assumed to remain linear during the window but also long enough (sufficient number of points) so that meaningful frequency resolution was achieved. The window started at time zero and was moved (displaced) along the time axis by 1 second intervals.

Based on the available records, four different types of transfer functions have been computed for this building as illustrated in Figure 3.1: between the roof and building base, between the roof and free field, between the building base and free field, and between an intermediate story level and the free field. However, for frequency determination, the transfer functions used were those computed between all the building levels and the free field since the base of the building responded throughout the earthquake as if it were an upper story level as illustrated in Figure 3.2. Table 3.1 lists the

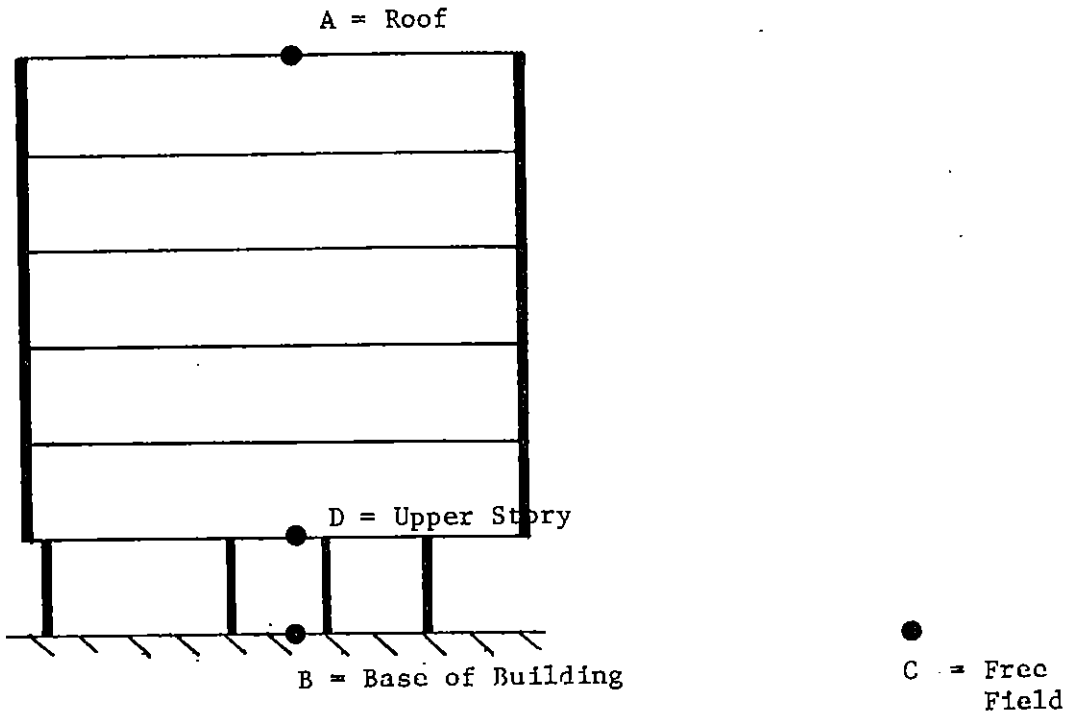

$|H_{AB}(\omega)|$ = Transfer function between the roof and the base of the building

$|H_{AC}(\omega)|$ = Transfer function between the roof and the free field

$|H_{BC}(\omega)|$ = Transfer function between the base of the building and the free field

$|H_{DC}(\omega)|$ = Transfer function between an upper story level and the free field

FIGURE 3.1 Location of Computed Transfer Functions $|H(\omega)| = |Y(\omega)/X(\omega)|$

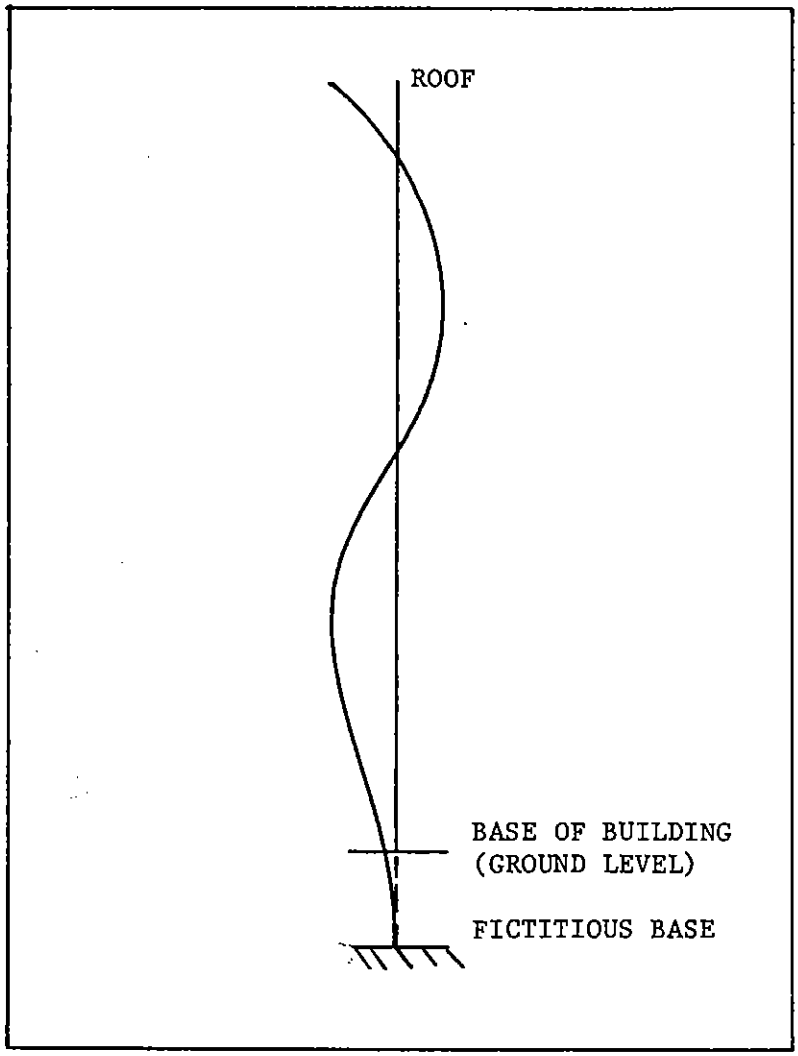

FIGURE 3.2 Base of Building Response in N-S and E-W Directions

TABLE 3.1 COMPUTED MOVING WINDOW FOURIER AMPLITUDE SPECTRA AND TRANSFER FUNCTIONS

Moving Window Fourier Amplitude Spectra	Figure
FF 092 (E-W Direction, Entire Record)	3.3a
FF UP (Vertical Direction, Entire Record)	3.3b
FF 002 (N-S Direction, Entire Record)	3.3c
FF 092	3.4
FF UP	3.5
FF 002	3.6
N/2/W - N/2/E (To determine torsion)	3.13
N/R/W - N/R/E (To determine torsion)	3.14

Moving Window Transfer Functions: $H(\omega) = Y(\omega)/X(\omega)$		Figure
$Y(\omega)$	$X(\omega)$	
E/R/C	FF 092	3.8
E/4/C	FF 092	3.9
E/2/C	FF 092	3.10
E/G/E	FF 092	3.11
E/R/C	E/G/E	3.12
N/R/W	FF 002	3.15
N/R/C	FF 002	3.16
N/R/E	FF 002	3.17
N/2/W	FF 002	3.18
N/2/E	FF 002	3.19
N/G/E	FF 002	3.20
N/R/E	N/G/E	3.21
U/G/E	FF UP	3.22

computed Fourier amplitude spectra and transfer functions used to determine the frequency content. All spectra considered were unsmoothed spectra. Due to the number of computed moving window spectra, spectra are shown only for the time intervals beginning at 0.0, 2.0, 4.0, 6.0, 8.0, 10.0, 12.0 and 14.0 seconds. Before discussing the results from the moving window analysis, several comments are pertinent regarding the application of this technique. First, the moving window technique violates the zero initial conditions in equation (3.1). Second, the window T neglects the effect of the input motion before the time interval T and hence the memory characteristics of the system are neglected. Third, the ground motion for this earthquake was highly nonstationary. Thus the moving window of length 5 seconds looked at a highly nonstationary time record. Transfer functions of such nonstationary records may have limited validity. Finally, it should be noted that the transfer function computed from equation (3.3) is the ratio of two Fourier spectra. If the modulus of the input spectrum has a very small value, then the ratio could be large, resulting in a peak. This peak may not represent the physical phenomena but may be the numerical problem of using a ratio method.

3.3 Frequency Content of Free Field

The frequencies recorded at the base of the building differed from the frequency characteristics of the nearby free field motion. Consider the free field motion. The Fourier amplitude spectra of the entire acceleration records for the free field station are shown in Figure 3.3. The spectra show that for the horizontal components, the major energy transfer occurred between 0 and 2.5 Hz, with amplitudes between 2.5 and 6.0 Hz uniformly but weakly amplified. The free field vertical component, on the other hand,

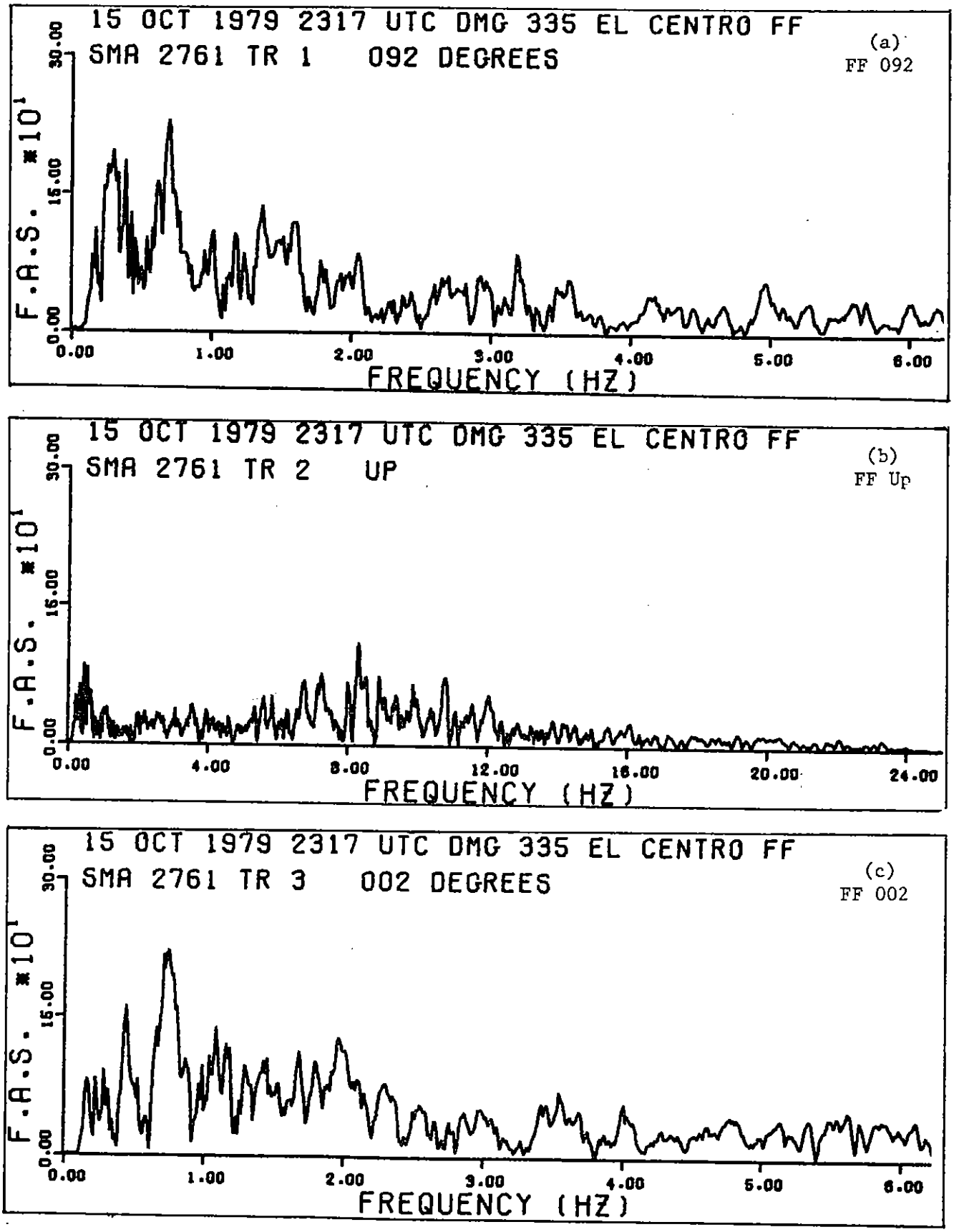

FIGURE 3.3 Fourier Amplitude Spectra of Free Field Components (Based on Entire Records)

showed fairly uniform amplitude of all frequencies between 0 and 12.5 Hz with peaks being amplified in the 0 to 1 Hz and 8 to 9 Hz ranges.

Because the free field motion was highly nonstationary, the frequency content was difficult to determine from the moving window Fourier amplitude spectra shown in Figures 3.4, 3.5 and 3.6 for the FF 092, FF Up and FF 002 components, respectively. However, for each component, a general envelope spectrum could be determined and frequency bandwidths, in a gross sense, could be assessed as illustrated in Figure 3.7. Note that the frequency bands for the horizontal components were similar to the ambient vibration test frequencies at the free field station shown in the spectra in Figure 1.10.

3.4 Frequency Content of the Building

The base of the building responded as an "upper story level" rather than as input motion to the structure. In both the E-W and N-S directions, the transfer functions computed between the base of the building and the free field contained the same frequency content as the transfer functions computed between the upper story levels and the free field. For example, in the E-W direction, the frequency content of the transfer functions computed between the building components at all levels and the free field, Figures 3.8, 3.9, 3.10 and 3.11, were the same. However, the transfer function computed between the E/R/C component and the base, Figure 3.12, had different frequency content than seen in all transfer functions computed between all building levels and the base. A comparison of Figures 3.17, 3.19, 3.20 and 3.21 shows similar base response in the N-S direction.

Consider the building response in the E-W direction shown in Figures 3.8 through 3.11. During the initial 6 seconds, the transfer functions and the corresponding phases show that the E-W motion started to vibrate at a high frequency, about 8.5 Hz. Considering that in the time domain, the

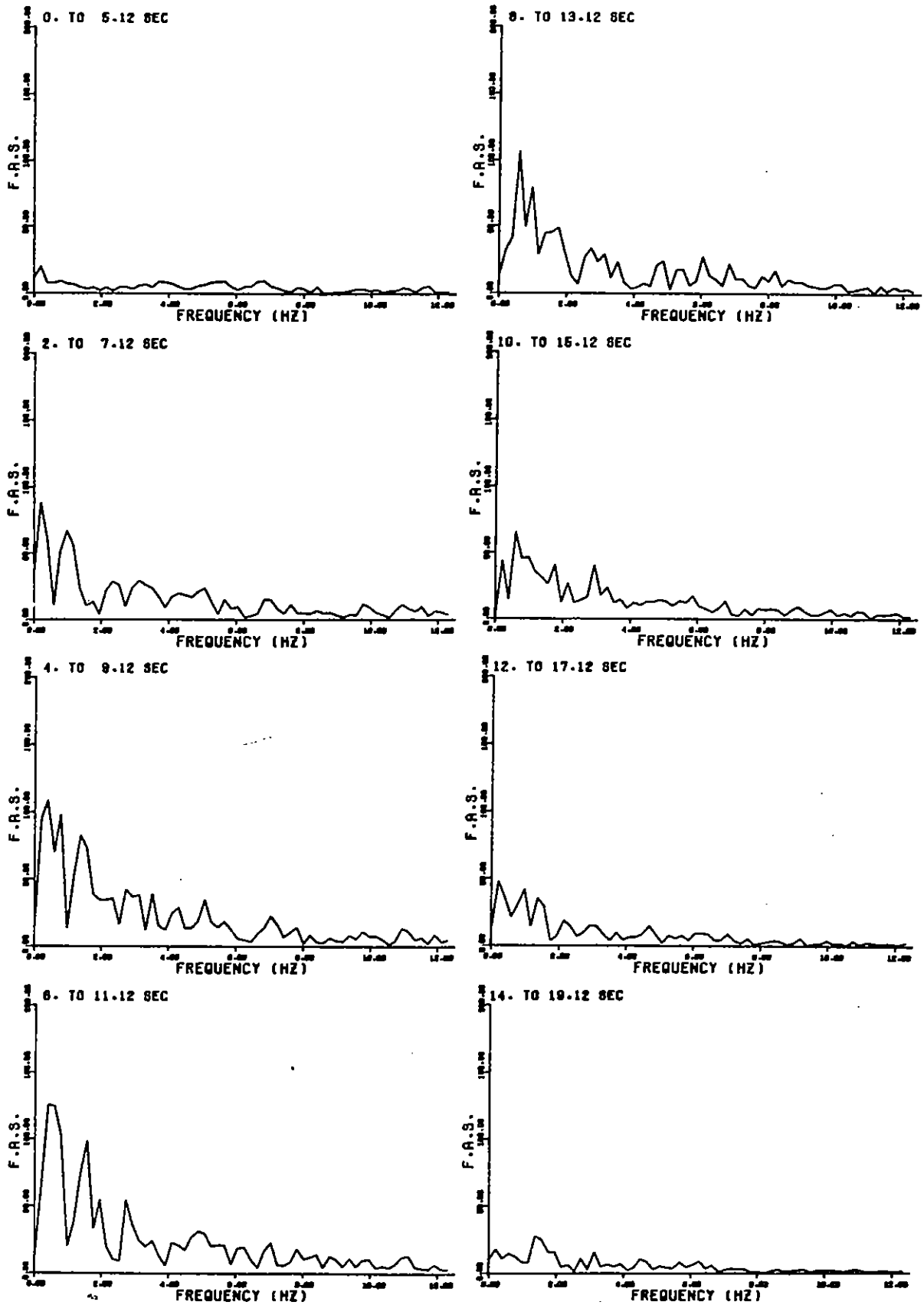

FIGURE 3.4 Moving Window Fourier Amplitude Spectrum, FF 092, E-W Free Field Component

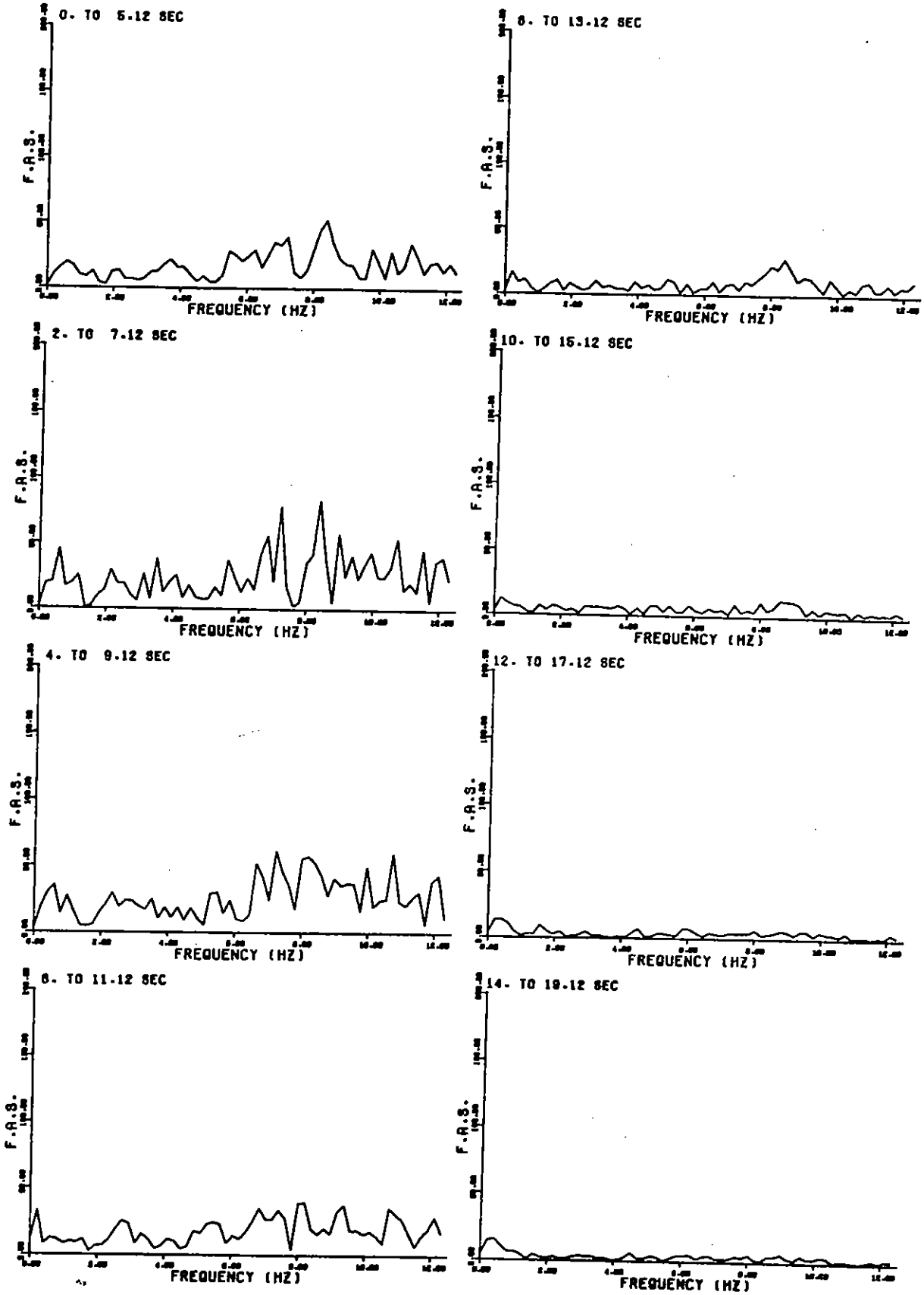

FIGURE 3.5 Moving Window Fourier Amplitude Spectrum, FF Up (Vertical Free Field Component)

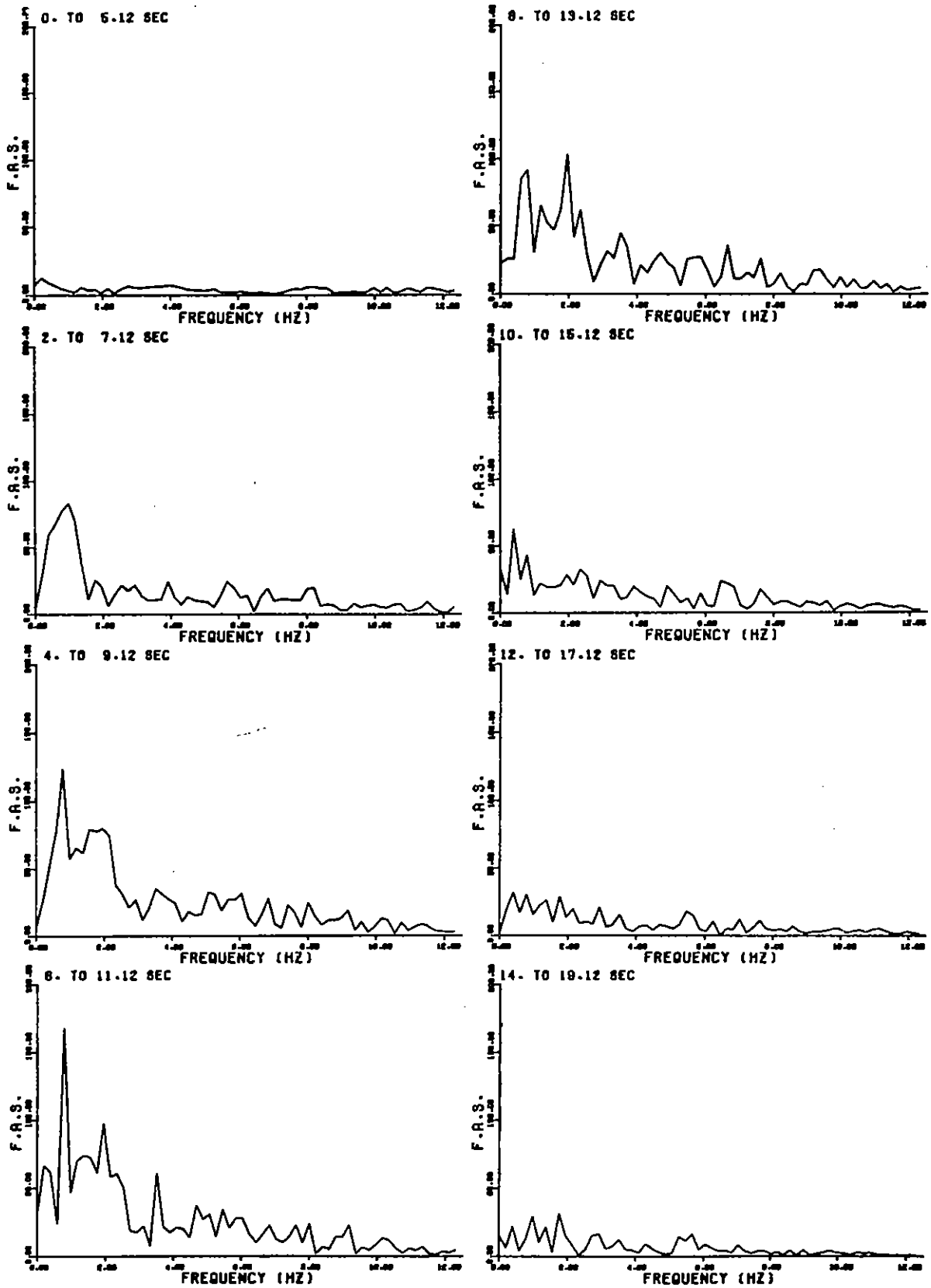

FIGURE 3.6 Moving Window Fourier Amplitude Spectrum, FF 002, N-S Free Field Component

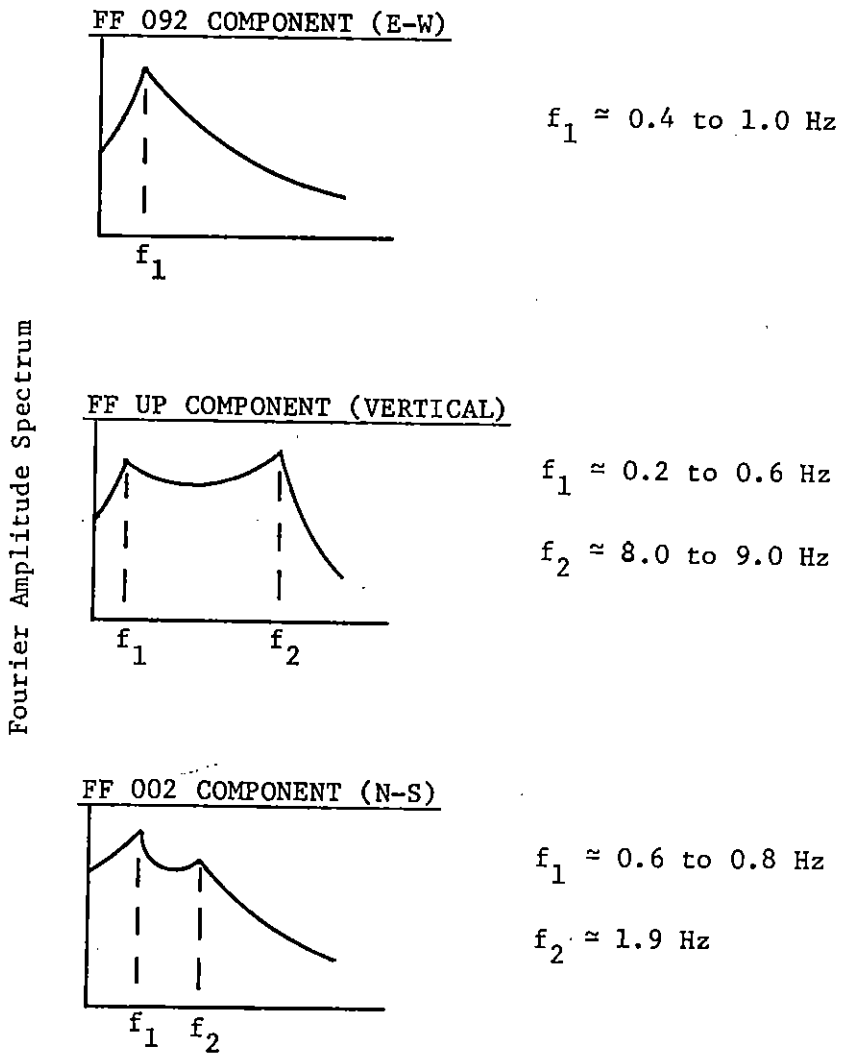

FIGURE 3.7 Summary of Frequency Content of Free Field Components (Based on Moving Time Window Analysis)

fourth floor moves out of phase with the roof and that the frequency of motion at all floor levels is about 8.5 Hz, it can be deduced that in this direction the building was initially vibrating in the third translational mode. Note that the identification of mode shapes using the transfer function technique requires that both the amplitude and the phase be known. Although both were used in this report, only the amplitudes are presented. From the pre-earthquake ambient vibration tests conducted in 1979, (Pardoen, 1979), the third mode frequency was calculated to be about 9 Hz. Hence, at slightly larger amplitudes (during the P wave phase) the third mode frequency was slightly reduced. Figures 3.8 and 3.11 show that this frequency was initially being excited at both the base and the roof but was not predominant in the corresponding free field motion.

During the ensuing strong motion (~6 to 12 seconds), the building response constantly changed. The moving time windows which include an initial part of the large amplitude strong motion show that the first and second translational modes of vibration, at 1.0 and 3.3 Hz, respectively, were establishing themselves in addition to the already present third mode. The third mode, however, decreased substantially from 8.5 Hz to 6.5 Hz. The peak which appeared near 9 Hz was therefore no longer the third mode but now the energy transfer at higher but undetermined modes. Towards the end of the strong motion, the frequencies of the first, second and third modes lowered from 1.0, 3.3 and 6.5 Hz to 0.6, 2.0-2.2 and 3.9 Hz respectively. Beyond 12 seconds (after column failure at ~11.2 seconds) the latter frequencies prevailed with most of the energy transfer occurring in the first and second modes. The transfer function between the roof and the free field, Figure 3.8, showed that the second mode was amplified quite robustly, although usually at the roof level the second mode signature is small. The above

time variation of the frequency content in the E-W direction is summarized in Table 3.2 and shown graphically in Figure 3.23.

The apparent coupling between the translational and torsional modes in the N-S direction complicated the frequency identification in this direction. The torsional frequencies are determined from moving window Fourier amplitude spectra of the difference between the N/2/W and N/2/E components (Figure 3.13) and the N/R/W and N/R/E components (Figure 3.14). The transfer functions between 0 and 5 seconds (Figures 3.13 to 3.20) show that the major portion of the energy transfer initially occurred at 2.0 Hz (first mode translation), 2.3 Hz (first mode torsion), 7.0 Hz (second mode torsion) and at about 9.0 Hz (second mode transverse). Between 5 and 10 seconds, the windows indicated no pronounced peaks except for some small amplification of all frequencies. Thus the building response was in transition with no dominant mode prevailing. During the end of the strong motion and beyond 12.0 seconds, the building vibrated in two bands: 1.0 to 1.5 Hz and 2.7 to 3.5 Hz. The bands were due to the close coupling between the first mode translation at 1.0 Hz and the first mode torsion at 1.4 Hz and between the second mode torsion at 2.7 Hz and second mode translation at 3.0-3.5 Hz. The time variation of the frequency content in the N-S direction is also summarized in Table 3.2 and shown graphically in Figure 3.23.

In both the E-W and N-S directions, the frequencies of vibration decreased substantially from the ambient vibration test. The N-S translational first mode decreased by a factor of 2.24, compared to a decrease of 2.6 in the E-W direction. It may be concluded that the first story east end column failures caused significant degradation of the stiffness of the building. However, the stiffness degradation at the first story cannot be the only

cause of such a large decrease in frequencies. The 1980 ambient vibration test on the shored up structure showed frequencies comparable to the 1979 ambient vibration test. Hence the amplitude of vibration, different behavior of soil for large amplitude values (soil-pile interaction), etc., may account significantly in the final explanation. In previous studies of buildings monitored during the 1971 San Fernando earthquake, similar effects, but on a smaller scale, were observed.

The apparent decrease in the translational first mode frequencies in the N-S and E-W directions beyond 12 seconds (beyond the large amplitude, strong motion response) can also be seen in the relative displacement time histories plotted in Figures 2.3. All upper story level traces in the N-S direction show that beyond 12 seconds,the fundamental frequency was about 1 Hz. Similar components in the E-W direction show that beyond 12 seconds the fundamental frequency was about 0.6 Hz.

Finally, consider the vertical transfer function between the ground level and the free field shown in Figure 3.22, which is the only one available for vertical vibration. This transfer function showed no definitive peaks in the low frequency range. Because higher frequencies, however, were being amplified, the possibility of rocking motion in at least the E-W direction could be eliminated.

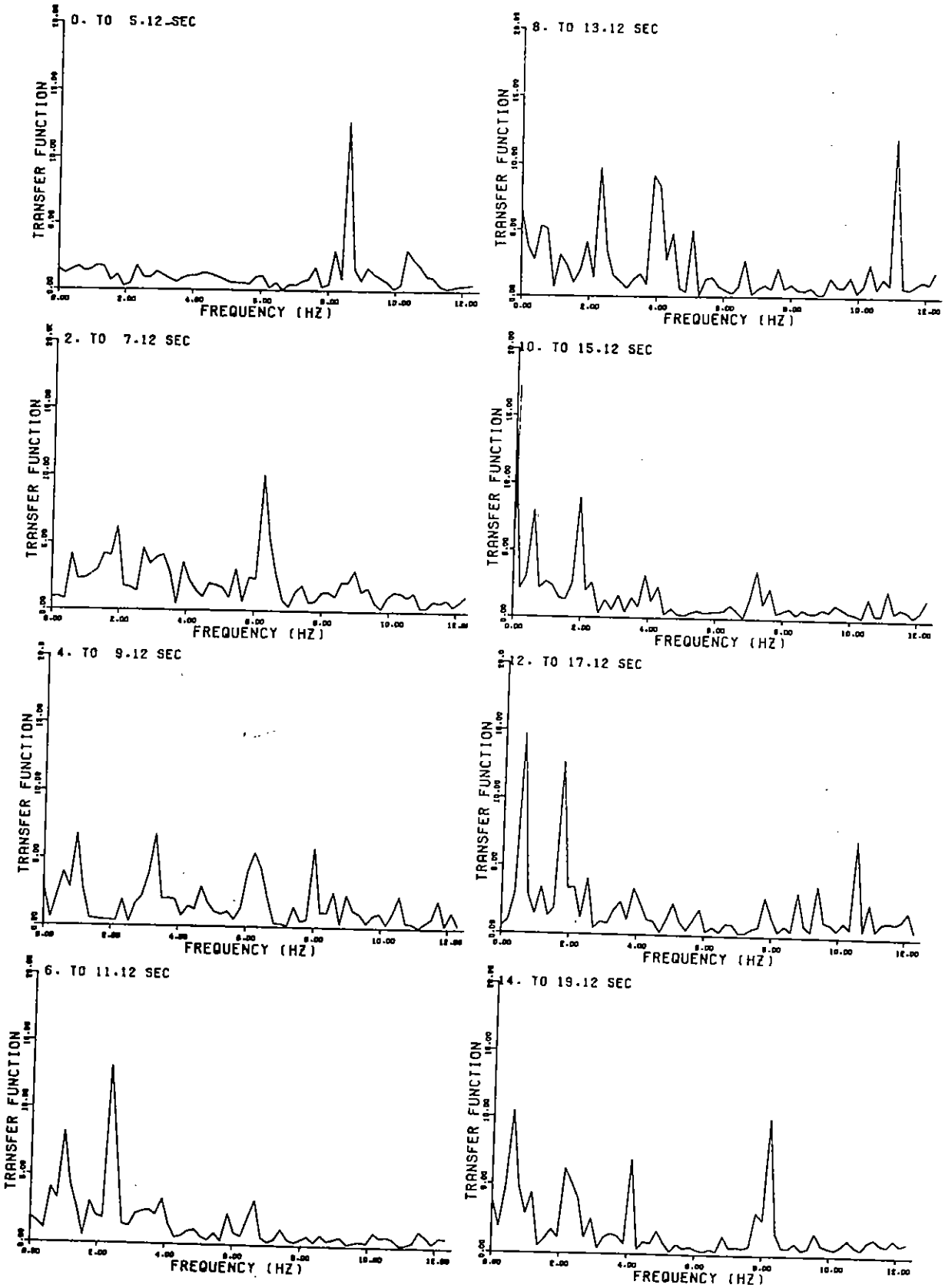

FIGURE 3.8 Moving Window Transfer Function Between E/R/C and FF 092

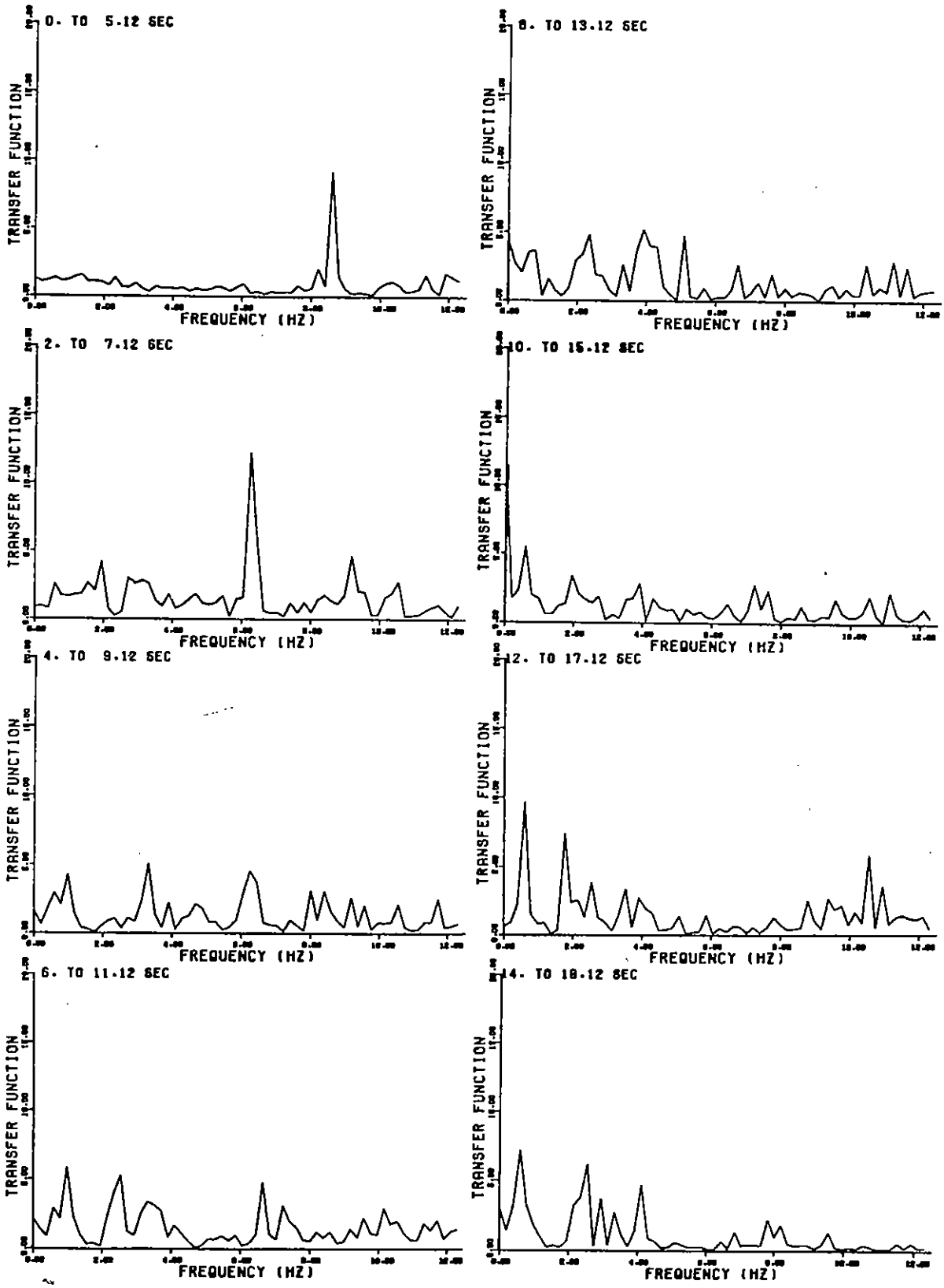

FIGURE 3.9 Moving Window Transfer Function Between E/4/C and FF 092

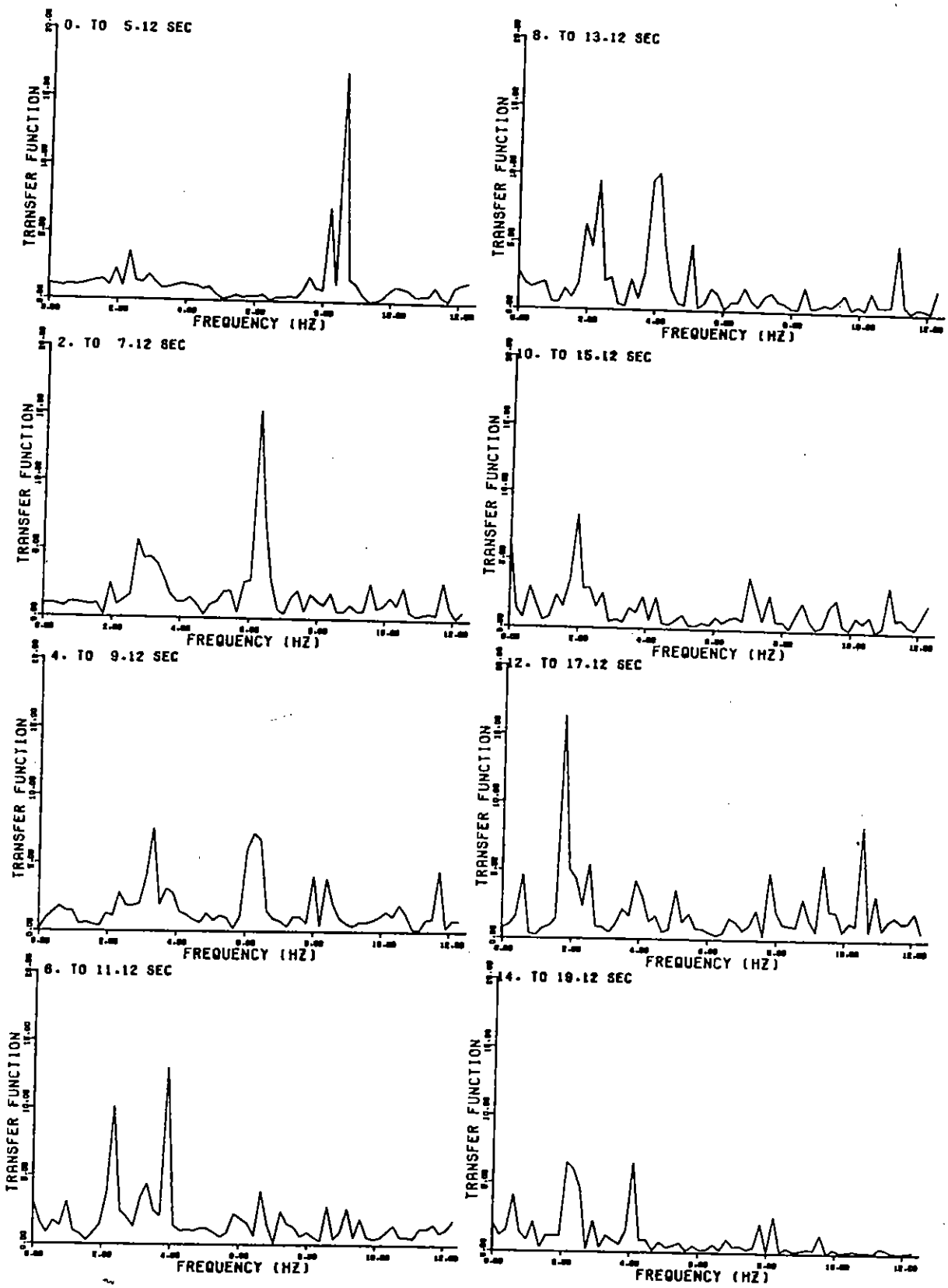

FIGURE 3.10 Moving Window Transfer Function Between E/2/C and FF 092

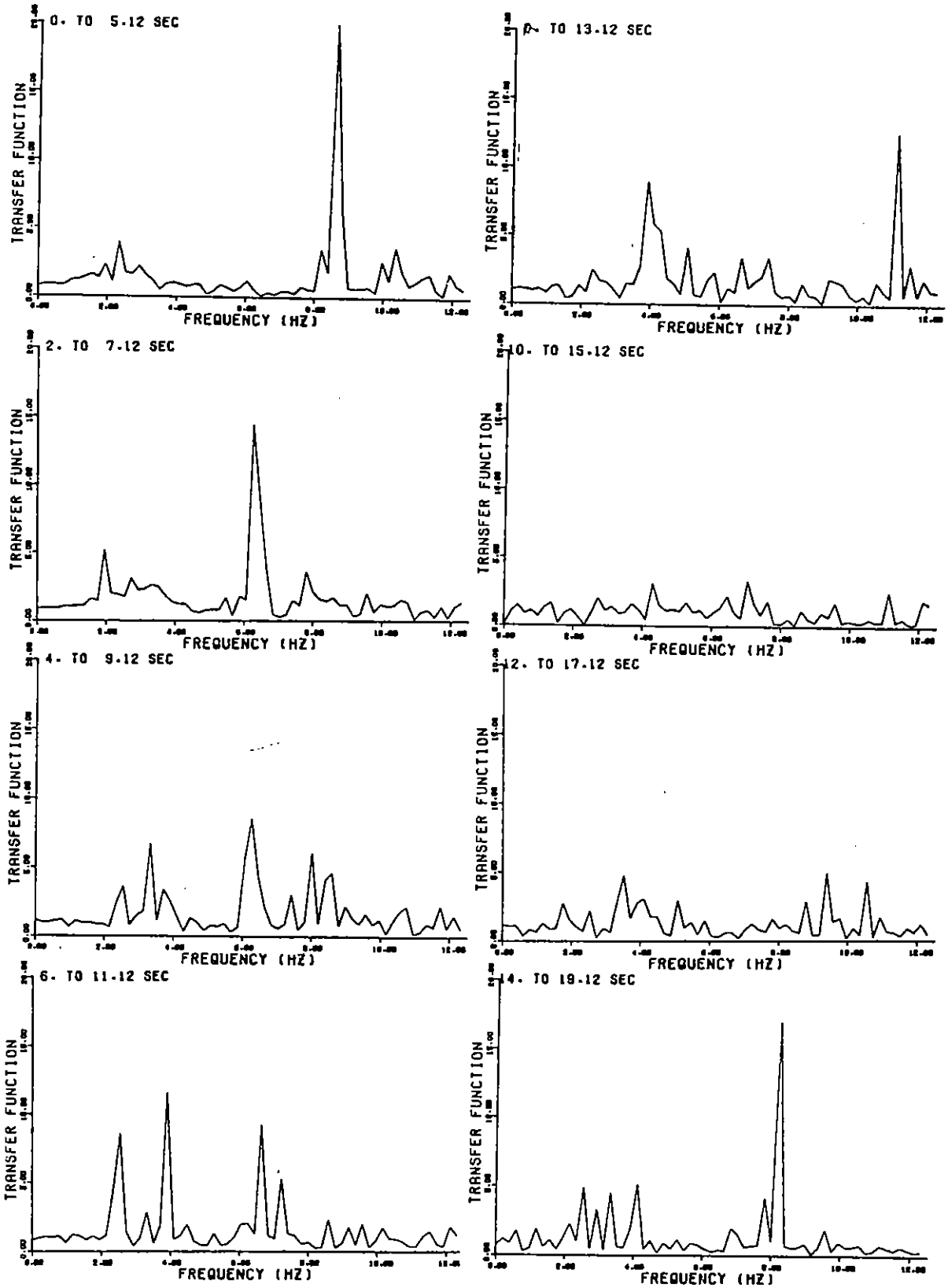

FIGURE 3.11 Moving Window Transfer Function Between E/G/E and FF 092

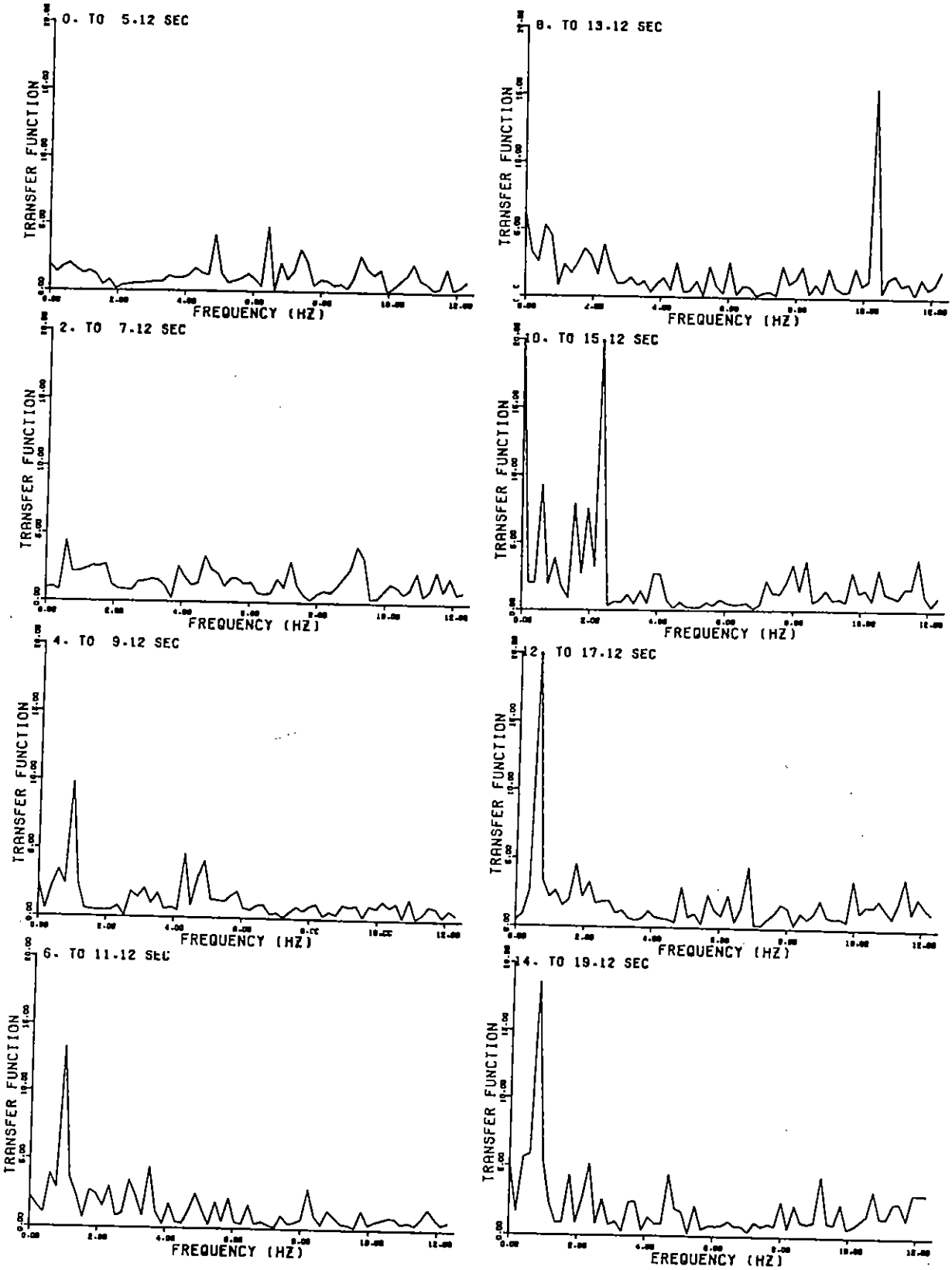

FIGURE 3.12 Moving Window Transfer Function Between E/R/C and E/G/E

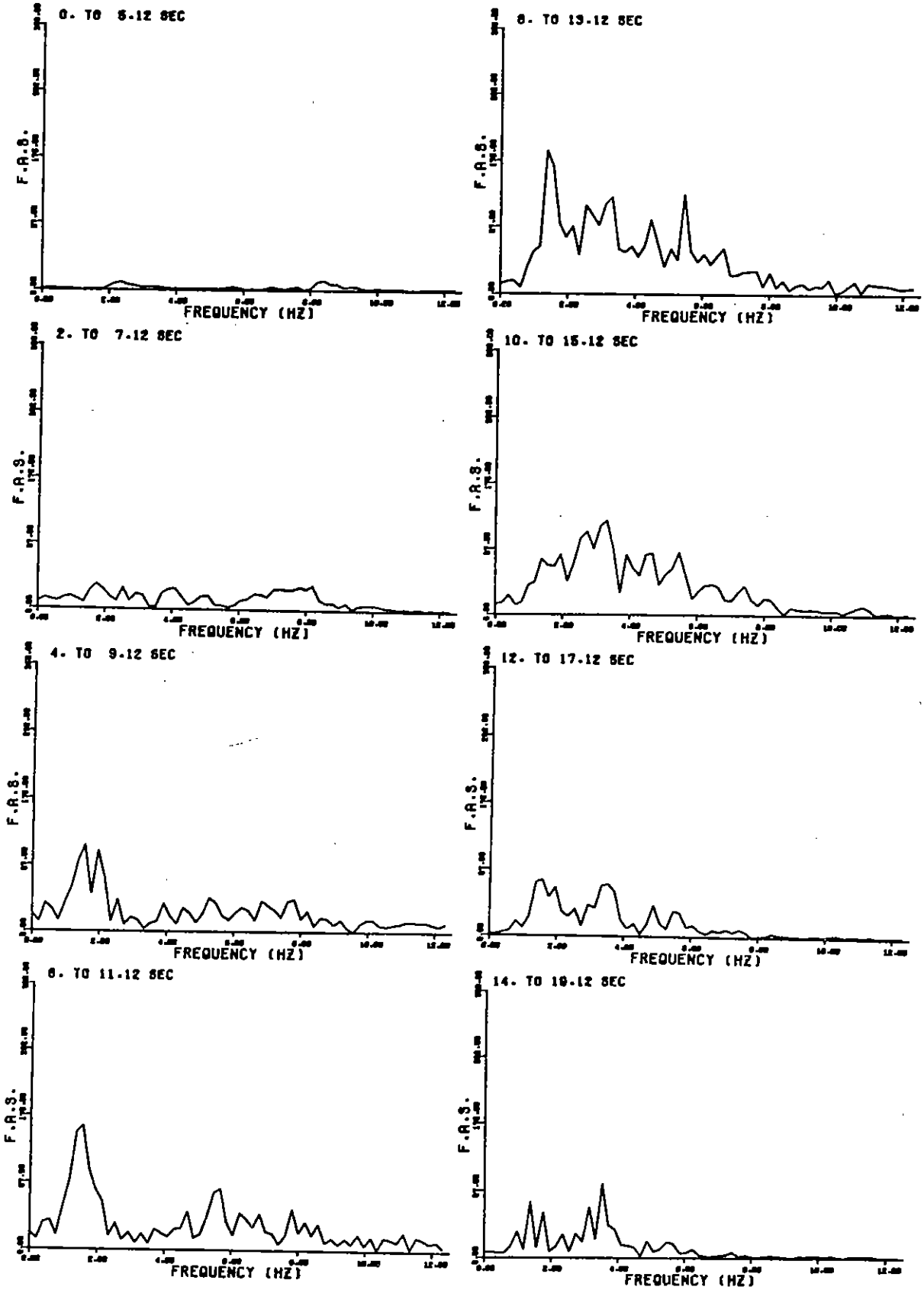

FIGURE 3.13 Moving Window Fourier Amplitude Spectrum, N/2/W - N/2/E

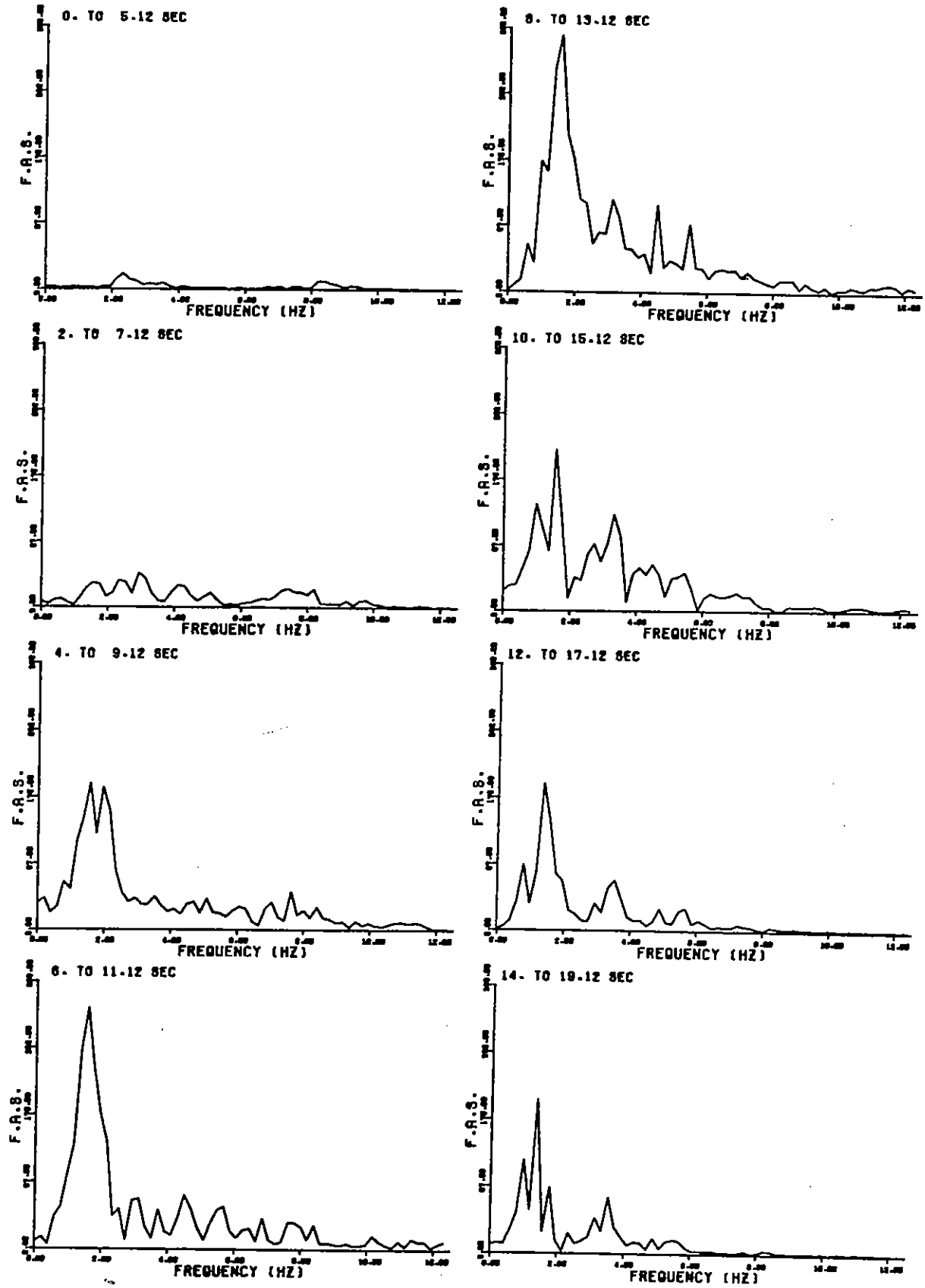

FIGURE 3.14 Moving Window Fourier Amplitude Spectrum, N/R/W - N/R/E

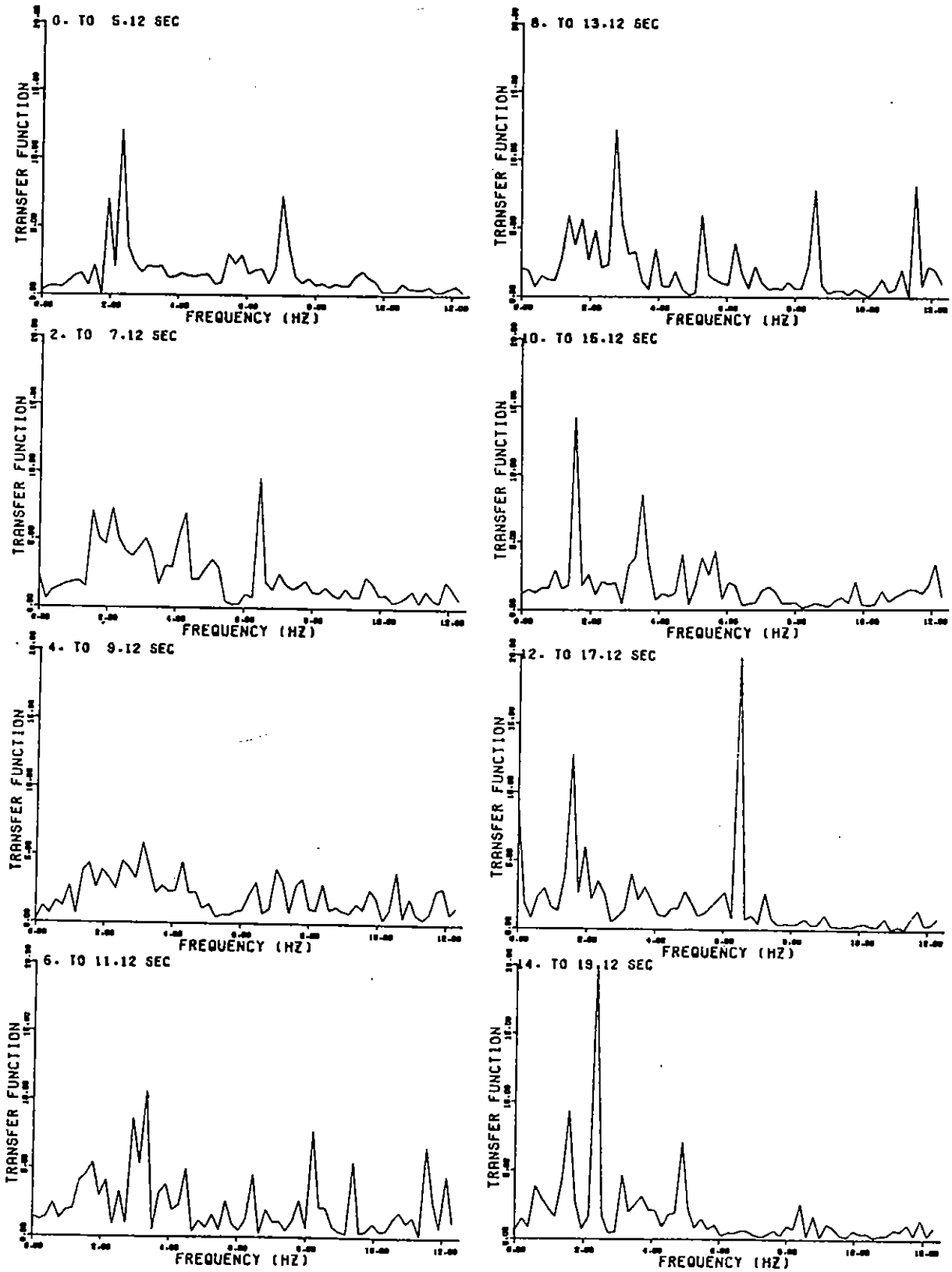

FIGURE 3.15 Moving Window Transfer Function Between N/R/W and FF 002

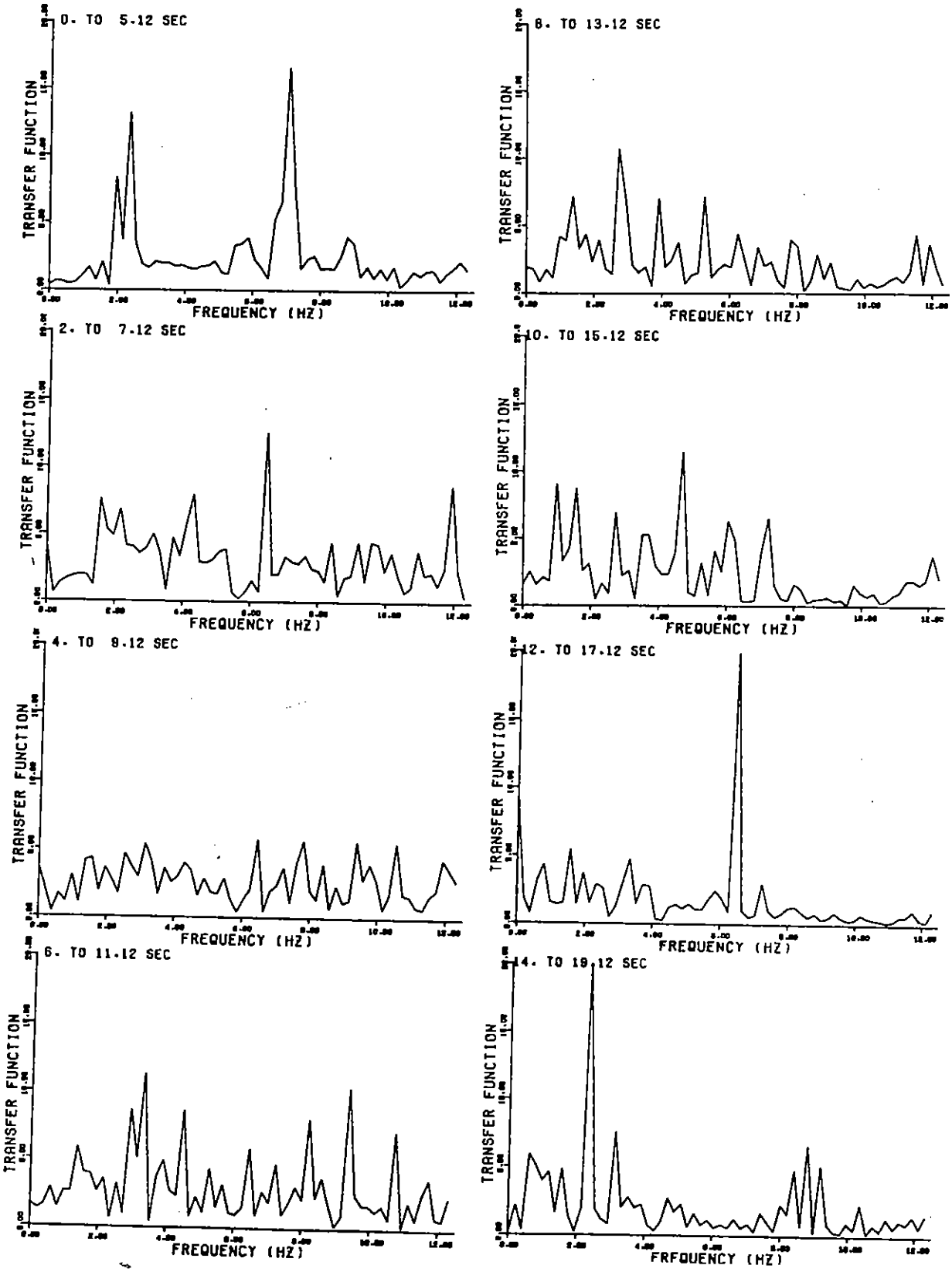

FIGURE 3.16 Moving Window Transfer Function Between N/R/C and FF 002

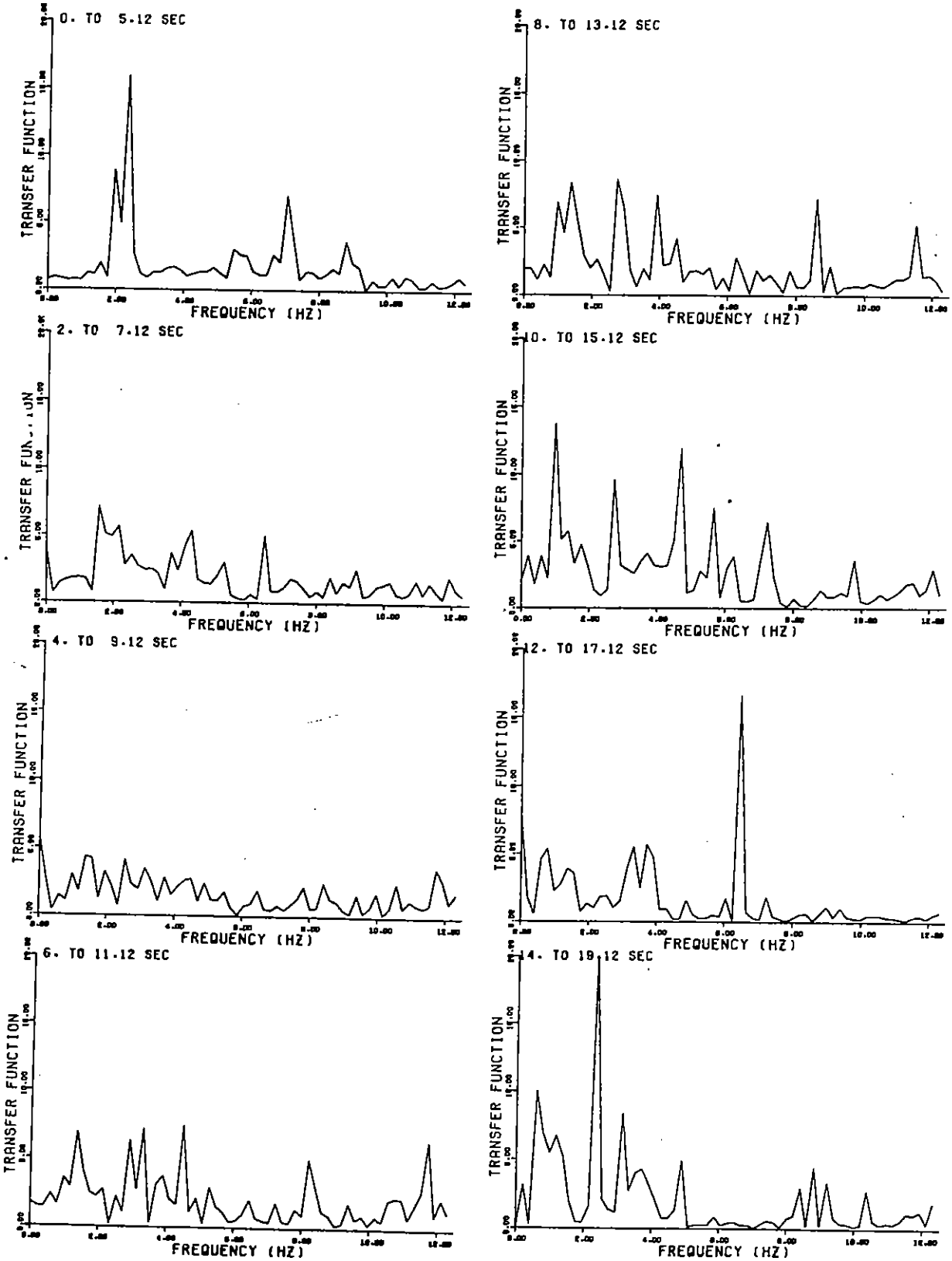

FIGURE 3.17 Moving Window Transfer Function Between N/R/E and FF 002

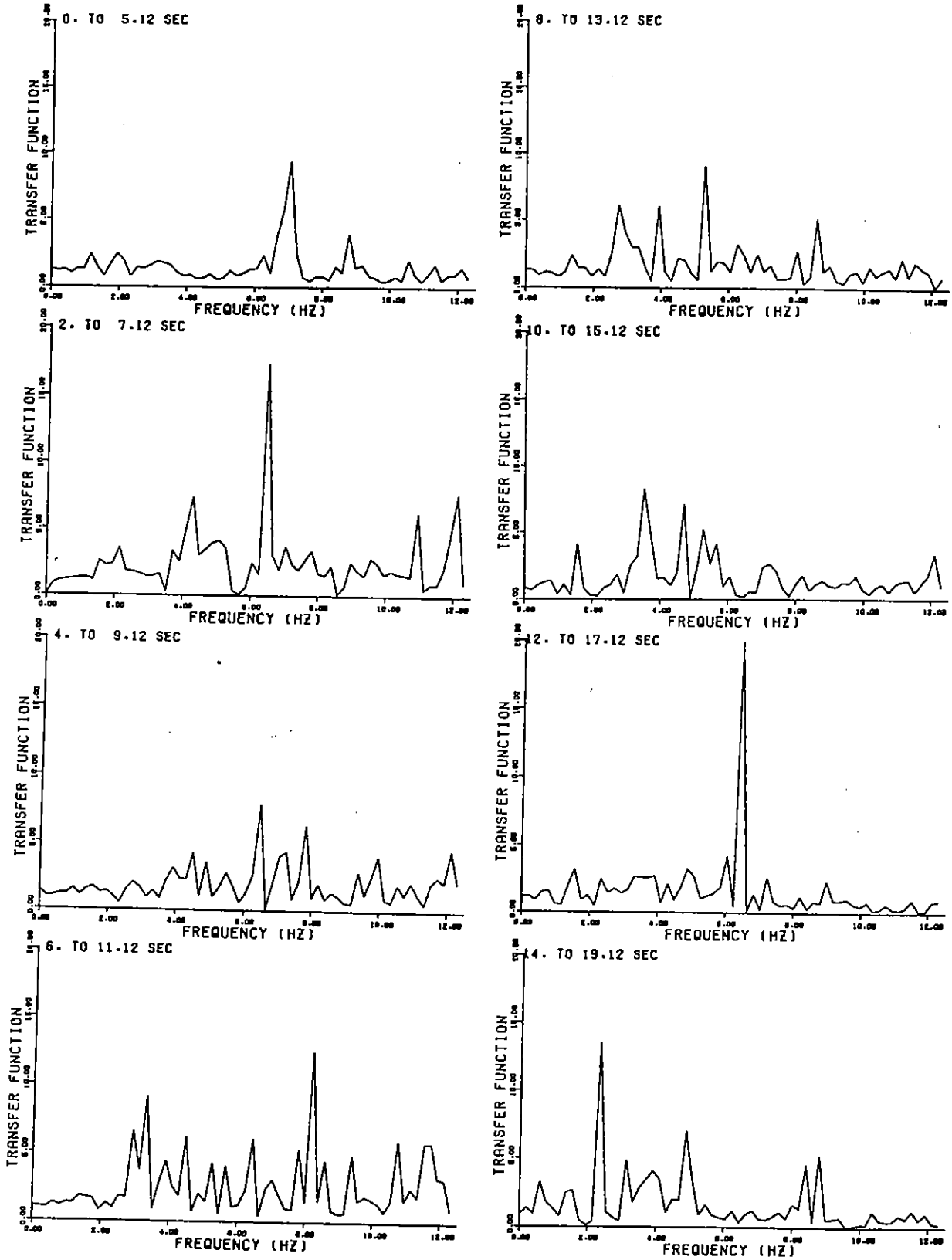

FIGURE 3.18 Moving Window Transfer Function Between N/2/W and FF 002

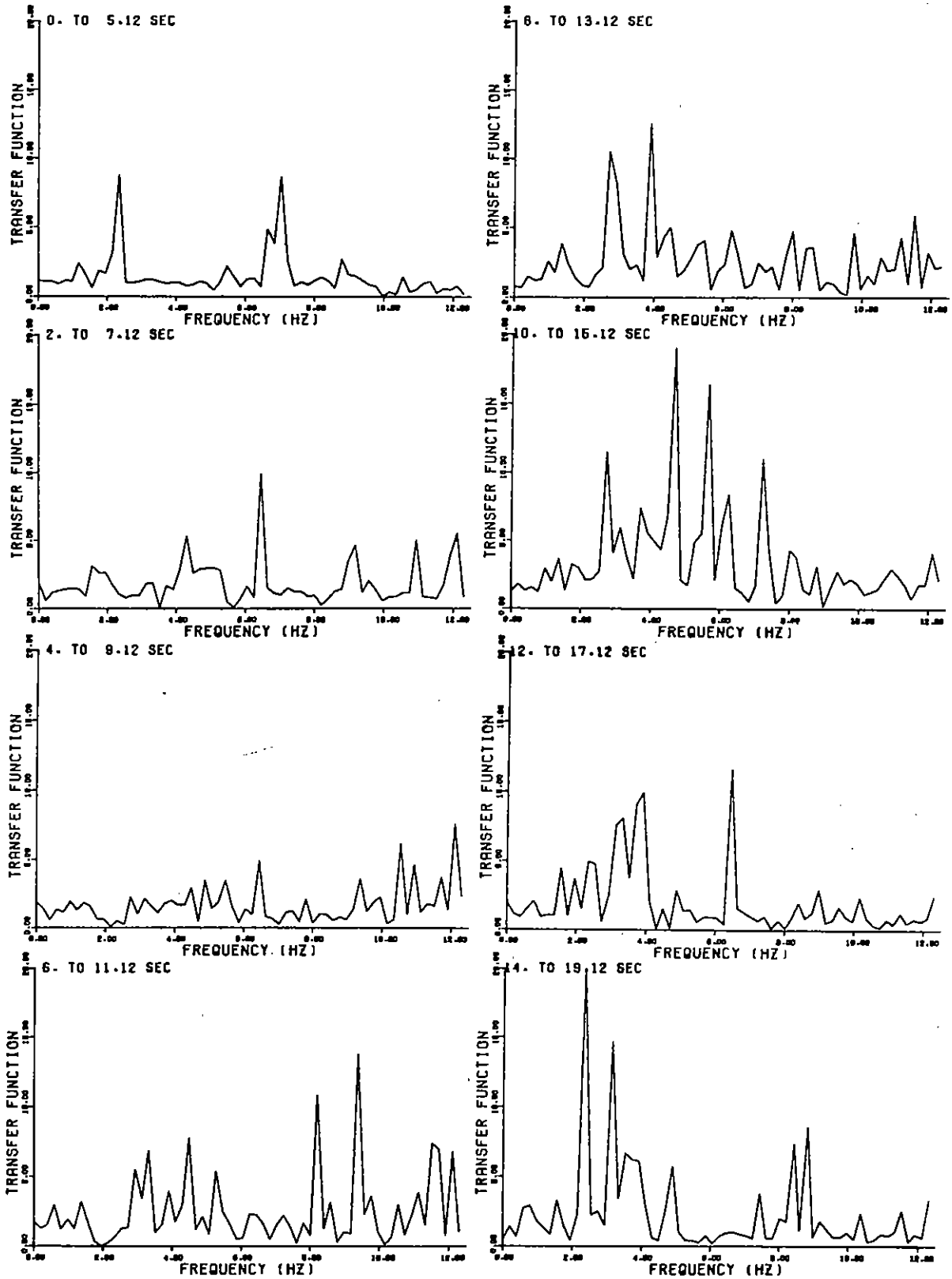

FIGURE 3.19 Moving Window Transfer Function Between N/2/E and FF 002

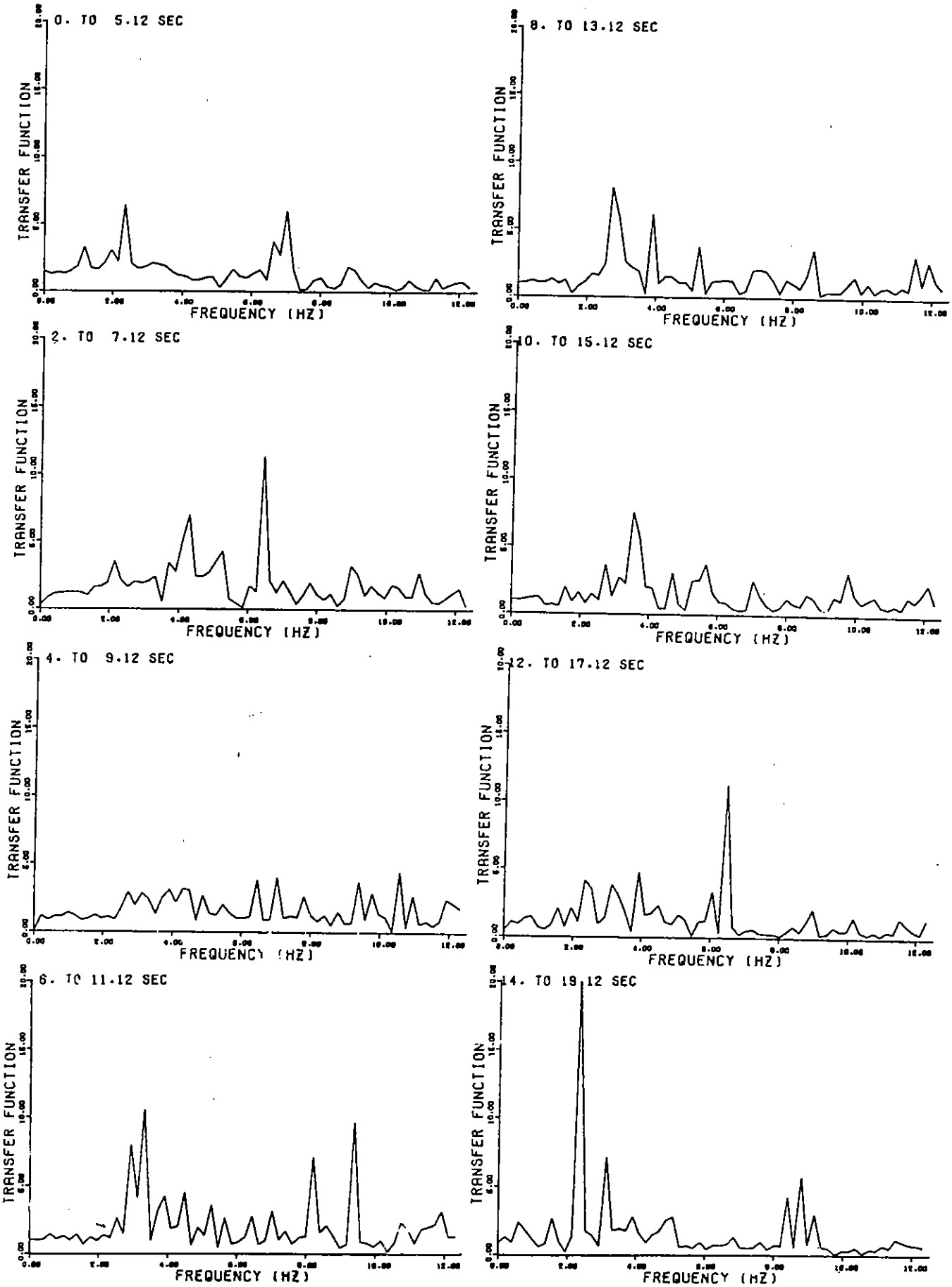

FIGURE 3.20 Moving Window Transfer Function Between N/G/E and FF 002

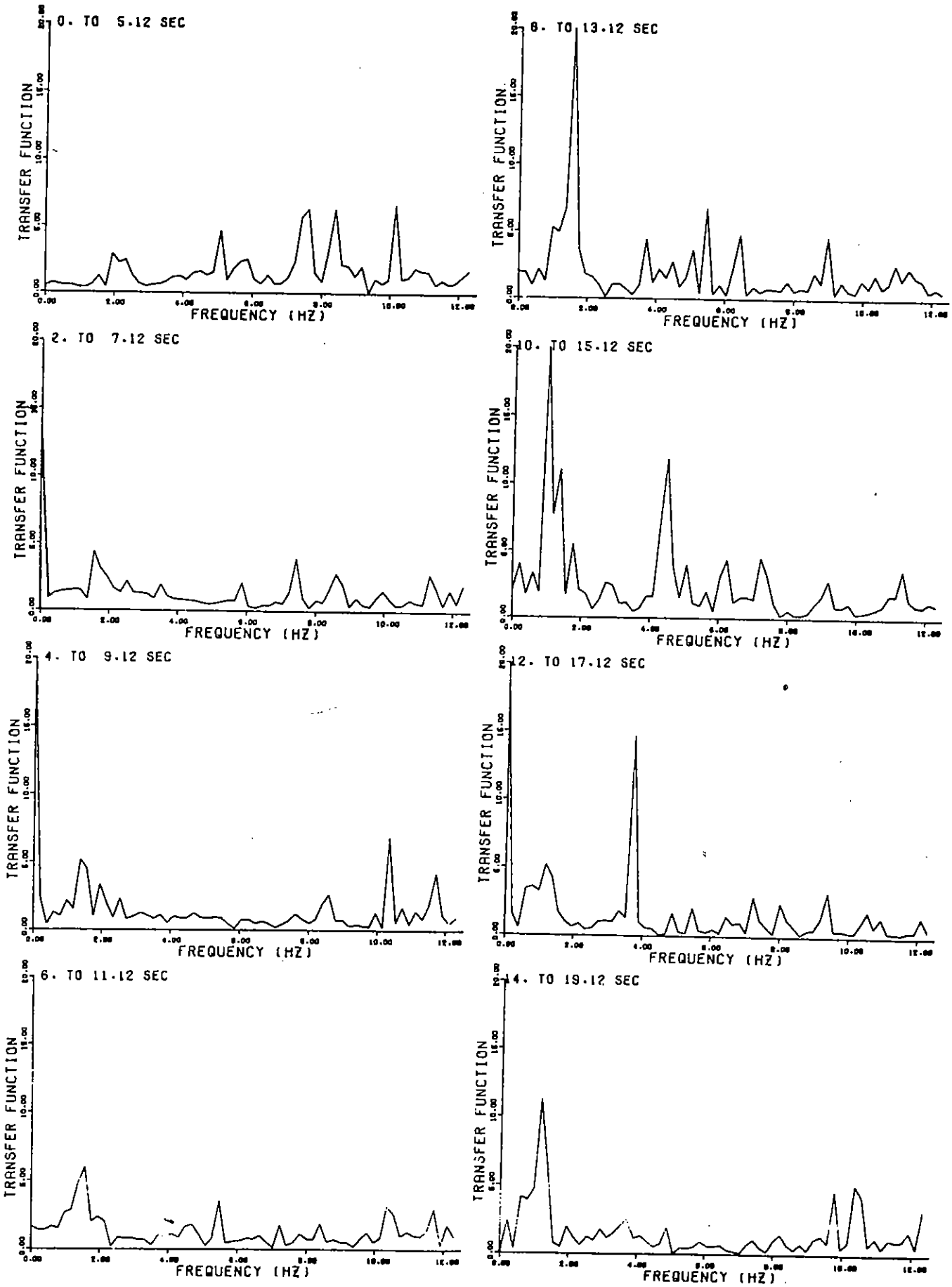

FIGURE 3.21 Moving Window Transfer Function Between N/R/E and N/G/E

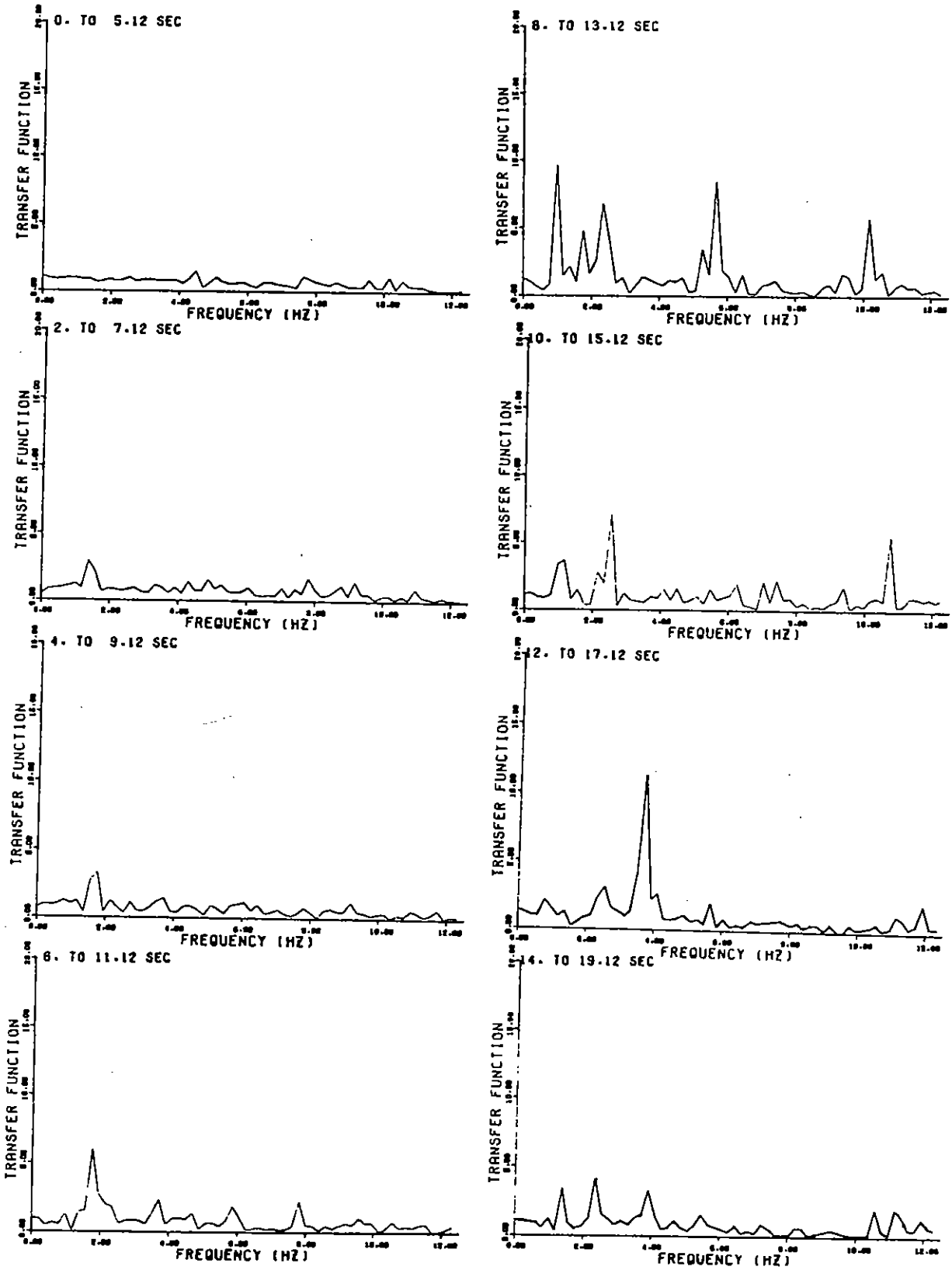

FIGURE 3.22 Moving Window Transfer Function Between U/G/E and FF Up

TABLE 3.2 SUMMARY OF TIME VARIATION OF FREQUENCY CONTENT OF THE IMPERIAL COUNTY SERVICES BUILDING

East-West Direction (Hz)

Measurement Time	Mode (Translation)		
	1	2	3
Ambient Vibration Test, February 1979	1.55	5.0	8.9
October 15, 1979 Earthquake:			
Seconds 0-6	-	4.8	8.6
Seconds 6-12	1.0	2.3-3.3	3.9-6.3
Seconds 12-End	0.6	2.0	3.9
Ambient Vibration Test, March 1980	1.20	2.88	7.28

North-South Direction (Hz)

Measurement Time	Mode			
	1st Trans-lation	1st Torsion	2nd Trans-lation	2nd Torsion
Ambient Vibration Test, February 1979	2.24	2.85	---	---
October 15, 1979 Earthquake:				
Seconds 0-6	2.0	2.3	9.0	7.6
Seconds 6-12	1.4	---	5.3	
Seconds 12-End	1.0	1.4	3.0-3.5	2.7
Ambient Vibration Test, March 1980	1.92	2.32	6.4(?)	---

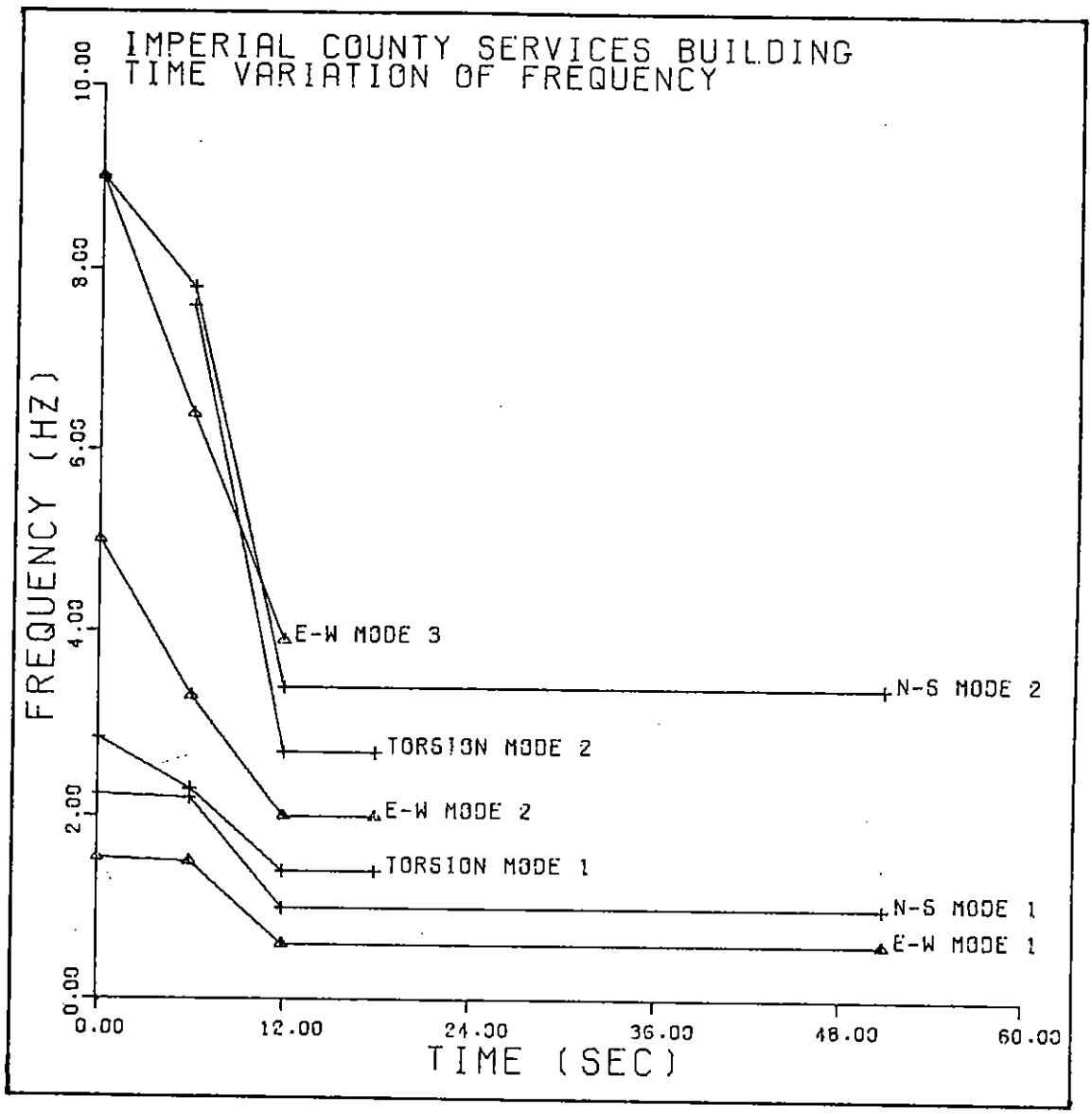

FIGURE 3.23 Summary of Time Variation of Frequency Content

CHAPTER 4: RMS ACCELERATION AND ARIAS INTENSITY

Recent research to develop root mean square (rms) acceleration and duration coupled as a means of characterizing strong ground motion, (McCann and Shah, 1979; McGuire and Hanks, 1979), provides the impetus to investigate rms acceleration as a structural response parameter. The availability of upper level records in the Imperial County Services Building from the October 15, 1979 earthquake makes such an investigation feasible. The rms acceleration is defined as:

$$a_{rms} = \left[\frac{1}{T} \int_0^T [a(u)]^2 du \right]^{1/2} \tag{4.1}$$

where a(u) is the acceleration time history and T is the duration of the record. The rms acceleration can be related to the Arias (1970) definition of strong motion intensity. The Arias intensity, I, is defined as the sum of the energy dissipated per unit mass for all single degree of freedom oscillators with frequencies from 0 to ∞. If $E(\omega)$ is the energy dissipation of an oscillator of natural frequency ω, then the Arias intensity is given as

$$I = \int_0^\infty E(\omega) d\omega \tag{4.2}$$

Arias has shown that equation (4.2) can be written for an individual oscillator as a function of critical damping, ξ, of the oscillator and the time history a(u) as

$$I = \frac{\arccos\xi}{g\sqrt{1-\xi^2}} \int_0^\infty [a(u)]^2 du \tag{4.3}$$

For zero percent critical damping, equation (4.3) simplifies to:

$$I = \frac{1}{g}\int_0^\infty [a(u)]^2 du \tag{4.4}$$

Parseval's theorem allows the Arias intensity in equation (4.4) to be expressed in terms of the rms acceleration defined in equation (4.1):

$$I = a_{rms}^2 \cdot T \tag{4.5}$$

Two interpretations of the rms acceleration are noted. First, the rms acceleration can be interpreted as the square root of an average constant intensity, a_{rms}^2, acting for duration T. Second, by considering the Arias intensity to be the energy (intensity) of the given motion, then the rms acceleration is the square root of the rate of energy arrival.

The discrete cumulative rms acceleration (McCann and Shah, 1979) and Arias intensity, derived from equations (4.1) and (4.4) respectively, are expressed as

$$a_{rms}(k) = \left[\sum_{i=1}^{k} \frac{\left(a(t_i)\right)^2}{k-1}\right]^{1/2} \tag{4.6}$$

$$I(k) = \sum_{i=1}^{k} [a(t_i)]^2 \tag{4.7}$$

As descriptors of the energy (intensity) of the strong ground motion and response, these cumulative functions should give insight into the characteristics of the motion of interest. The cumulative rms function describes the average rate of energy (intensity) arrival as a function of duration and peaks where the motion is most intense. If the rate of energy dissipation of the structure was known, then the initiation of yielding would occur when the rate of energy arrival exceeds the rate being dissipated.

The cumulative Arias intensity is a simple summation and therefore should change slope dramatically as sudden increases or decreases in energy arrival occur. The maximum Arias intensity value occurs at the end of the record.

The cumulative rms acceleration and Arias intensity are shown in Figures 4.1 and 4.2, respectively, for the three free field and thirteen building acceleration records. The maximum values are listed in Table 4.1. A study of the cumulative functions gives several insights into the building response:

- From the shape of cumulative rms functions as shown in Figure 4.1, it can be seen that the majority of the energy buildup occurs between 5 and 12 seconds. Between 5 and 12 seconds, the rate of energy buildup shows three distinct regions of energy arrival. Between 5 and 7 seconds, the slope of the cumulative rms functions for all records shows a constant but steep rate of increase in the energy arrival. This corresponds to the suddenly increasing large amplitude accelerations evident in all traces during this time interval. From 7 to 8 seconds, the rate of energy arrival is in transition, as shown by the abrupt flat or slightly decreasing average rate of energy arrival. At this time the acceleration traces show a high amplitude, long period (approximately 1 second) pulse. From 8 seconds to the time of the maximum cumulative rms (see Table 4.1), the cumulative rms increases again but the slope of the curve is not as steep as between 5 to 7 seconds. Beyond 12 seconds, the large amplitude motion decreases and hence the cumulative rms decreases to the end of the record.

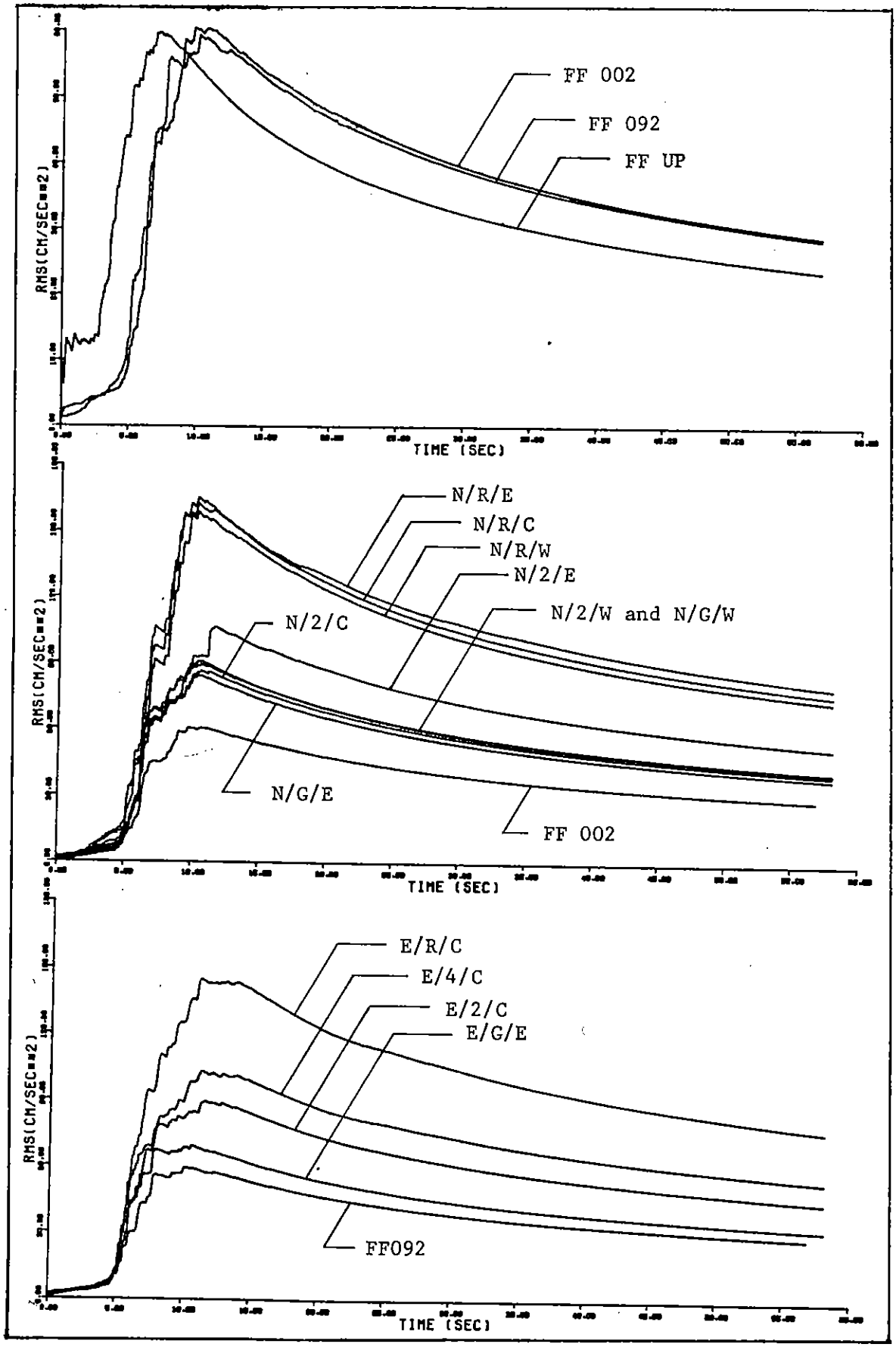

FIGURE 4.1 Cumulative RMS Acceleration Functions

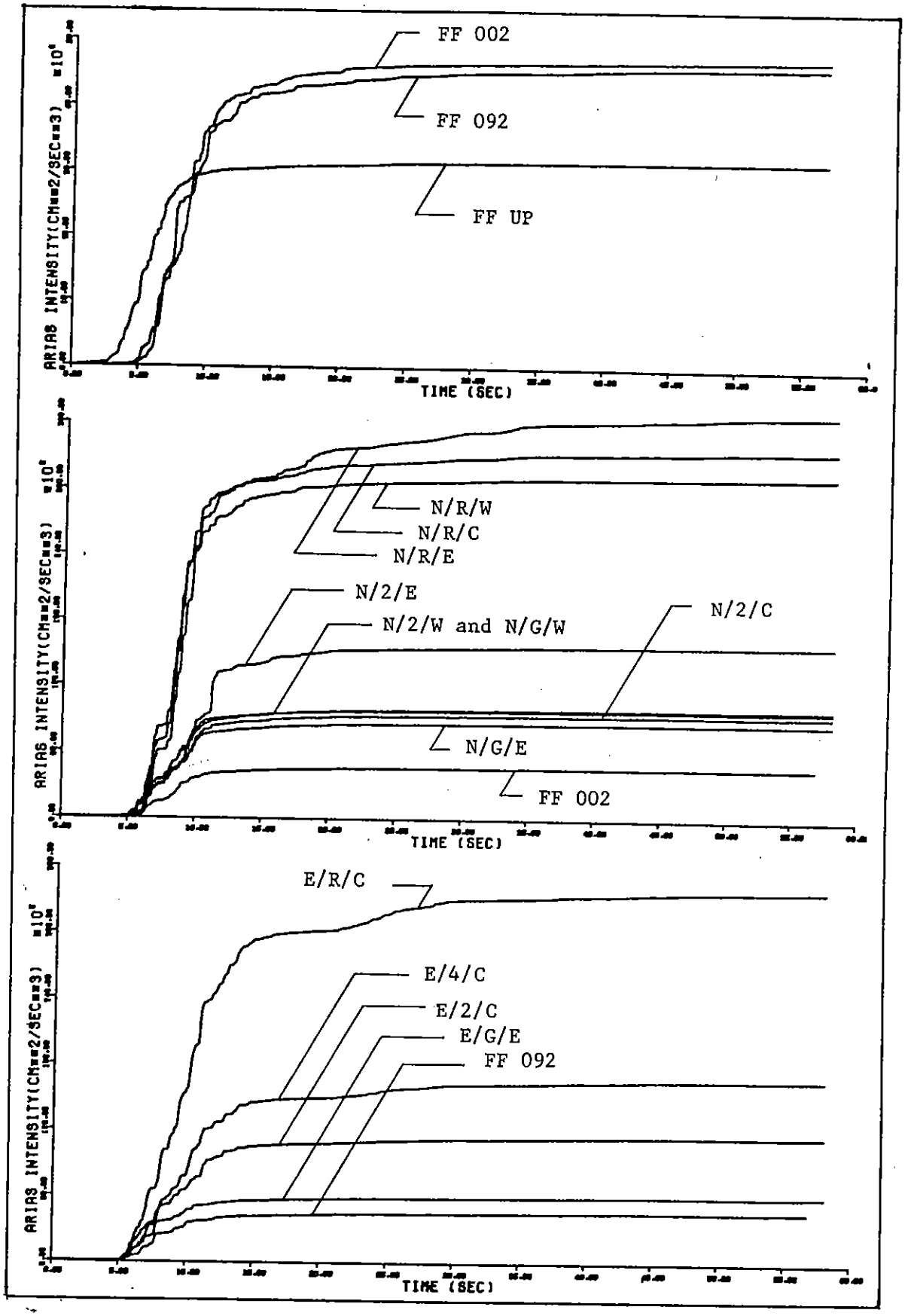

FIGURE 4.2 Arias Intensity Functions

TABLE 4.1 SUMMARY OF CUMULATIVE RMS AND ARIAS INTENSITY FUNCTIONS

Trace	Maximum Cumulative RMS Acceleration (cm/sec^2)	Time of RMS_{max} (sec)	$\int_0^T a^2 dt$ (cm/sec^3) x 10^2	Value of $\int a^2 dt$ at RMS_{max} x 10^2	% of $\int a^2 dt$ at RMS_{max}	Absolute Acceleration (cm/sec^2)	Time of Maximum Acceleration (sec)
FF 092	59.3	10.13	46114	35593	0.77	-231.44	7.75
FF UP	59.7	7.14	31605	25406	0.80	230.90	5.10
FF 002	60.4	9.78	47235	35614	0.75	209.02	8.95
N/R/W	158.9	10.26	312816	258874	0.83	531.34	9.12
N/R/C	165.5	10.26	336184	280912	0.84	-551.56	8.89
N/R/E	162.8	10.26	368807	271817	0.74	-569.38	8.89
E/R/C	144.9	11.20	337842	235119	0.70	-443.90	10.92
E/4/C	103.0	11.32	166010	120095	0.72	258.21	6.97
E/2/C	89.2	11.57	114210	92145	0.81	-268.54	7.77
N/2/W	89.4	10.67	99923	85209	0.85	355.80	6.40
N/2/C	86.4	10.66	94138	79605	0.85	307.44	6.42
N/2/E	106.5	11.60	157791	131551	0.83	-641.95	11.20
N/G/E	84.2	10.65	86688	75540	0.87	284.03	6.44
N/G/W	90.9	10.66	98337	88046	0.90	330.57	6.41
E/G/E	69.1	10.63	59894	50778	0.85	-324.96	7.72
U/G/E	35.8	6.85	12659	8780	0.69	-174.26	5.79

Finally it should be noted that these three time regions of energy arrival are also seen in the corresponding plots of Arias intensity.

- It is of interest to note that the maximum cumulative rms, i.e., the maximum rate of energy arrival, occurred at exactly the same time (10.26 seconds) at the roof level for all three N-S components (N/R/W, N/R/C and N/R/E). At the second floor, the maximum cumulative rms occurred at almost the same time for traces E/2/C (11.57 seconds) and N/2/E (11.60 seconds).
- In all traces, the Arias intensity was at least 70% of its maximum value at the time of the maximum cumulative rms value.
- The horizontal components of free field motion have almost identical cumulative rms and Arias intensity functions (Figures 4.1 and 4.2) indicating very similar motion.

The durations of strong motion for the three free field and thirteen building responses were determined from the definitions of duration given by Trifunac and Brady (1975), Bolt (1973), and McCann and Shah (1979). The Trifunac and Brady duration is the time interval required to accumulate the Arias intensity between 5 and 95 percent of its maximum value. Bolt's definition is based on the total time elapsed during the record between the first and last crossing of a given acceleration level. In this report, the Bolt cutoff level is 0.05g. Finally, the duration from McCann and Shah is determined from the derivative of the cumulative rms function. The rms acceleration over each calculated duration is then computed. Table 4.2 lists the duration and the corresponding rms values. The maximum rms computed from the cumulative rms function is also listed and hence corresponds to a duration between 0 seconds and the time of the maximum value. A general trend is evident.

TABLE 4.2 COMPARISONS OF DURATION AND RMS ACCELERATION

Trace	Duration (sec)			RMS (cm/sec^2)			
	Trifunac-Brady	Bolt	McCann-Shah	Trifunac-Brady	Bolt	McCann-Shah	Maximum Cumulative RMS
FF 092	15.6	11.7	12.2	51.7	60.2	59.1	59.3
FF UP	8.0	8.1	9.2	59.6	60.4	56.4	59.7
FF 002	12.1	11.2	10.7	59.4	62.6	63.6	60.4
N/R/W	9.9	25.6	8.2	169.2	109.9	186.9	159.9
N/R/C	13.2	30.3	6.5	151.7	104.6	213.3	165.5
N/R/E	22.9	43.4	12.9	120.7	91.7	158.7	162.8
E/R/C	19.7	24.4	23.7	124.4	116.1	117.6	144.9
E/4/C	19.9	23.3	19.1	86.8	82.9	89.9	103.0
E/2/C	15.8	19.4	9.8	80.8	75.2	103.5	89.2
N/2/W	10.5	13.0	8.5	92.8	85.9	103.6	89.4
N/2/C	10.0	15.4	10.9	92.3	77.1	90.5	86.4
N/2/E	12.6	15.8	12.8	106.5	98.3	107.5	106.5
N/G/W	9.1	12.7	6.4	98.9	86.5	118.0	90.9
N/G/E	9.7	15.2	10.6	90.0	74.6	87.8	84.2
E/G/E	11.6	11.6	7.5	68.4	69.6	84.4	69.1
U/G/E	18.0	6.8	11.3	25.2	39.3	31.8	35.8

For many of the building and free field components, the rms values are reasonably similar and hence the definition of strong motion duration does not affect the value. Furthermore, Figures 4.3a and b now show for building response a similar linear relationship between rms and peak acceleration as found by Mortgat (1976) for free field motion.

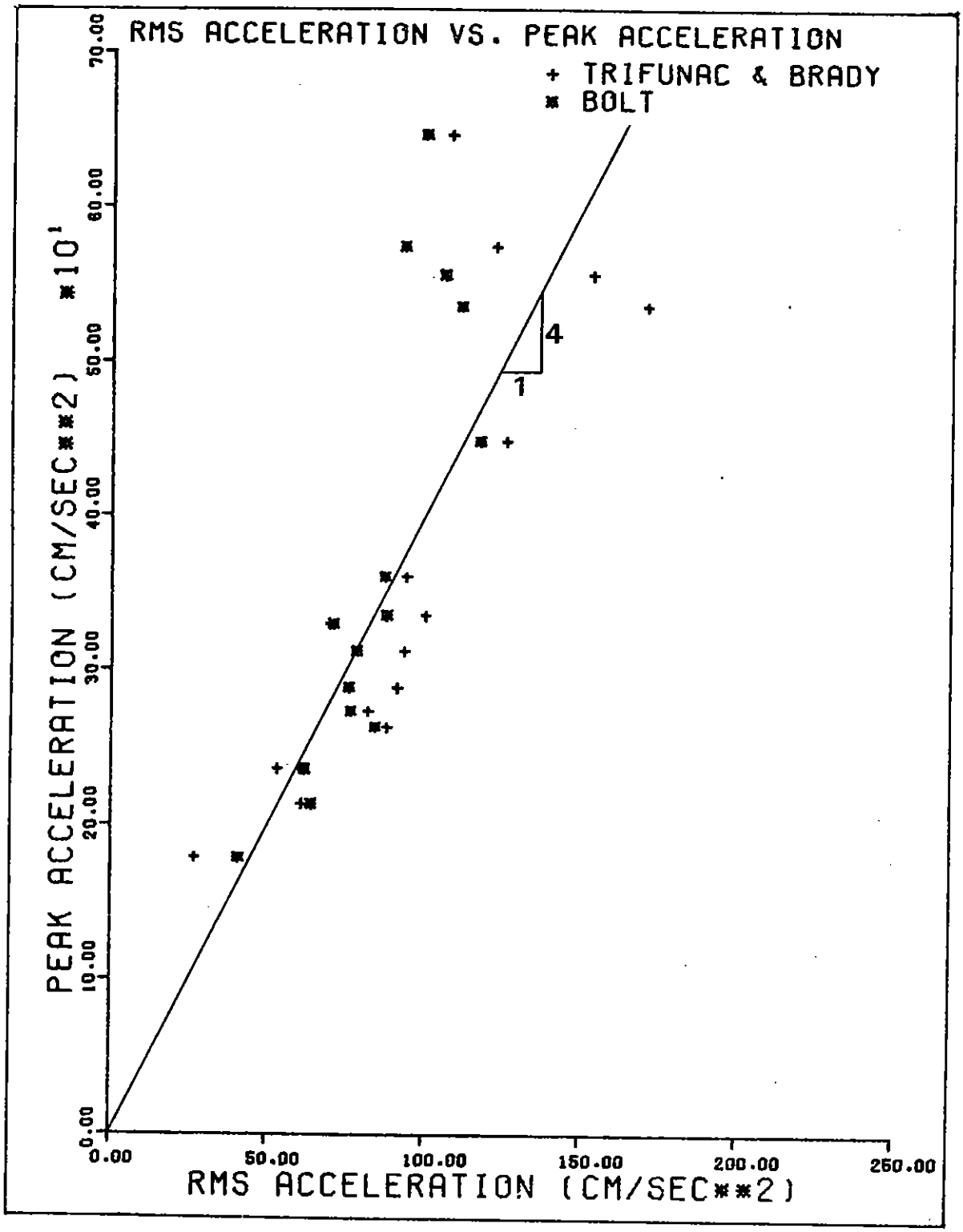

FIGURE 4.3a Peak Acceleration vs. RMS Acceleration Using Definitions of Duration by Trifunac & Brady and Bolt

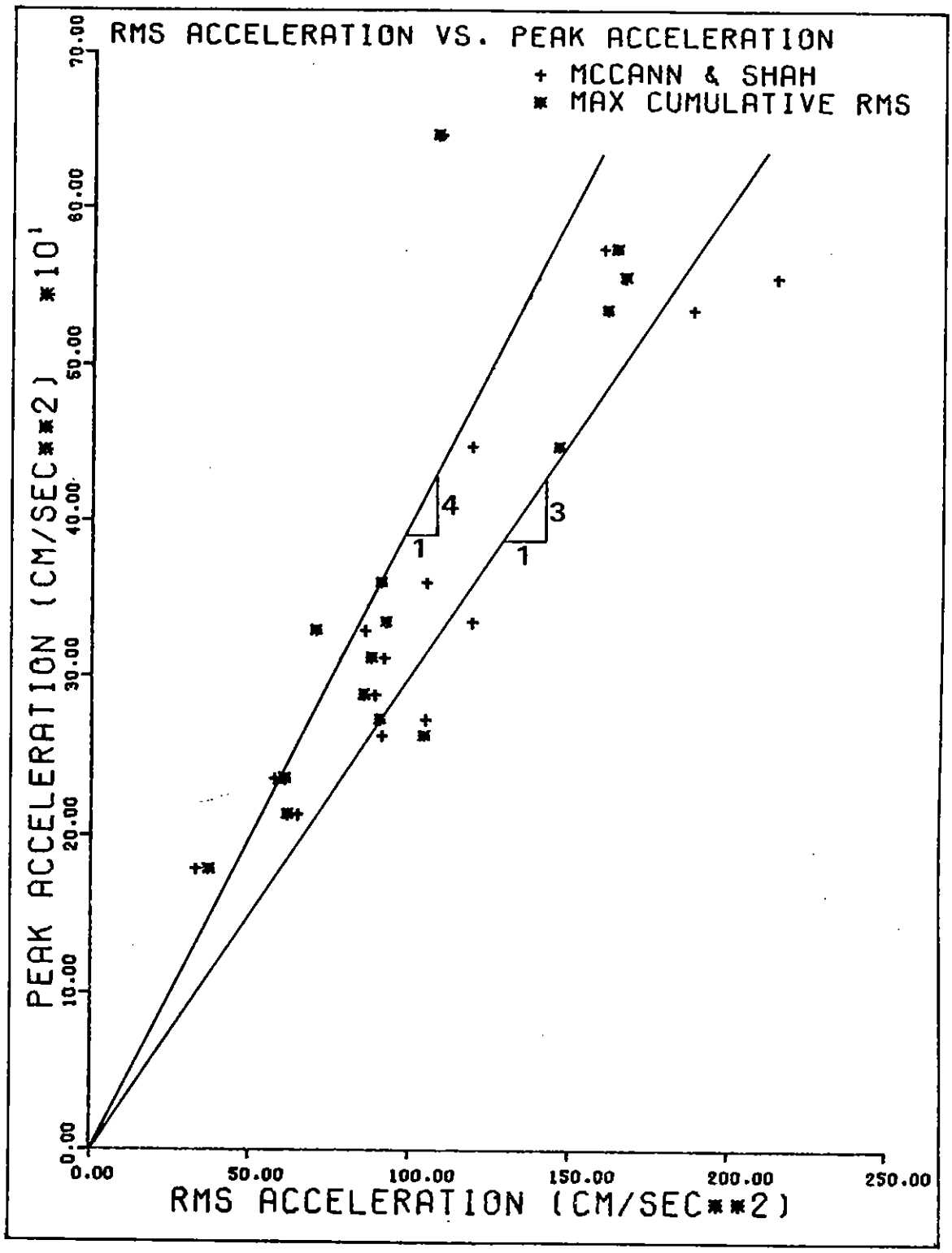

FIGURE 4.3b Peak Acceleration vs. RMS Acceleration Using Definitions of Duration by McCann & Shah and Determined from the Maximum Cumulative RMS Acceleration Function

CHAPTER 5: INTERPRETATION OF RESPONSE

From the analyses performed in the preceding chapters, the response of the Imperial County Services Building during the earthquake of October 15, 1979 showed the following features:

- The ground motion at the free field of the building was a highly nonstationary process. The horizontal components contained low frequency content (0 to 3 Hz). During the first 6 seconds (P wave phase), the horizontal components had amplitudes less than 30 cm/sec^2. Between 6 and 12 seconds, the amplitudes increased about 10 times (maximum was 0.23g) corresponding to the S wave influence. At about 12 seconds, the amplitudes rapidly decayed to about 50 cm/sec^2 and less and by 24 seconds, were less than 15 cm/sec^2. The vertical component, on the other hand, showed less variation with time and a predominant high frequency content (8 to 9 Hz). Rotational components of ground motion were not significant.
- In an average sense, the 0.23g horizontal PGA was amplified to values at the roof of the building of 0.45g in the E-W direction and 0.5g to 0.6g in the N-S direction. The largest PGA of 0.64g occurred in the N-S direction at the second floor level, east end of the building, (N/2/E component), at 11.2 seconds. Large relative displacements of 23.5 cm were computed at the roof (E/R/C) and 8.9 cm at the second floor (E/2/C) in the E-W direction. In the N-S direction, maximum relative displacements of 7 cm were observed at the roof (N/R/E) and 3.4 cm at the second floor (N/2/E).
- Pile-soil interaction occurred during the earthquake since the horizontal motion at the base of the building reflected the response

of the building (similar frequency content). The vertical transfer function between the free field and the base showed only high frequency amplification (16-18 Hz) and hence eliminated the possibility of rocking in the E-W direction. Horizontal peak ground accelerations were 150% higher at the base of the building than at the free field and the peak vertical ground acceleration was 130% lower.

- The dynamic characteristics of the building changed dramatically during the earthquake. Using moving time window Fourier analysis, the frequency content in the N-S (first and second translational and torsional modes) and E-W directions (first, second, and third translational modes) was determined. During the first five seconds of low amplitude vibration, a reduction of the frequencies from the ambient vibration values was already apparent. At the end of the strong motion (12 seconds) and beyond, the frequencies for all identifiable modes had decreased to 0.4 times the pre-earthquake ambient vibration test frequencies. Post earthquake ambient vibration tests for the shored up structure showed frequency values only 0.80 times smaller than the pre-earthquake ambient vibration test.
- Due to the high frequency content of the first 5 seconds, high frequency modes were excited; in particular, the second torsional mode prevailed during most of the record. This second torsional mode was clearly influenced by the discontinuity of the exterior shear walls at the first story and by the slight eccentricity in plan at the first story.

- With the arrival of the S waves, the predominant frequencies shifted to the lower end of the spectrum (0.5 to 2 Hz) and the first modes of vibration were excited. The rapid increase in amplitude (≈10 times) in the 1 to 2 Hz frequency range caused an apparently large decrease in the building frequencies and a consequent increase in the relative displacements.
- Yielding may have occurred at the ground level columns between 6 and 7 seconds when the first large relative displacements occurred between the base and the second floor. It is hypothesized that the second torsional mode configuration combined with the first large N-S second story displacements caused rotation of the upper level exterior shear walls which in turn imposed the first large axial loads on the east and west end columns. These axial loads, coupled with the resulting P-Δ effect from the E-W frame motion, initiated yielding in these columns.
- During the next 6 seconds until collapse of the east end columns, large amplitude motion continued with coupling between the transverse and torsional modes.
- Collapse of the four east end columns may have occurred near 11.2 seconds when the E-W and N-S motions obtained simultaneously their near maximum relative displacements at the second floor after an overall 5 to 7 cycles of high amplitude displacements. At this time, the axial loads from the N-S motion on the east end columns were high and coupled with an important P-Δ effect from the E-W frame vibration. Failure of the west end columns was prevented by the presence of a single bay shear wall along the west end ground level column line.
- It is interesting to note that large deformations occurred at the second floor and roof diaphragms (about 2 cm maximum) as observations of minor cracking suggest. Usually,

in design practice these elements are considered as in-plane rigid bodies.

- Finally, from the thirteen records in the building, a reasonably complete analysis of the dynamic behavior during the earthquake was obtained. However, two important points are mentioned: 1) There were no vertical records in the upper story levels and hence the influence of the vertical component could not be assessed, and 2) A study performed to determine filter effects on the relative displacements showed that while the relative interstory displacements obtained from the accelerations were sensitive (20 to 40%) to filtering techniques, the phases were not. Therefore some of the conclusions based on relative displacements may be subjected to additional adjustments if the method of processing records is revised.

The above analysis of the dynamic behavior of the Imperial County Services Building motivates several areas of further needed research:

- Dynamic Analysis Techniques:

  Could the observed behavior of the building and the change in the building properties during nonlinear response have been predicted if the input free field motion were known? Are the present approximate methods of analyses, e.g., static, response spectra, etc., adequate to analyze this structure? What values should be chosen to represent the fundamental frequencies? Particularly, why did the apparent frequencies change so dramatically? What is the role of soil-pile interaction?

- Strong Ground Motion Vs. Response Parameters:

  If the building had been subjected to strong ground motion triggered at other locations, would failure of the east end columns also have occurred? Is root mean square (rms) acceleration a better measure of the response than PGA?

- Design Implications:

  Had the building been designed with shear walls down to the foundation level, would collapse have occurred? What structural damage would be expected if the first story level had been designed with complete symmetry?

- Instrumentation:

  Keeping in mind that this building was the best instrumental building to suffer extensive damage, can we retrace the behavior from the start of the earthquake to the end? If not, what is the value of such instrumentation?

REFERENCES

1. Arias, A. (1970), "A Measure of Earthquake Intensity," in Seismic Design of Nuclear Power Plants, R. Hansen, ed., M.I.T. Press.

2. Beck, J.L. (1978), "Determining Models of Structures from Earthquake Records," Report No. EERL-78-01, California Institute of Technology.

3. Bolt, B.A. (1973), "Duration of Strong Ground Motion", Fifth World Conference on Earthquake Engineering, Rome, Italy, Vol. I., pp. 1304-1315.

4. Kaya, I. and McNiven, H.D. (1978), "Investigation of the Nonlinear Characteristics of a Three Story Steel Frame Using System Identification", Report No. EERC 78/25, University of California, Berkeley.

5. Leivas, E. et al. (1980), "Geological Setting, Historical Seismicity and Surface Effects of the Imperial Valley Earthquake," in Reconnaissance Report, Imperial County, California, Earthquake, October 15, 1979, EERI, February, 1980, pp. 5-19.

6. McCann, M.W. (1980), "RMS Acceleration and Duration of Strong Ground Motion," John A. Blume Earthquake Engineering Center, Technical Report No. 46, Stanford University, Stanford, CA, October 1980.

7. McCann, M.W. and Shah, H.C. (1979), "Determining Strong-Motion Duration of Earthquakes," Bulletin of the Seismological Society of America, Vol. 69, No. 4, pp. 1253-1265.

8. McGuire, R.K. and Hanks, T.C. (1979), "RMS Accelerations and Spectral Amplitudes of Strong Motion During the San Fernando Earthquake," submitted to the Bulletin of Seismological Society of America.

9. McVerry, G.H. (1979), "Frequency Domain Identification of Structural Models from Earthquake Records," Report No. EERL 79-02, California Institute of Technology.

10. Mortgat, C.P. (1976), "A Bayesian Approach to Seismic Hazard Mapping: Development of Stable Design Parameters," Ph.D. Thesis, Department of Civil Engineering, Stanford University.

11. Pardoen, G.C. (1979), "Imperial County Services Building - Ambient Vibration Test Results," Research Report 79/14, Department of Civil Engineering, University of Canterbury, Christchurch, New Zealand.

12. Pardoen, G.C., Hart, G.C. and Bunce, B.T., "Damage Assessment of the Imperial Co. Services Building," Presented at ASCE Convention, Florida, October 27-31, 1980, Preprint 80-680.

13. Rojahn, C. and Ragsdale, J.T. (1980), "Strong Motion Records from the Imperial County Services Building, El Centro," in Reconnaissance Report, Imperial County, California Earthquake, October 15, 1979, EERI, February, 1980, p. 173-184.

14. Trifunac, M.D. and Brady, A.G. (1975), "A Study of the Duration of Strong Earthquake Ground Motion," Bulletin of the Seismological Society of America, Vol. 65, No. 3, 1975.

15. Udwadia, F.E. and Marmelis, P.Z. (1976), "The Identification of Building Structural Systems: I. The Linear Case", Bulletin of the Seismological Society of America, Vol. 66, No. 1, pp. 125-151.

16. Udwadia, F.E. and Trifunac, M.D. (1974), "Time and Amplitude Dependent Response of Structures," Earthquake Engineering and Structural Dynamics, Vol. 2, pp. 359-378.

17. Ulrich, F.P. (1941), "The Imperial Valley Earthquakes of 1940," Bulletin of the Seismological Society of America, Vol. 31, January 1941, pp. 13-31.

18. Wosser, T. et al. (1980), "On the Earthquake Induced Failure of the Imperial County Services Building," in Reconnaissance Report, Imperial County, California Earthquake, October 15, 1979, EERI, February, 1980, pp. 159-172.